DISSERTATION

Analyse zum Vorkommen von Autoantikörpern gegen hirneigene Antigene bei an Demenz Erkrankten
Fokus auf GFAP als Antigen

Analysis of the occurrence of autoantibodies against brain antigens in patients with dementia
Focus on GFAP as antigen

zur Erlangung des akademischen Grades
Medical Doctor - Doctor of Philosophy (MD/PhD)

vorgelegt der Medizinischen Fakultät
Charité – Universitätsmedizin Berlin

von

Paula Charlotte Barthel

Erstbetreuung: PD Dr. Markus Höltje

Datum der Promotion: 29.11.2024

Table of Contents

List of Tables

List of Figures

Abbreviations

AD	Alzheimer's disease
AIS	Androgen insensity syndrome
AMPA	Alpha-amino-3-hydroxy-5-methyl-4-isoxazolepropionic acid
ANNA-3	Anti-Neuronal Nuclear Antibody 3
AP3B2	Adaptor-related protein complex 3, beta 2
AT1A3	α3 subunit of Na+/K+-ATPase
BSA	Bovine serum albumin
CAA	Cerebral amyloid angiopathy
CARPVIII	Carbonic anhydrase-related protein VIII
CASPR2	Contactin-associated protein-like 2
COVID-19	Coronavirus disease 2019
CRC	Colorectal cancer
CSF	Cerebrospinal fluid
DAPI	4′, 6- diamidino-2-phenylindole
DNEM	Dulbecco’s Modified Eagle Medium
DPPX	Dipeptidyl-peptidase-like protein-6
ERC1	Anti-ELKS/RAB6-interacting/CAST family member 1
FCS	Fetal calf serum
FLAIR	Fluid-attenuated inversion recovery sequence
FTD	Frontotemporal dementia
GABA	Gamma-aminobutyric acid
GAD65	Glutamic acid decarboxylase 65-kilodalton isoform
GADPH	Glyceraldehyde-3-phosphate dehydrogenase
GFAP	Glial fibrillary acidic protein
Glu-RD2	Glutamate receptor d2
HBP	High blood pressure
HBSS	Hank’s balanced salt solution
hCMEC/D3 cells	Human cerebral microvascular endothelial cells
HEK cells	Human embryonic kidney cells
hIgG	Human Immunoglobulin G
ICH	Intracerebral hemorrhage
IgG	Immunoglobulin G

ITPR1	Inositol 1,4,5-trisphosphate receptor type 1
KCNA2	Potassium voltage-gated channel subfamily A member 2
LBD	Lewy body dementia
LGI1	Leucine-rich-glioma-inactivated 1
mAbs	Monoclonal antibodies
MAP2	Microtubule-associated protein 2
MCI	Mild cognitive impairment
mGlu-R1	Metabotropic glutamate receptor 1
mGlu-R5	Metabotropic glutamate receptor 5
MMSE	Mini Mental State Examination
MOCA	Montreal-Cognitive-Assessment
MOG	Myelin Oligodendrocyte Glycoprotein
MRI	Magnetic resonance imaging
NB-medium	Neurobasal-medium
NMDA	N-methyl-D-aspartate
NMDAR	N-methyl-D-aspartate receptor
NPH	Normal pressure hydrocephalus
PBS	Phosphate-buffered saline
PD	Parkinson's disease dementia
PEI	Polyethyleneimine
PFA	Paraformaldehyde
pTau	Phospho-Tau
RA	Rheumatoid arthritis
SAE	Subcortical arteriosclerotic encephalopathy
SAH	Subarachnoid hemorrhage
Sez6l2	Seizure-related 6 homolog like 2
T2D	Type 2 diabetes
TIA	Transient ischemic attack
TPC	Total protein count
Tr/DNER	Anti-Tr/anti-Delta/Notch-like epidermal growth factor-related receptor
TRIM	Turbo inversion recovery magnitude sequence

Abstract

Einleitung: Die vorliegende Dissertation umfasst drei Publikationen. Die Hauptpublikation mit Erstautorenschaft beschäftigt sich mit dem Vorkommen von Autoantikörpern bei Patient*innen mit Demenz, mit besonderem Fokus auf GFAP als Antigen. Zwei weitere Publikationen zum Antikörperrepertoire bei COVID-19 und zu Gefäß-Autoantikörpern stehen dazu in engem inhaltlichem Zusammenhang und werden in der Diskussion weiterführend erläutert.
Seit der Entdeckung der Anti-NMDA-Rezeptor-Enzephalitis sind autoantikörpervermittelte neurologische Erkrankungen zunehmend in den Wissenschaftsfokus gelangt. Seitdem wurden zahlreiche weitere Autoantikörper identifiziert, die ein breites Spektrum an Symptomen hervorrufen können. Daher stellten wir die Hypothese auf, dass im Serum von Patient*innen mit Demenz Autoantikörper gegen hirneigene Antigene zu detektieren sind. Diese Autoantikörper könnten eine chronisch verlaufende autoimmune Enzephalitis bedingen, welche die Symptome einer dementiellen Erkrankung hervorruft. Als Antigene kommen u.a. astrozytäre Antigene, beispielsweise GFAP, in Betracht.

Ziel der Studie: Ziel ist es, das Vorkommen von Autoantikörpern bei Patient*innen mit Demenz zu untersuchen und spezifische Antigene zu identifizieren.

Material und Methoden: Die Kohorte umfasst 127 Patient*innen mit Demenz aus der neurologischen Klinik der Charité. Als Kontrollkohorten dienten 82 Proben aus der Biobank der Charité sowie von 15 gesunden Personen. In einem mehrstufigen Screeningverfahren wurden die Seren zunächst mittels immunzytochemischer Färbungen auf primären murinen embryonalen hippokampalen/kortikalen Zellkulturen das generelle Vorhandensein von Autoantikörpern untersucht. Nachfolgend wurden zusätzliche Methoden, u.a. (Ko-)Färbungen auf Astrozytenkulturen, GFAP-transfizierten HEK-Zellen und murinen Hirnschnitten, Livefärbungen sowie Western Blots angewandt.

Ergebnisse: Insgesamt 45 von 127 Demenzpatient*innen wurden im ersten Screeningschritt positiv auf das Vorhandensein von Autoantikörpern getestet. Am häufigsten waren Autoantikörper gegen Astrozyten in 28 (22%) Demenzseren und 3 (4.7%) Biobankseren ($p \leq 0.001$ Demenz vs. Biobank $p \leq 0.001$ Demenz vs. Gesamtkontrollen). GFAP-spezi-

fische Autoantikörper wurden bei 14 (11%) Demenzseren und einem (1.6%) Biobankserum ($p = 0.007$ Demenz vs. Biobank; $p = 0.003$ Demenz vs. Gesamtkontrollen) nachgewiesen.

Diskussion und Schlussfolgerungen: Autoantikörper, insbesondere gegen GFAP, traten signifikant häufiger in der Demenzkohorte als in den Kontrollkohorten auf. Die pathogene Relevanz dieser Autoantikörper kann, auf Grundlage der aktuellen Forschung, nicht abschließend geklärt werden. Das Auftreten von GFAP-Autoantikörpern definiert eine Subgruppe von Patient*innen mit Demenz, die ein vielversprechendes zukünftiges Forschungsfeld eröffnet. Wichtige Aspekte sind u.a. die Rolle von Infektionen wie COVID-19 und Blutgefäß-Autoantikörpern, diagnostische Marker sowie Langzeit- und Therapiestudien.

Introduction: This dissertation includes three publications. The main, first-authorship publication investigates the occurrence of autoantibodies in patients with dementia, focusing on GFAP as a potential antigen. Two additional publications about the antibody repertoire in patients with COVID-19 and about blood-vessel autoantibodies are closely related to the main topic and will be further explained in the discussion section.
Since the discovery of the autoimmune NMDAR encephalitis, autoantibody-mediated neurological diseases have increasingly become a focus of research. Since then, numerous other autoantibodies have been identified that can cause a wide range of symptoms. We therefore hypothesized that autoantibodies against brain antigens can be detected in the serum of patients with dementia. These autoantibodies might cause a chronic, slowly progressing form of autoimmune encephalitis with symptoms of dementia. Possible antigens include astrocytic antigens, for example GFAP.

Aim of the study: To investigate the occurrence of autoantibodies in patients with dementia and to identify specific antigens.

Material and methods: The cohort includes 127 patients with dementia from the Charité Neurology Department. Our control cohorts consisted of 82 Charité Biobank samples and samples from 15 healthy people. Using a successive screening strategy, the sera were

first stained on primary embryonic murine hippocampal/cortical cell cultures for the presence of autoreactivity. We then applied additional methods, including (co-)staining on purified astrocyte cultures, GFAP-transfected HEK cells and murine brain sections, live staining, and Western blots.

Results: A total of 45 of 127 dementia patients tested positive for the presence of autoantibodies in the first screening step. Autoantibodies against astrocytes were the most common in 28 (22%) dementia sera and 3 (4.7%) biobank sera ($p \leq 0.001$ dementia vs. biobank $p \leq 0.001$ dementia vs. total controls). GFAP-specific autoantibodies were detected in 14 (11%) dementia sera and one (1.6%) biobank serum ($p = 0.007$ dementia vs. biobank; $p = 0.003$ dementia vs. total controls).

Discussion and conclusion: Autoantibodies, especially against GFAP, were significantly more frequent in the dementia cohort than in the control cohort. Based on the current research, the question about the pathogenic relevance of these autoantibodies cannot be answered yet. GFAP autoantibody-positivity defines a subgroup of patients with dementia which should be addressed by further research. Important aspects include the role of infections such as COVID-19 and blood-vessel autoantibodies, biomarkers, as well as long-term follow-up and therapy-studies.

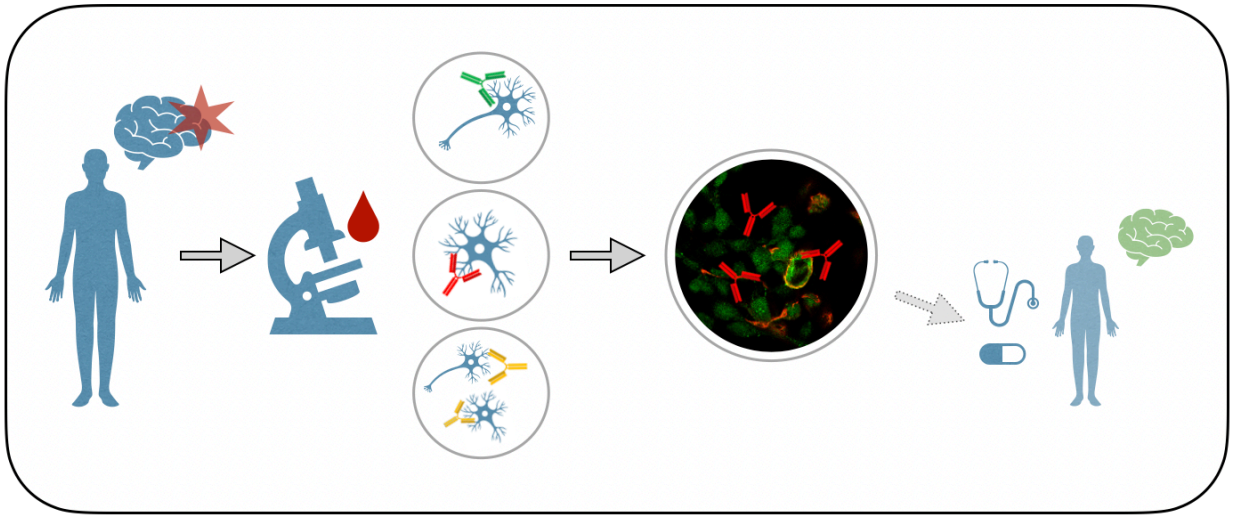

Figure 1: Graphical abstract (own representation: Paula Charlotte Barthel)

We aimed to investigate our hypothesis, that autoantibodies are present in patients with dementia, potentially contributing to the disease resembling acute autoimmune encephalitis. Furthermore, we stated that specific antigens such as astrocytic GFAP can be identified. Therefore, we screened 127 serum samples from patients with dementia for the presence of autoantibodies, using a successive screening strategy with immunocytochemical staining on primary murine embryonic hippocampal/cortical cell cultures as a first screening step. We then utilized additional methods to refine our findings and to identify specific antigens, including (co-)staining on GFAP-transfected HEK cells (shown), purified astrocyte cultures, and murine brain sections, live staining, and Western Blots. A total of 45 out of 127 dementia patients tested positive for the presence of autoantibodies in the first screening step. Autoantibodies were either directed against neurons, astrocytes, or both. Autoantibodies against astrocytes were the most common, which led to our special focus and further investigation of this subgroup of autoantibodies. Using GFAP-transfected HEK cells, we were able to identify GFAP as a specific autoantibody target in 14 (11%) dementia sera. These autoantibodies, especially against GFAP, occurred significantly more often in the dementia cohort than in our control cohorts. However, the question about the pathogenic relevance of these autoantibodies cannot be fully answered yet. GFAP autoantibody-positive patients are subgroup of patients with dementia, which is a promising topic for further research.

1 Introduction

1.1 Dementia

Dementia is among the most prevalent neuropsychiatric diseases and is one of the biggest and quickly growing challenges for healthcare systems worldwide. It affects people worldwide and the absolute number of people who live with dementia is increasing. An analysis for the Global Burden of Disease Study 2019 estimated the global prevalence of dementia and forecasted the evolution until 2050 (1). They found that in 2019 around 57.4 million people were living with dementia and predicted that numbers will rise to 152.8 million people in 2050. There were noticeable geographic differences in the estimated number of people with dementia. The increase was predicted to be the highest in low- and middle-income countries and lowest in high-income countries (1).

Regarding the public health perspective, the “Dementia prevention, intervention, and care: 2020 report of the Lancet Commission”, identified twelve modifiable risk factors: excessive alcohol consumption, head injury, air pollution, lower education, hypertension, hearing impairment, smoking, obesity, depression, physical inactivity, diabetes, and infrequent social contact. The modification of these factors might prevent or delay up to 40% of dementias (2).

Dementia does not only affect our society at the high level of our communities and health care systems but is also a deeply personal challenge for every single patient and the people who care for them. The disease stops the patient from being able to live an independent life, even affecting his personality and relationships. The available data shows the need to take action to address dementia as a disease that affects millions worldwide and underscores the great challenge for our healthcare system. This includes improvement on a worldwide level, for example public health programs, addressing the big risk factors, as well as better care on a personal level for every patient and the people who care for them (2). It is therefore crucial to continue and improve scientific research about dementia to better understand the disease, identify risks, investigate pathogenesis, therapies and maybe even a cure.

Dementia does not describe a single, specific disease but is a broad term for various diseases that present with symptoms including impaired memory, orientation, and learning, as well as changes in personality, leading to the inability to live independently. Secondary dementias where symptoms are caused by another underlying disease must be

distinguished from primary neurodegenerative dementia syndromes. Despite years of ongoing research, the pathogenesis of these neurodegenerative diseases is still poorly understood. Therapies, if available, can address the various symptoms of the disease, but there is still no cure for neurodegenerative dementias. Many hypotheses have been developed over time and, at the moment, it seems most likely that various factors contribute to the disease. Even neurodegenerative dementias need to further be distinguished in subgroups with different disease mechanisms (3), (4), (5), (6).

There is growing evidence that one of the factors contributing to dementia might be autoimmunity, possibly even causing a subgroup of patients with “autoimmune dementia”, where symptoms are caused primarily by an autoimmune reaction rather than being primarily neurodegenerative. In these cases, dementia might be caused by a slowly progressing form of autoimmune encephalitis (7).

1.2 Autoimmune Encephalitis

Autoimmune anti-N-methyl-D-aspartate receptor (NMDAR) encephalitis was first described in 2007 in a case series of twelve woman with ovarian or mediastinal teratoma, causing a new form of immunotherapy-responsive, paraneoplastic encephalitis with pathogenic autoantibodies directed against extracellular neuronal autoantigens (8). Until then, paraneoplastic encephalitis was associated with autoantibodies, such as anti-Hu or Anti-Ma2, targeting intracellular antigens. This kind of autoimmune encephalitis is most likely T cell-mediated, with autoantibodies occurring as a co-phenomenon, and is poorly responsive to immunotherapy (9). The twelve women with NMDAR encephalitis initially presented with prodromal symptoms such as fever, headache and cough. These first unspecific symptoms were followed by predominantly psychiatric symptoms including behavioral changes, cognitive decline and memory loss. The patients declined, developing seizures, reduced level of consciousness, autonomic instability or insufficient breathing. Extensive diagnostics revealed no explanation for the illness. Finally, immunocytochemical and immunohistochemical tests identified autoantibodies targeting the NMDA receptor in patients’ cerebrospinal fluid (CSF) and/or sera. Most patients improved with immunotherapy (8).

Since 2007, research and knowledge about autoimmune encephalitis has increased dramatically, creating a completely new and highly relevant class of neurologic diseases. This spectrum is still expanding with the discovery of new autoantibodies.

Autoimmune encephalitis may be associated with tumors, as described in first case reports of NMDAR encephalitis. Further research revealed multiple factors, including genetic predisposition or prior treatment with immunocheckpoint inhibitors that can cause or contribute to autoimmune encephalitis (10), (11). Infections, which can trigger an autoimmune reaction against brain structures, are an important factor. For example, NMDAR encephalitis commonly manifests after, or can clinically mimic, a herpes simplex virus encephalitis (12), (13). Other infections associated with autoimmune encephalitis are, for example, varicella zoster virus infection (14) and, especially relevant right now, coronavirus disease 2019 (COVID-19) (15), (16). To this day, autoantibodies targeting a myriad of antigens have been discovered, so that only some of them can be mentioned exemplarily in this report. In classical forms of autoimmune encephalitis, autoantibodies are directed against cell surface antigens, which makes them more likely to be directly pathogenic. For example, it has been proven that patient-derived monoclonal NMDAR antibodies are directly pathogenic, causing neuronal damage in cultured hippocampal neurons (17). Other antibodies against cell surface proteins are directed, for example, against the gamma-aminobutyric acid (GABA) receptor, alpha-amino-3-hydroxy-5-methyl-4-isoxazolepropionic acid (AMPA) receptor or glycin receptor (18), (19), (20). Autoantibodies which target intracellular antigens, such as autoantibodies against synapsin (21), can also be pathogenic.

Autoimmune reactions are not restricted to neuronal antigens but can also attack other cells, such as the endothelial cells of the blood-brain barrier (22) or glial cells like astrocytes or oligodendrocytes. For example, autoantibodies against the Aquaporin-4 water channel on the surface of astrocytes or against myelin-oligodendrocyte glycoprotein can cause neuromyelitis optica spectrum disorder, characterized by acute, relapsing, remitting, optic neuritis and transverse myelitis (23).

Symptoms of autoimmune encephalitis depend on the specific autoantibody, but clinical presentation can also differ from patient to patient or mimic other neurologic diseases, which sometimes complicates the diagnosis. In addition to the clinical examination, other diagnostic tools are used to support the diagnosis or to rule out differential diagnoses. This includes screening for infections, cerebral imaging, electroencephalography, cognitive testing, and psychiatric, rheumatologic, and immunological evaluation (24). In clinical practice, when autoimmune encephalitis is suspected, testing for common autoantibodies in patients' CSF and/or serum is necessary to confirm the diagnosis, using well established commercial assays in specialized laboratories. However, these assays may miss

autoantibodies which are not yet known (25). Therefore, broader screenings are necessary to discover new potential antigens.

1.3 Autoimmune Dementia

As described above, the topic of autoimmune encephalitis has steadily gained attention and the spectrum of autoantibodies and various possible symptoms is still growing. We already know that different autoantibodies can cause a broad number of different symptoms, sometimes even mimicking other neurologic diseases. However, most research in the field of autoimmune encephalitis focuses on acute manifestations, whereas less is known about slowly progressing forms. The spectrum of possible symptoms and disease courses of autoimmune encephalitis is extremely broad and heterogeneous. Therefore, it is plausible that some forms of autoimmune encephalitis could also cause a slowly progressing disease, with subacute or chronic cognitive impairment, manifesting as autoimmune dementia. It is important to identify these patients since they, in contrast to patients with primary neurodegenerative dementia, might benefit from immunotherapy.

In 2010, Flanagan et al. established the term “autoimmune dementia” for a subgroup of dementia patients where the underlying disease is caused by autoimmunity rather than a primary neurodegenerative process (7). Authors stated “red flags” to identify these patients with autoimmune dementia such as acute or subacute disease onset, rapid progressing dementia, fever or headache, young age, co-existing autoimmune or oncologic disease, unusual neurologic symptoms e.g. seizures (26), (27). In these cases, immunological testing is recommended, but screening for autoantibodies is not routinely performed when diagnosing patients with dementia.

Case reports mention patients who had initially presented with symptoms suggesting neurodegenerative diseases such as atypical dementia, Lewy body dementia, Creutzfeldt-Jakob disease, rapidly progressive dementia or frontotemporal dementia but were later diagnosed with autoimmune dementia and successfully treated with immunotherapy (28), (29), (30), (31), (32). Interestingly, autoantibodies with yet unknown relevance also occur in patients with correctly diagnosed neurodegenerative disorders (33), (34), (35).

Regarding autoimmune dementia, many aspects are still unclear, and more research is needed to better understand its epidemiology, etiology, pathogenesis and potential diag-

nostic criteria and treatment options. Therefore, it is necessary to systematically investigate great cohorts of patients with dementia for the presence of autoantibodies against brain structures, which might contribute to the disease.

1.4 GFAP astrocytopathies

In regard to autoimmune dementia, we hypothesize that autoantibodies may not only target neuronal proteins, but may also target glial cells, especially astrocytes, which are essential for a healthy brain. Astrocytes have complex interactions with neurons and other brain cells, both in vitro and in vivo; they support neurons' metabolism, synaptic transmission, and neurogenesis and are part of the blood-brain barrier. Furthermore, astrocytes undergo a complex process of aging and may also play a role in neurodegenerative diseases as shown e.g. for Alzheimer's disease (36).

Glial fibrillary acidic protein (GFAP) is a protein which is highly expressed in the cytoskeleton of astrocytes. GFAP functions as a type III intermediate filament protein and is the main protein of the astrocytic cytoskeleton, ensuring their form and function. Human GFAP is encoded by the gene locus 17q21 and has a molecular weight around 50 kDa. There are different GFAP splice variants; GFAPα is the most abundant form (37), (38), (39).

Many factors which influence the brain's status modulate GFAP expression level. Astrocytes become activated when the brain is damaged, such as through inflammation or trauma, causing a reactive gliosis. Therefore, GFAP levels in patients' sera or CSF can be used as a diagnostic or prognostic marker for brain damage in diseases like multiple sclerosis or traumatic brain injury (40), (41). A recent systematic review and meta-analysis focused on the role of serum GFAP as a biomarker for Alzheimer's disease. After analyzing numerous studies, the authors concluded that GFAP levels are increased in these patients and that GFAP is therefore a promising new biomarker for diagnosis and prognosis of Alzheimer's disease (42). A study that followed up 160 mild cognitive impairment (MCI) patients for 4.7 years found that serum GFAP can predict the progression of MCI into Alzheimer's disease (43).

GFAP was identified in 2016 as target of autoantibodies in autoimmune GFAP astrocytopathy (44). Patients typically present with acute or subacute meningomyeloencephalitis, suffering from symptoms including fever, headache, ataxia, tremor, optic papillitis, seizure or psychosis. The disease may be paraneoplastic, postinfectious or idiopathic.

Diagnosis is made based on the presence of GFAP IgG autoantibodies in serum and/or CSF detected by cell-based assays (45), (46), (47). CSF autoantibodies are more sensitive for the classic meningomyeloencephalitis phenotype, whereas some patients are only seropositive and are more likely to have atypical symptoms (48), (49). The pathogenesis behind the GFAP astrocytopathy is not fully understood, but animal studies and pathological analysis indicate that the disease is most likely mediated by T cells. However, B cells might also play a role (50), (51), (46). A pooled analysis of 324 cases until 2021 showed that the mean age of disease onset was 45 years without sex-specific prevalence and around 20% had co-existing malignancies, most commonly ovarian teratoma. Co-existing neuronal autoantibodies were detected in 25%, most commonly NMDAR autoantibodies. Nearly half of the patients showed characteristic radiological features, especially perivascular radial enhancement and extensive longitudinal myelitis. Most patients (86.5%) responded to acute immunotherapy with methylprednisolone, intravenous immunoglobulin or plasma exchange. CSF abnormalities, elevated white blood cell and protein count, as well as positive oligoclonal bands, were detected (48). Case reports in literature also describe patients with atypical disease manifestations such as intracranial hypertension and bilateral vision loss, hypertrophic pachymeningitis or Area postrema syndrome (52), (53), (54). Focusing on dementia, there are also single case reports which mention patients with GFAP autoantibodies who present with reversible parkinsonism (and cognitive impairment), chronic progressive cognitive impairment or rapid progressive dementia, which responded to immunotherapy (55), (56), (57), (58).

1.5 Aim of the study

Our study investigated two main hypotheses:

I. We hypothesize that autoantibodies against brain structures are present in patients with dementia.
II. Furthermore, specific antigens can be identified.

At the moment, autoantibody tests are performed on a case-by-case basis, but are not part of the standard diagnostic procedures for diagnosing dementia. Therefore, the cur-

rent available data is not sufficient to fully answer questions about the prevalence of autoantibodies in dementia patients or their antigens, pathogenesis, and implications for clinical practice.

Therefore, the aim of our study is to expand the current knowledge about autoimmune dementia by systematical screening for the presence of any autoantibodies against brain structures in a large cohort of 127 patients diagnosed with various forms of dementia. This broad screening uses immunocytochemical methods on primary murine hippocampal/cortical cell cultures. Additional cell-based assays and immunohistochemical methods are performed to identify target structures, focusing on GFAP as a potential autoantigen. In addition to the investigation of prevalence and potential target structures of these autoantibodies, patient clinical and paraclinical data will be reviewed.

2 Material and Methods

2.1 Patients

In total, our study included serum samples from three cohorts of patients: the dementia cohort plus two age-matched control groups. The dementia cohort consisted of 127 patients from the Memory Clinic of the Department of Neurology, Charité Universitätsmedizin Berlin and German Center for Neurodegenerative Diseases Berlin. They had been diagnosed with dementia based on clinical and neuropsychological examination, blood- and CSF-testing, as well as imaging studies. Patients with any form of dementia or mild cognitive impairment were included in this study, without any additional exclusion criteria. Serum samples were obtained from January 2018 until April 2021 and stored at − 80 °C. Our first age-matched control group consisted of serum samples from the Charité Biobank, obtained from 82 patients, with various neurologic diseases except dementia. Consequently, exclusion criteria were a diagnosis of any form of dementia, mild cognitive impairment or dementia-associated diseases. Our second control group was obtained from 15 healthy individuals who accompanied the patients from the dementia cohort to their appointments in the Memory Clinic.
The study was approved by the Ethics Committee of Charité Universitätsmedizin Berlin and all participants provided written informed consent to participate.

2.2 Screening strategy

The screening for the existence of autoantibodies in the serum samples was performed in two main steps. The first one was a broad screening to detect any autoantibodies in the sera, using immunostaining on primary murine embryonic hippocampal/cortical cell cultures as the primary detection method. These mixed cultures contain neurons and glial cells. Second, autoantibody positive sera were further characterized in order to determine specific antigens. Samples which showed reactivity to astrocytes, were tested on GFAP-transfected HEK cells to detect autoantibodies against this specific antigen. Additional immunohistochemical and immunocytochemical methods, including (co-)staining on murine brain sections, murine purified astrocyte cultures and live cell cultures, screening for co-existing autoantibodies or Western Blot was used to further characterize our findings. Immunoreactivity was always assessed by two independent observers.

All methods followed our already established protocols from previous studies and are summarized in the present paper (59).

2.3 Cell cultures

2.3.1 Primary murine embryonic hippocampal/cortical cell cultures

Murine hippocampal/cortical cultures were prepared from SWISS-mice embryos. At day E16-17, the pregnant mice were killed, and their embryos were removed. After collecting the embryonic brains in 0.6% PBS-glucose solution, we isolated parts of the cortex and the hippocampi from the embryonic brains and transferred them to NB-medium. N-medium was added, followed by the first round of centrifugation (800 rpm for 2 min at 4 °C) and resuspension of the cells in N-medium without collagen. The cells were centrifuged a second time and diluted in NB-starter medium. The cell-solution was seeded (8×10^4/ml) on coverslips in 24-well plates, which had been incubated overnight with poly-L-lysine solution in PBS (1:20) and coated with N-medium with collagen afterwards. Finally, we incubated the cells (10–14 days at 37 °C) and used them for immunostaining.

2.3.2 Murine purified astrocyte cultures

Murine purified astrocyte cultures were prepared from SWISS-mice aged between postnatal days 2 and 3. The mice were killed and their whole brains were isolated and suspended in Hank's balanced salt solution (HBSS, Sigma). We centrifuged the suspension (300×*g* for 3 min) and resuspended them with a pipette in HBSS. The cells were seeded on 6-well plates (1/2 brain per well), coated with poly-L-Lysine (100 µg/ml in PBS), after repeating the centrifugation two more times resuspending with pipettes with smaller diameters. The cells were then incubated in DMEM, supplemented with 10% FCS, 100U/ml pen/strep and 2 mM L-glutamine at 37 °C and 5% CO_2. We shook the plates regularly to remove microglia and replaced the medium twice. Incubation time was seven days for immunostaining and 12 to 14 days for immunoblots. For immunostaining, we coated 24-well plates with poly-L-lysine (100 µg/ml in PBS) and seeded the cells (4×10^4 cells per well) for further use.

2.3.3 GFAP-transfected HEK cells

HEK293 cells were transfected with a plasmid encoding for human glial fibrillary acidic protein (GFAP alpha (I), based on a VB900131- 8024ppx plasmid backbone, Vector Builder, Chicago, IL, USA), using established protocols. In detail, we diluted the DNA in 0.9% NaCl, added polyethyleneimine (PEI) as the transfection agent and incubated for 30min at RT. Next, we added the solution to the cells in 24-well plates which previously had received half of the standard volume fresh HEK cell medium. We incubated the cells for 4h at 37°C and added the remaining half of the HEK cell medium. Then, the cells were incubated for the transfection time of 24h. Finally, we fixed the cells for 20min with 4% PFA and used them for immunostaining. To test whether the transfection was successful and efficient, we co-stained the cells with a commercial monoclonal anti-GFAP antibody.

2.4 Staining of cultured cells

2.4.1 Hippocampal/cortical cell cultures and purified astrocyte cultures

Fixed cells: To prepare the cells for staining, we first removed the medium from the 24-well plates and washed the cells twice with 10% PBS. After that, we fixed the cells with 80% ice-cold methanol for 20min. Then, we removed the methanol and incubated the cells in blocking solution (1h at RT). Next, we incubated the cells with the patient's serum (diluted 1:200 in blocking solution) for 24h at 4°C and washed them twice with PBS. We diluted the secondary antibody (FITC- conj. goat anti-human IgG) 1:100 in secondary antibody solution, applied it to the cells for 90min at RT and washed them with PBS again. Next, we incubated the cells with DAPI (4′, 6- diamidino-2-phenylindole) for 10 min to stain the cell nuclei. Finally, the cells were mounted to the slides with Immu-Mount (Thermo Fisher Scientific, Waltham, MA).

Live cells: For live staining, the first step was to add the patient's serum (diluted 1:200 in culture medium) to the 24-well plates which contained the living cells. The cells were incubated with the serum for 24h, washed with PBS and fixed with 80% ice-cold methanol for 20min. After that, the next steps, including incubation with secondary antibody, staining with DAPI and mounting, followed the same protocol as for staining fixed cells.

2.4.2 HEK cells

HEK293 cells were stained according to the same protocol as described for fixed hippocampal/cortical cell cultures and purified astrocyte cultures. The only difference was the use of 4% PFA in PBS for fixation instead of methanol.

2.5 Staining of murine brain sections

Brain sections for immunostaining were obtained from adult SWISS-mice. We perfused the mice and dissected their brains. After cryoprotecting and freezing at -80°C, coronary and sagittal sections of 20µm thickness were cut. The resulting sections included our brain regions of interest, especially hippocampus, cortex and cerebellum. For the staining, we first washed the sections in PBS, added blocking solution and incubated them for 30min at RT. After that, we removed the blocking solution, added the serum samples to the sections (diluted 1:200 in primary antibody solution) and incubated the sections for 24h at 4°C. The secondary antibody (FITC-conj. goat anti-human IgG 1:100 in secondary antibody solution) was applied after washing the sections with PBS. Again, we incubated the sections for 1h at RT, washed them with PBS and mounted them to the slides using Immu-Mount.

2.6 Co-staining with commercial antibodies

We performed co-staining on cell cultures and brain sections with commercial antibodies to confirm cell-types and structures such as astrocytes (monoclonal mouse anti-GFAP antibody) or neurons (monoclonal mouse anti-MAP2 antibody). The protocols were the same as for staining without commercial antibodies. We added the commercial primary antibodies together with the patient's serum in blocking solution or primary antibody solution. Commercial secondary antibody (Alexa-red goat anti-mouse 594) were also applied together in addition to FITC-conj. goat anti-human IgG antibody.

2.7 Screening for co-existing autoantibodies

Screening for co-existing autoantibodies was available for 12 of the 15 GFAP-positive sera. The standard and research autoimmune diagnostic panels by the Euroimmun AG (Lübeck, Germany), tested for the following antigens: Hu, Ri, ANNA-3, Yo, Tr/DNER, Ma/Ta, GAD65, Amphiphysin, Aquaporin4, MOG, NMDA-R, AMPA-R, GABAB-R, LGI1,

CASPR2, IGLON5, ZIC4, DPPX, Myelin, CARPVIII, Glycine-R, mGlu-R1, mGlu-R5, GABAA-R, RHO activating GTPase 26, Recoverin, Glu-RD2, Flotillin 1/2, ITPR1, Homer3, Neurochondrin, Neurexin-3-alpha, ERC1, Sez6l2, AP3B2, Contactin1, Neurofascin 155, Neurofascin 186, AT1A3, KCNA2, Dopamin-R2.

2.8 Western Blots

We used cells from astrocyte cultures and whole brains from adult SWISS-mice for immunoblotting. Astrocyte cultures were used after an incubation time of 14 days. First, we homogenized our substrate in PBS with added protease inhibitors (glass-Teflon homogenizer, 10 strokes at 900 rpm). Next, we centrifuged our homogenates at 1500×*g* for 10 min to remove the cell nuclei and diluted the remaining supernatant in Leammli buffer. We submitted it to an SDS-PAGE. After transferring the proteins from SDS-PAGE to a membrane, we washed the membrane for 1h with blocking solution and incubated it with the patient's serum diluted 1:200 in antibody solution (overnight at 4°C). Next, the membrane was washed before and after incubation with the secondary antibody (Horseradish peroxidase coupled goat anti-human kappa light chain secondary IgG, horse anti-mouse IgG, goat anti-rabbit IgG) for 1h at RT. Finally, we used enhanced chemiluminescence (GE Healthcare Europe GmbH, Freiburg, Germany), to visualize immunoreactivity. In addition to the patient's serum, we also used a mouse monoclonal anti-GFAP primary antibody (the same as used for immunofluorescence) as positive control and a negative serum from our control cohort. Protein loading was confirmed with a mouse monoclonal anti-GAPDH antibody or a rabbit polyclonal anti-Actin antibody.

2.9 Image acquisition

We used the upright Leica DMLB epifluorescence microscope and the Leica SL confocal microscope for image acquisition.

2.10 Statistics

We used Microsoft Excel 2016 for our statistical analysis. To determine the statistical significance of our findings, we used the Chi-square test and considered P- values ≤0.05 as significant.

2.11 Summary of antibodies and agents

Table 1: Summary of commercial antibodies (own representation: Paula Charlotte Barthel)

Antibody	Manufacturer
FITC- conj. goat anti-human IgG	Dianova, #109095003
Monoclonal mouse anti-GFAP	Synaptic Systems, Göttingen, Germany, #173011
Monoclonal mouse anti-MAP2	Chemicon Merck Chemicals #MAB3418
Alexa-red goat anti-mouse 594	MoBiTec, #A11032, Göttingen, Germany
Monoclonal mouse anti-glyceraldehyde-3-phosphate dehydrogenase	GAPDH, Merck Millipore, Darmstadt, Germany; #MAB374
Polyclonal rabbit anti-Actin	Sigma-Aldrich, St. Louis, MO, USA, #A5060
Horseradish peroxidase coupled goat anti- human kappa light chain secondary IgG	Life Technologies, Carlsbad, CA, USA; #A18859
Horse anti-mouse IgG and goat anti-rabbit IgG	Vector Laboratories, Burlingame, CA, USA; #PI-2000 and #PI-1000

Table 2: Summary of agents (own representation: Paula Charlotte Barthel)

Solution	Composition
NB-medium	10 ml B27; 5 ml penicillin/streptomycin (pen/strep); 1.25 ml L-glutamine; 485 ml Neurobasal Medium
N-medium	50 ml fetal calf serum (FCS); 5 ml pen/ strep; 5 ml L-glutamine; 10 mM HEPES; 1 mg/ml insulin; 44 mM glucose; 5 ml collagen G; filled

Solution	Composition
	up to 500 ml with Dulbecco's Modified Eagle Medium (DMEM)
NB-starter medium	25µl Na-glutamate (100mM); 100ml NB-medium
HEK cell medium	95ml DMEM (Gibco #41966-029); 5ml FCS superior (Biochrom #50613); 1ml PIS (Biochrom #A2213); 1ml Glutamax (Gibco #35050-038)
Blocking solution (Cells)	0.1% Triton; 5% NGS; 2.0% BSA; PBS
Secondary antibody solution (Cells)	2% BSA in PBS
Blocking solution (Brain slices)	10% NGS in PBS; 0.3% Triton-X-100
Primary antibody solution (Brain slices)	10% NGS in PBS; 0.3% Triton-X-100; 0.1% NaN_3
Secondary antibody solution (Brain slices)	5% NGS in PBS; 0.1% Triton-X-100
Blocking solution (Western blots)	5% low fat milk powder, 0.1% Tween-20 in in Tris buffer
Antibody solution (Western Blots)	1.5% BSA in Tris buffer

3 Results

3.1 General autoimmune reactivity and staining pattern

To analyze the immunoreactivity of sera from 127 dementia patients, we first performed a broad and unspecific screening for any immunoreactivity, using primary murine embryonic hippocampal/cortical cell cultures. A positive staining indicated the presence of autoantibodies in the sample and led to further testing. Our two age-matched control cohorts included 82 serum samples from the Charité Biobank from patients with various neurologic diseases except dementia and dementia-associated diseases, and 15 serum samples from individuals who accompanied the patients to the Memory Clinic and had no history of neurologic diseases.

Immunoreactivity against fixed hippocampal/cortical cell cultures was observed in 45 of 127 dementia patients, revealing three main groups of staining patterns. A summary of all staining results and general staining pattern is given in table 3 and figure 2. Autoantibodies against neurons were detected in 10 (8%) dementia patients and 4 (4.9%) patients from the biobank cohort ($p=0.40$ dementia vs. Biobank $p=0.25$ dementia vs. total controls). In dementia patients, 7 (5.5%) stained positive for neurons and astrocytes, whereas one sample from the biobank cohort was also positive ($p \leq 0.001$ dementia vs. Biobank $p \leq 0.001$ dementia vs. total controls). Autoimmunity against astrocytes was observed in 28 (22%) dementia patients and 3 (4.7%) biobank samples ($p \leq 0.001$ dementia vs. Biobank $p \leq 0.001$ dementia vs. total controls). The age-matched healthy control cohort (15 samples) showed no immunoreactivity at all.

Our study focused mainly on immunostaining on fixed cell cultures and brain sections. Using this technique, the fixation leads to the permeabilization of the cells and the exposure of intracellular antigens which can then be recognized by the applied antibodies. However, all 127 dementia serum samples were also tested with live staining on hippocampal/cortical cell cultures where antibodies against surface antigens can be detected. Three sera reacted positive in live staining, indicating the presence of autoantibodies against unspecified surface antigens in these samples (Fig.3).

Table 3: Summary of staining results (from Barthel et al., 2023)

	Dementia cohort	Charité Biobank cohort	Age-matched control cohort	P-value
Number	127	82	15	
Immunoreactivity in primary hippocampal cell culture				
Neurons, n (%)	10 (8)	4 (4.9)	0 (0)	p = 0.40 dementia vs. Biobank p = 0.25 dementia vs. total controls
Neurons and astrocytes, n (%)	7 (5.5)	1 (1.6)	0 (0)	p ≤ 0.001 dementia vs. Biobank p ≤ 0.001 dementia vs. total controls
Astrocytes, n (%)	28 (22)	3 (4.7)	0 (0)	p ≤ 0.001 dementia vs. Biobank p ≤ 0.001 dementia vs. total controls
Immunoreactivity with HEK293 cells expressing GFAP, n (%)	14 (11)	1 (1.6)	0 (0)	p = 0.007 dementia vs. Biobank p = 0.003 dementia vs. total controls

Immunocytochemical findings obtained from stainings of mixed neuronal and glial hippocampal/cortical primary cultures as well as GFAP-transfected HEK293 cells at a dilution of 1:200 (n = 127 dementia patient sera, n = 97 sera from age-matched patients or healthy subjects). Data are presented as absolute numbers and proportions. Statistical significance was verified using Chi-square test.

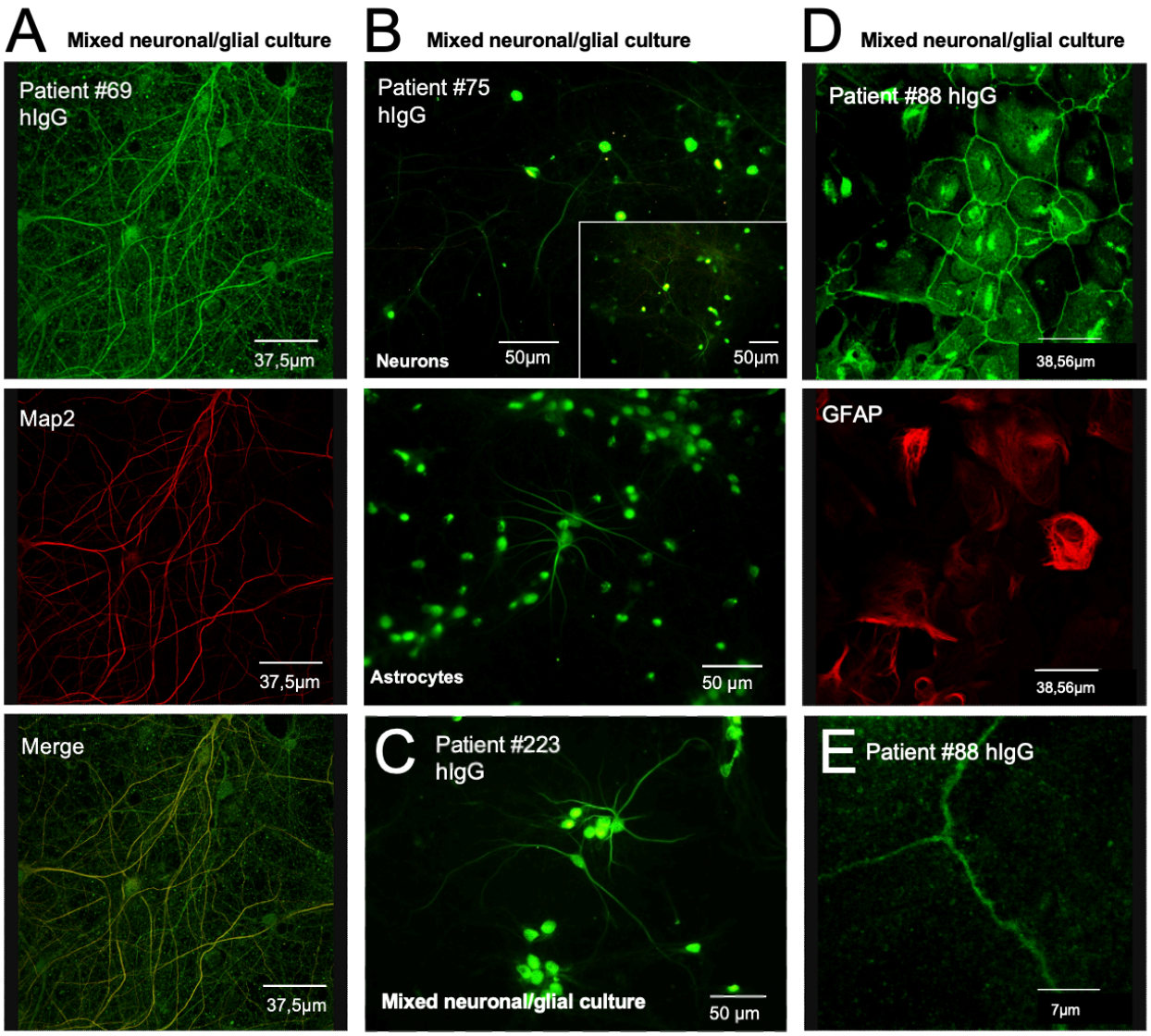

Figure 2: General staining pattern on fixed hippocampal/cortical cell cultures (own representation: Paula Charlotte Barthel)

The cells (mixed neuronal/glial culture) were fixed with 80% ice-cold methanol for 20min and then blocked and stained first with the patient's serum 1:200 and followed by an anti-human IgG secondary antibody to detect autoantibodies against brain structures. The staining revealed three main patterns: Positive sera either stained neurons, astrocytes or both. A) Confocal imaging: Serum of patient #69 had an intense neuronal staining pattern. Co-staining with a commercial anti-Map2 antibody, a marker protein for neurons, showed a high degree of overlap. B) Serum #75 stained neurons but also astrocytes in mixed culture, indicating the presence of autoantibodies against both cell types. C) A distinct astrocytic staining pattern was seen in serum #223. However, it did not react with GFAP-transfected HEK293 cells and might therefore target another unknown astrocytic antigen. D) Confocal imaging: Within the subgroup of astrocytic-positive sera, an interesting staining pattern occurred in some samples. Serum #88 is shown exemplarily, staining not only stellar astrocytes but also the cell membrane of flattened, polygonal astrocytes (confirmed

by co-staining with a commercial anti-GFAP antibody.). E) Confocal imaging: Another image of serum #88, staining the cell membrane of flattened, polygonal astrocytes.

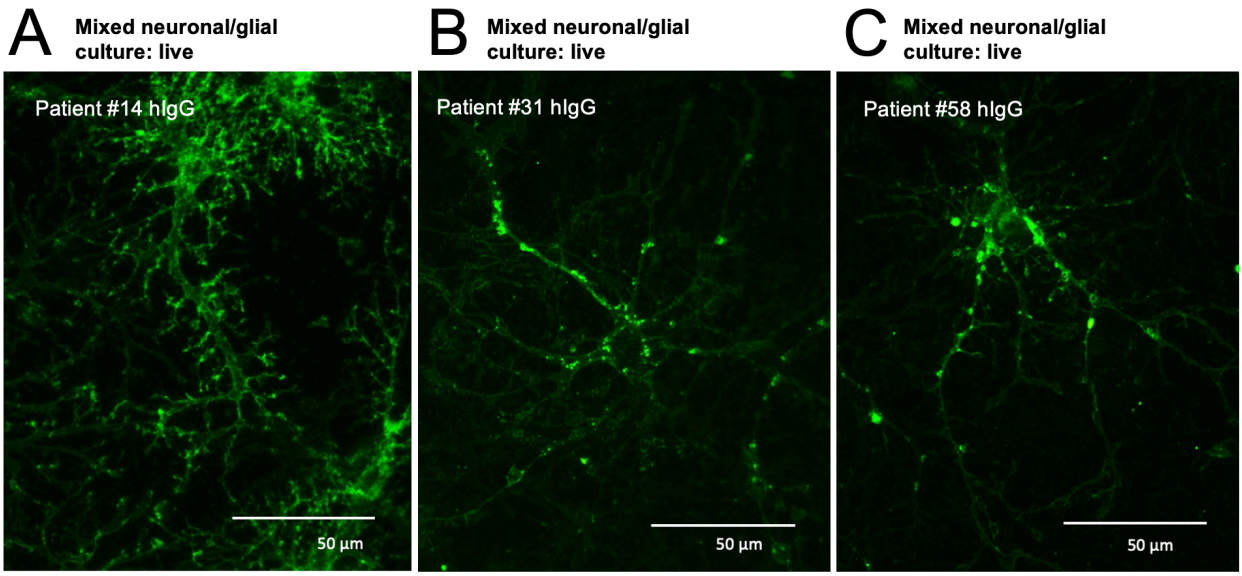

Figure 3: Results of live staining on hippocampal/cortical cell cultures (modified from Barthel et al., 2023)

The serum samples were diluted 1:200 in culture medium, added to the living cells in 24-well plates and incubated for 24h at 37°C. Afterwards, the cells were washed with PBS, fixed with 80% ice-cold methanol for 20 min and stained with the secondary antibody, following the same protocol as described for fixed cells. A) Serum #14, which also stained astrocytes on fixed cells and tested GFAP-positive on fixed HEK cells, stained an unspecified surface antigen on living cells. B) and C) Sera #31 and #58 also stained living cells in a punctured or clustered pattern.

3.2 Specific autoimmune reactivity against GFAP

Samples (n=35) which showed immunoreactivity against astrocytes on hippocampal/cortical cell cultures were further stained on HEK cells expressing GFAP, a protein which is highly expressed in astrocytes and is therefore a potential antigen. 14 sera (11%) stained positive, indicating the presence of autoantibodies against GFAP in these samples. One sample (1.6%) from the biobank cohort was also positive for GFAP autoantibodies. Again, the healthy age-matched control cohort was completely negative ($p = 0.007$ dementia vs. Biobank; $p = 0.003$ dementia vs. total controls). A follow-up after 16 to 22 months was available for three dementia patients. Staining on GFAP-expressing HEK cells as well as staining on hippocampal/cortical cell cultures was still positive in all patients. Additional

experiments, including staining on astrocyte cultures, murine brain sections and Western Blots were performed for the 14 GFAP-positive samples. As described above, all GFAP-positive sera reacted positive when stained on primary murine embryonic hippocampal/cortical cultures, which contain astrocytes resembling their typical, ramified in vivo morphology. Serum #2 reacted with ramified astrocytes in purified astrocyte culture and serum #9 also co-stained isolated, flattened, polygonal astrocytes, usually expressing lower levels of GFAP (Fig. 7A/4G). Serum #11 and #13 stained astrocytes on fixed murine brain sections, especially in the corpus callosum and olfactory bulb (Fig. 5D). When co-stained with commercial GFAP antibodies, all sera showed co-localization. Seven of the 14 GFAP-positive sera (#1; #3; #4; #6; #9; #13; #14), were positive in Western Blots obtained from hippocampal/cortical cell cultures or astrocyte cultures. They showed a positive band between 50 and 55 kDa, corresponding to the molecular weight of GFAP (Figs. 4/6). Representative (co-)stainings, Western blots and MRI-images for GFAP-positive patients are shown in figure 4-7.

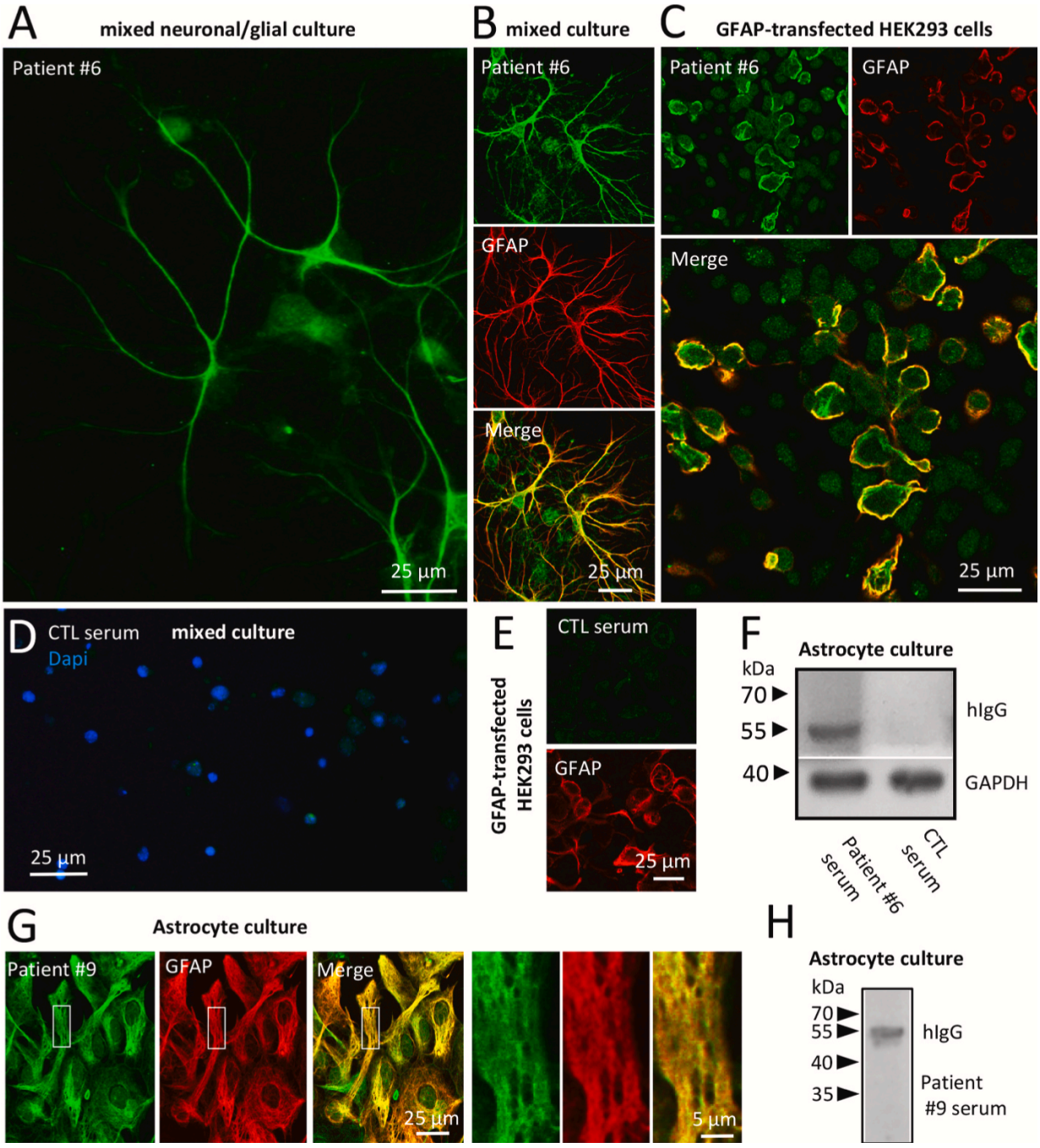

Figure 4: Serum autoantibodies against glial fibrillary acidic protein (GFAP) in two patients with Alzheimer's disease (from Barthel et al., 2023)

A) Patient serum #6 intensely stained large, branched cells that morphologically appeared like astrocytes in mixed embryonic hippocampal/cortical cultures. B) Patient serum antibodies co-localize with GFAP in cultured astrocytes. Cultures were double stained for human IgG and commercial monoclonal GFAP antibody. Both signals stained filament-like structures in stellate astrocytes and showed a high degree of overlap in the soma and astrocytic processes. Confocal imaging C) Patient serum antibodies react with GFAP-transfected HEK293 cells. HEK293 cells were transfected with a human GFAP plasmid. Only transfected cells reacted with patient IgG and

signals showed a high degree of overlap with commercial GFAP staining. Confocal imaging D) Mixed embryonic hippocampal/cortical cultures were incubated with a serum from a 73-year old healthy control. No staining occurred. E) Likewise, control serum did not show any immunoreactivity to GFAP-transfected HEK cells. F) Purified astrocyte cultures were subjected to Western blotting and probed with patient serum and an age-matched control serum. For loading control, glyceraldehyde 3-phosphate dehydrogenase (GAPDH) was used. Incubation with patient serum resulted in a single immunoreactive band at around 55 kDa, corresponding to the expected molecular weight of GFAP. Control serum yielded no staining. G) Purified astrocyte cultures were fixed and double stained for binding of IgG from another patient (patient #9) and GFAP, thereby showing a high degree of overlap (see insets). H) In line with this, autoantibodies of patient #9 show a major immunoreactive band at around 55 kDa in Western blots. Reactivity to GFAP was verified using HEK293 cells transfected with human GFAP (not shown).

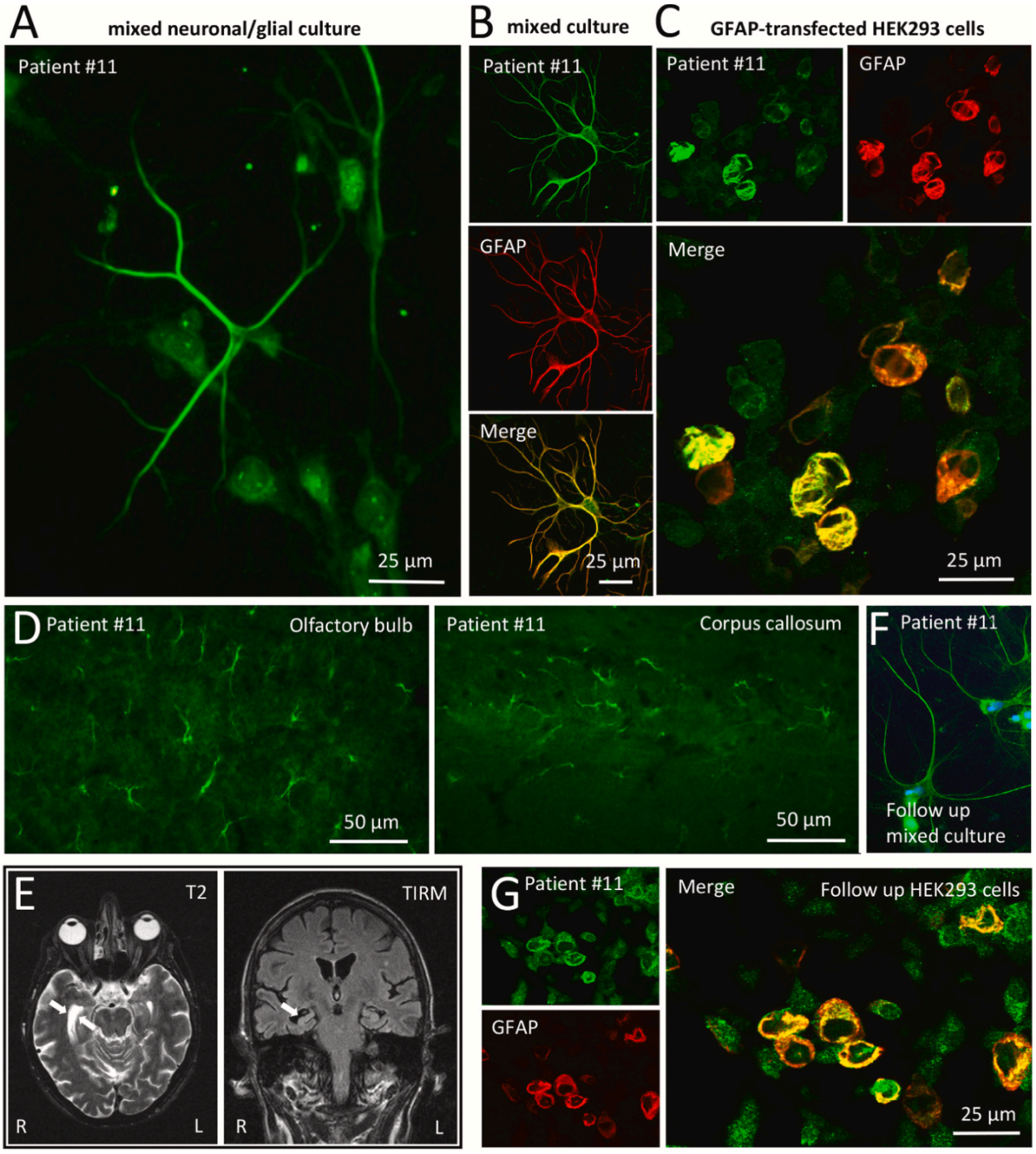

Figure 5: Follow-up evaluation of serum autoantibodies against glial fibrillary acidic protein (GFAP) in a patient with Alzheimer's disease (from Barthel et al., 2023)

A) Patient serum #11 intensely stained large, branched cells that morphologically appeared like astrocytes in mixed embryonic hippocampal/cortical primary cultures. B) Patient serum antibodies co-localize with GFAP in cultured astrocytes. Cultures were double stained for human IgG and GFAP. Both signals stained filament-like structures in stellate astrocytes and showed a high degree of overlap in the soma and astrocytic processes. Confocal imaging C) Patient serum antibodies react with GFAP-transfected HEK293 cells. Only transfected cells reacted with patient IgG and signals showed a high degree of overlap with commercial GFAP staining. Confocal imaging

D) Astrocyte staining by patient autoantibodies in brain sections. Patient serum #11 stained astrocytes in various brain areas, being most prominent in the olfactory bulb and Corpus callosum. E) Axial and coronal MRIs (T2 and turbo inversion recovery magnitude sequence) of patient #11 demonstrate moderate decrease in brain volume with right mesiotemporal emphasis (arrows). F) Follow up test for the presence of autoantibodies to GFAP in mixed cortical/hippocampal cultures and transfected HEK293 cells. Patient serum was collected again 18 months after first testing and used in the described detection assays. Recurrently, stellate astrocytes were stained in the primary culture and only GFAP-transfected cells HEK293 reacted with patient IgG and both signals showed a high degree of overlap.

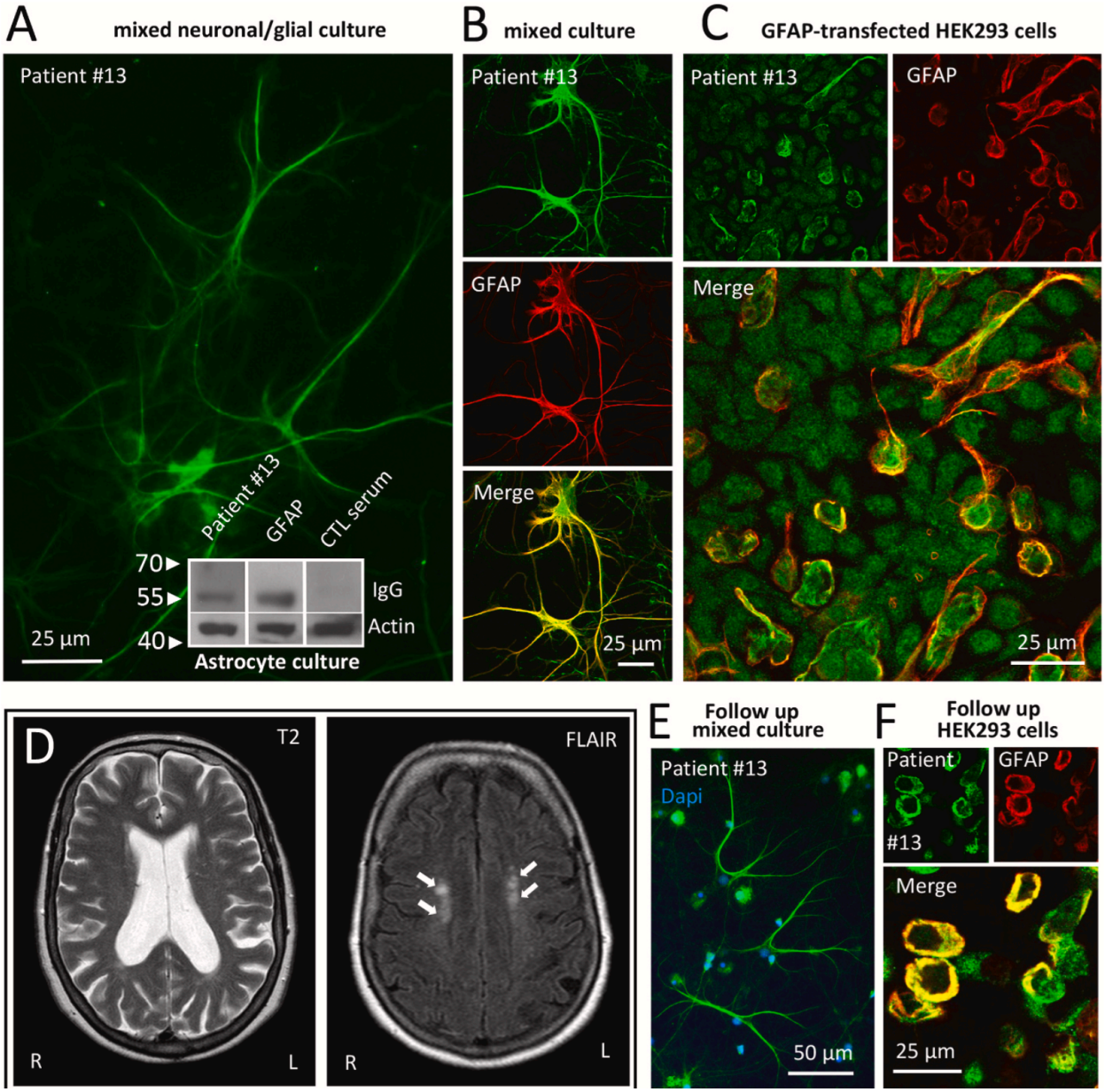

Figure 6: Follow-up evaluation of serum autoantibodies against glial fibrillary acidic protein (GFAP) in another patient with Alzheimer's disease (from Barthel et al., 2023)

A) Patient serum #13 intensely stained large, branched cells that morphologically appeared like astrocytes in mixed embryonic hippocampal/cortical cultures. Inset: Biochemical evaluation showed that incubation with patient serum resulted in a single immunoreactive band at around 55 kDa in purified astrocyte culture corresponding to commercial GFAP staining. Control serum yielded no staining. B) Patient serum antibodies co-localize with GFAP in astrocytes of mixed cultures. Cultures were double stained for human IgG and GFAP. Both signals stained filament-like structures in stellate astrocytes and showed a high degree of overlap in the soma and astrocytic processes. Confocal imaging C) Patient serum antibodies react with GFAP-transfected HEK293 cells. Only transfected cells reacted with patient IgG and signals showed a high degree of overlap with commercial GFAP staining. Confocal imaging D) Axial MRIs (T2 and fluid-attenuated inversion recovery sequence) of patient #13 demonstrate mild to moderate frontoparietal atrophy with corresponding enlargement of the lateral ventricles and periventricular white matter lesions (arrows). E) Follow up test for the presence of autoantibodies to GFAP in mixed cortical/hippocampal cultures and transfected HEK293 cells. Patient serum was collected again 22 months after first testing and used in the described detection assays. Recurrently, stellate astrocytes were stained in the primary culture and only GFAP-transfected cells HEK293 reacted with patient IgG and both signals showed a high degree of overlap.

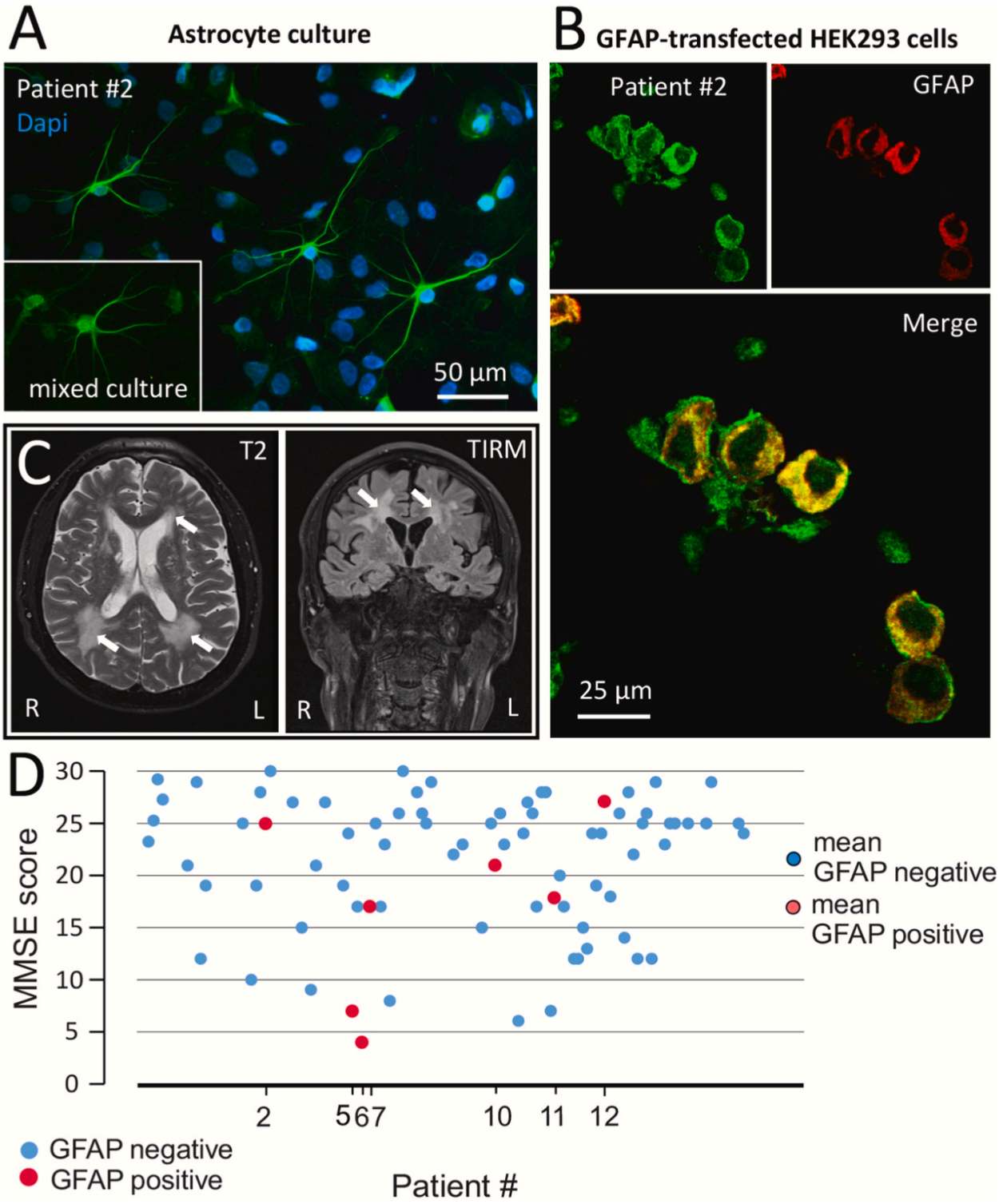

Figure 7: Serum autoantibodies against glial fibrillary acidic protein (GFAP) in a patient with Cerebral Amyloid Angiopathy (from Barthel et al., 2023)

A) Patient serum #2 intensely stained mainly large stellate astrocytes in purified astrocyte cultures. Polygonal flattened cells were only weakly stained. Inset: Patient serum also recognized astrocytes in mixed neuronal/glial cultures. B) Patient serum antibodies react with GFAP-transfected HEK293 cells. Only transfected cells reacted with patient IgG and signals showed a high degree of overlap with commercial GFAP staining. Confocal imaging C) Axial and coronal MRIs

(T2 and turbo inversion recovery magnitude sequence) of patient #2 demonstrate marked ubiquitously occurring white matter gliosis (arrows). D) Cognitive screening by Mini Mental State Examination (MMSE) was available for a total of 79 dementia patients. Blue dots indicate GFAP-negative patient sera, red dots indicate 7 screening scores available for GFAP-positive patients. Mean values are indicated on the right.

3.3 Clinical and paraclinical findings

Our study included patients with any form of mild cognitive impairment or dementia without any additional exclusion criteria. Demographic data for the dementia cohort and the control cohorts is shown in table 4. The dementia cohort included 127 patients, 56 (44%) of them were female and 71 (56%) male. The most common diagnosis was Alzheimer's disease (n=59; 46%), followed by mild cognitive impairment (n= 24; 19%) and frontotemporal dementia (13; 10%). Mean age at blood draw was 73.8 years (± 9.4y SD), 73.0 years (± 9.3y SD) for females and 74.6 (± 9.6y SD) for males. The Charité Biobank cohort included 44 (53.7%) females and 38 (46.3%) males. Mean age at blood draw was in total 70.8 years (± 7.7y SD), 70.8 years (± 7.0y SD) for females and 70.9 (± 8.5y SD) for males. The second control cohort with 15 healthy subjects included 9 (60%) females and 6 (40%) males. Mean age at blood draw was in total 75.8 years (± 5.1y SD), 75.9 years (± 5.4y SD) for females and 75.7 (± 4.6y SD) for males.

Table 4: Demographic data of dementia cohort and control cohorts (from Barthel et al., 2023)

A) Dementia cohort.

Mean ± SD age at blood draw N = 127		**Sex**		**Sex %**	**Type of dementia**		**Type of dementia %**
73,8 ± 9,4		female	56	44	AD	59	46
female	male	male	71	56	MCI	24	19
73,0 ± 9,3	74,6 ± 9,6				FTD	13	10
					SAE	11	9

A) Dementia cohort.

Mean ± SD age at blood draw N = 127	Sex	Sex %	Type of dementia		Type of dementia %
			SAE/AD	10	8
			LBD/PD	6	5
			CAA	4	3

B) Charité CSF/serum Biobank cohort

Mean ± SD age at blood draw N = 82		Sex		Sex %
70, 8 ± 7,7		female	44	53,7
female	male	male	38	46,3
70,8 ± 7,0	70,9 ± 8,5			

C) Healthy subjects

Mean ± SD age at blood draw N = 15		Sex		Sex %
75,8 ± 5,1		female	9	60
female	male	male	6	40
75,9 ± 5,4	75,7 ± 4,6	Mean MMST ± SD 29 ± 0,6/30		

A) Demographic and dementia type data of the 127 patients analyzed in this study. Data are given in absolute numbers and proportions. AD = Alzheimer's disease; MCI = mild cognitive impairment; FTD = frontotemporal dementia; SAE = subcortical arteriosclerotic encephalopathy; LBD = Lewy body dementia; PD=Parkinson's disease dementia; CAA = cerebral amyloid angiopathy B, C) Demographic data of the two age-matched cohorts used for control. Neuropsychological testing was available for the 15 healthy subjects.

The patients were diagnosed with dementia in the Charité Memory Clinic, based on clinical and neuropsychological evaluation, laboratory findings and imaging studies. A summary of this data is shown in table 5 for the 14 GFAP-positive dementia patients in comparison with the GFAP-negative dementia patients. Regarding clinical and neuropsychological evaluation, results of Mini Mental Status Evaluation (MMSE) were available for seven GFAP-positive and 72 GFAP-negative patients and the 15 healthy subjects.

MMSE-scores between GFAP-positive and GFAP-negative patients are visualized in figure 7D. Laboratory testing focused on the parameters that are included in the standard diagnostics for dementia and are usually abnormal in dementia patients. This was also the case in our dementia patients (GFAP-positive and GFAP-negative patients): Values for pTau(181), total tau and total protein count (TPC) were increased and the values for Amyloid-beta (1–42) and beta-Amyloid ratio 42/40 were decreased. We found no statistically significant difference in any parameter between GFAP-positive and GFAP-negative patients. Only Amyloid-beta (1–42) and beta-Amyloid ratio 42/40 was reduced in GFAP-positive patients compared with GFAP-negative patients, but this finding was not statistically significant. Screening for co-existing autoantibodies was positive for three GFAP-positive patients. Autoantibodies were directed against Rho GTPase-activating protein, myelin and, in one patient, a yet unknown surface antigen. Exemplary MRI imaging results for four GFAP-positive patients are shown in figure 5-7. They revealed pathologies that were consistent with their dementia diagnosis, for example atrophy (seven patients) and medullary gliosis (six patients).

In summary, the results of our study revealed a high prevalence of autoantibodies in patients with dementia which is statistically significantly higher than the frequency of autoantibodies in patients with various neurologic diseases except dementia and healthy individuals. Focusing on GFAP as a specific antigen, the prevalence was once again statistically significantly higher in dementia patients than in our control groups. Clinical and paraclinical data did not significantly differ between GFAP-positive and negative dementia patients.

Table 5: Demographical data, dementia type, secondary diagnoses, neuropsychological testing and laboratory findings of 14 GFAP-positive patients (from Barthel et al., 2023)

Patient ID	Age at blood draw	Sex	Type of dementia	Secondary diagnosis	Coexisting Autoantibodies	MMSE	pTau(181)	Total-Tau	Aβ (1–40) [pg/ml]	Aβ (1–42) [pg/ml]	Aβ Ratio	TPC (mg/l)
1	54	m	FTD		negative							
2	73	m	CAA	s/p ICH (2018)	anti-Rho GTPase-activating protein	25/30	91	839.18	11245	502	0.45	608.3
3	79	m	AD	Suspicion of NPH (2017)	negative		62	297.42	29962	537	0.18	809.5
4	61	f	AD	APP gene mutation (c2149 G > A); Epilepsy	negative							301
5	78	m	AD	s/p CRC	negative	7/30	136	1200.97	13213	483	0.37	525.8
6	67	m	AD		anti-myelin	4/30						
7	78	m	AD/SAE	s/p AIS (2012)	n.d.	17/30	31	227.34	7904	557	0.71	410.7

Patient ID	Age at blood draw	Sex	Type of dementia	Secondary diagnosis	Coexisting Autoantibodies	MMSE	pTau(181)	Total-Tau	Aβ (1–40) [pg/ml]	Aβ (1–42) [pg/ml]	Aβ Ratio	TPC (mg/l)
8	79	m	AD	s/p TIA (2017); s/p SAH (2017); RA	negative							
9	82	m	AD	Movement disorder; Lung tumor	negative		136	949	13485	699	0.52	389
10	74	m	AD	HBP, nicotine abuse; T2D	negative	21/30						593.7
11	75	f	AD		n.d.	18/30	73	535.29	17751	575	0.32	306.6
12	78	f	MCI	Suspicion of NPH (2016); organic depression disorder DDX anxiety disorder; s/p CRC	negative	27/30	100	519.8	23683	987	0.42	448.2
13	76	f	AD		negative		54	527	10467	539	0.51	504.6
14	54	f	FTD		unknown surface antigen							

Patient ID	Age at blood draw	Sex	Type of dementia	Secondary diagnosis	Coexisting Autoantibodies (this study)	MMSE	pTau(181)	Total-Tau	Aβ (1–40) [pg/ml]	Aβ (1–42) [pg/ml]	Aβ Ratio	TPC (mg/l)
Mean GFAP+	72±9					17/30±8.0	85±35	637±311	15963±6981	610±155	0.44±0.14	489,7 ±146,9
Mean GFAP–	74±9,4					22/30±6.3	81±40	617±422	15566±7682	756±361	0.72±1.1	508,07 ±211,47

Means are given and compared to GFAP-negative patients. Laboratory findings were available for 8 GFAP-positive and 53–69 (parameter-depending) GFAP-negative patients. GFAP-positivity was verified by transfected HEK293 cells. AD = Alzheimer's disease; AIS = androgen insensity syndrome; CAA = cerebral amyloid angiopathy; CRC = colorectal cancer; FTD = frontotemporal dementia; HBP = high blood pressure; ICH = intracerebral hemorrhage; MCI = mild cognitive impairment; NPH = normal pressure hydrocephalus; RA = rheumatoid arthritis; SAE = subcortical arteriosclerotic encephalopathy; SAH = subarachnoid hemorrhage; TIA = transient ischemic attack; T2D = type 2 diabetes; TPC = total protein count.

4 Discussion

4.1 Summary

We screened sera from 127 dementia patients and two age-matched control cohorts for the presence of autoantibodies against brain structures, using a successive screening strategy, with staining on primary murine embryonic hippocampal/cortical cell cultures being the first step. A positive staining result, indicating the presence of any autoantibodies, led to further testing. Immunoreactivity against hippocampal/cortical cell cultures was observed in 45 of 127 dementia patients, either against neurons (n=10; 8%), astrocytes (n=28; 22%), or both (n=7; 5.5%). Overall immunoreactivity, as well as reactivity against the specific cell types was statistically significantly more frequent in the dementia cohort than in the two control cohorts. We were able to identify GFAP as specific antigen in 14 (11%) of the dementia samples that previously stained astrocytes in hippocampal/cortical cell culture. Again, the results for autoreactivity against GFAP were statistically significant. Clinical and paraclinical data of GFAP-positive dementia patients did not differ statistically significantly from GFAP-negative dementia patients.

4.2 Interpretation and correlation with the current research state

The immunoreactivity against brain structures, especially against GFAP, which occurs significantly more often in dementia patients than in age-matched controls, raises questions about the significance of these autoantibodies. Why do patients with dementia develop autoantibodies, and what are the underlying immunological mechanisms? Do the autoantibodies occur as a secondary phenomenon caused by the dementia defining neurodegeneration and/or are they directly pathogenic, causing or contributing to the disease course?

4.2.1 General immunological mechanisms and risk factors

The complex immunological mechanisms which cause autoimmunity against various brain structures and result in manifold symptoms are an important focus of ongoing research but still only partially understood. Highly simplified, possible mechanisms include central and peripherally dysfunctional B cell tolerance which fails to negatively select autoreactive B cells during their maturation. T cell assistance plays an important role in the

activation process of autoreactive B cells and some autoimmune diseases are also mediated by cytotoxic T cells. These autoreactive B cells may become activated by certain proteins that are expressed e.g. by tumors or following virus-induced cell death. Placing the focus on dementia, neurodegeneration could also be an important trigger in this process (25).

4.2.1.2 Autoantibodies and dementia related to COVID-19

One of the most important risk factors for autoimmune encephalitis are infections. Since 2019, COVID-19 is especially relevant in this context and consequently also for autoimmune dementia (15), (16). Therefore, this topic is exemplarily discussed here and was investigated as part of the present MD/PhD thesis (60). Our study investigated the antibody repertoire of patients with COVID-19. We derived 598 monoclonal antibodies (mAbs) from ten patients' sera and investigated e.g. their virus-neutralizing capacity, crystal structure and in vivo efficiency in a COVID-19 hamster model. We found 40 mAbs that had strong virus-neutralizing potential and selected the strongest for in vivo evaluation where we could show that the prophylactic or therapeutic application of this antibody protects infected hamsters from COVID-19-induced lung pathology and weight loss. Interestingly, we found that, in addition to virus-neutralizing antibodies, patients also had autoantibodies. We further investigated these autoantibodies, using immunohistochemical staining on unfixed murine brain, lung, heart, liver, kidney and gut tissue. Additional assays included immunocytochemical staining on primary murine embryonic hippocampal/cortical cell cultures. This revealed various autoreactive binding patterns e.g. against hippocampal neuropil, bronchial, vascular and intestinal walls (60). To this point, the pathological relevance of these autoantibodies remains unclear but, given what we already know in terms of autoimmune encephalitis, it seems plausible that autoimmunity is one of many factors that contribute to the disease. Another study tested serum and CSF from 11 critically ill COVID-19 patients with neurologic symptoms for the presence of autoantibodies. They found that all patients had autoreactivity in serum or CSF. Some had known autoantibodies e.g. against the NMDA receptor, while many had previously undescribed autoantibodies that reacted with yet unknown neuronal, glial or endothelial epitopes. The authors stated that their finding might suggest a causal relationship between the development of autoantibodies and symptoms and may indicate these patients would benefit from immunotherapy (16). There are also studies investigating the relationship between cognitive impairment, neurodegeneration, autoimmunity and COVID-19.

One of them found serum or CSF autoantibodies in 52% of 50 patients with self-reported cognitive impairment in post-COVID-19 syndrome. The presence of antineuronal autoantibodies in CSF was strongly associated with objective cognitive impairment measured by an abnormal MOCA-assessment (61). Given the fact that dementia is a chronic, usually slowly progressing disease, long-time-effects of COVID-19 will become apparent in the coming years and are an important topic for future research.

4.2.2 Pathogenic relevance

The pathogenic relevance of GFAP autoantibodies specifically whether they are primarily causing the disease or are a secondary phenomenon, was investigated by studies with heterogenous results.

Autoantibodies against GFAP are known to occur in patients with GFAP astrocytopathy, an autoimmune neurologic disease that was first described in 2016 (44). Patients typically present with acute or subacute meningomyeloencephalitis, suffering from symptoms including fever, headache, ataxia, tremor, optic papillitis, seizure or psychosis (45), (46), (47). However, there are some cases in the literature where patients with GFAP autoantibodies had atypical symptoms. Regarding dementia, some case reports mention patients presenting with rapid progressive dementia or primary progressive aphasia (58), (62). The pathogenesis behind GFAP astrocytopathy is not fully understood, but current research indicates that the disease is most likely T cell mediated; the autoantibodies against GFAP likely occur as a secondary phenomenon and are not directly pathogenic themselves (50), (51), (46).

Important for that hypothesis is the fact that GFAP is an intracellular antigen. In our study, the rate of immunopositivity was by far higher when the samples were stained on fixed cells and brain sections that expose intracellular antigens than with live staining that detects autoantibodies against surface antigens. Regarding the knowledge about autoimmune encephalitis, autoantibodies against extracellular antigens are more likely to be directly pathogenic, as shown for NMDAR autoantibodies (17), than autoantibodies against intracellular antigens. There are not only autoantibodies against neuronal surface proteins but also against astrocytic surface antigens, for example, autoantibodies against the Aquaporin-4 water channel which is expressed on the surface of astrocytes. They are directly pathogenic, activating the complement cascade in a complex autoimmune reaction that involves various immune cells, cytokines and a disrupted blood-brain barrier. This process damages astrocytes and consequently also disrupts neuronal function (63),

(64). Nevertheless, some autoantibodies against intracellular antigens are also known to be pathogenic, for example, autoantibodies against synapsin which become internalized by FcγII/III-mediated endocytosis in neuronal cell culture and therefore can reach their target, causing synaptic dysfunction (21).

In addition to the fact that GFAP is an intracellular antigen, there are other studies and aspects that support the hypothesis that GFAP autoantibodies are a secondary phenomenon and not directly pathogenic themselves. A study investigating the clinical and radiological characteristics of 59 patients with GFAP autoantibodies in CSF or serum, presenting with the typical phenotype of mengingomyeloencephalitis, came to the hypothesis that the present GFAP autoantibodies are a non-specific, secondary phenomenon, caused by inflammation of the nervous system (47).

Autoantibodies against GFAP with unknown relevance also occur in other neurologic diseases like traumatic brain injury or epilepsy (65), (66). In our study, GFAP autoantibodies were significantly more common in the dementia cohort than in the Charité Biobank cohort that included patients with various neurologic diseases except dementia. However, one patient with motor neuron disease was also positive for GFAP autoantibodies. These findings might support the hypothesis that GFAP autoantibodies are a secondary phenomenon due to brain injury or neurodegeneration, not only in a subgroup of dementia patients, but also in other neurologic diseases.

However, our findings showed that GFAP autoantibodies do not occur equally in all neurologic diseases. Instead, there seem to be some diseases in which a subgroup of patients develops GFAP autoantibodies. Further research is needed to compare patients with different diseases which share GFAP autoantibodies as a common denominator.

Interestingly, autoantibodies against GFAP frequently occur together with co-existing autoantibodies, for example NMDAR autoantibodies (48). Accordingly, co-existing autoantibodies were also present in three of our GFAP-positive dementia patients. Some of these co-existing autoantibodies might be considered as pathogenic, whereas the pathogenicity of GFAP autoantibodies in unclear. In these cases, it might be even more challenging to distinguish the possible pathogenic effects of each single type of autoantibody. The experimental production of monoclonal antibodies, as shown e.g. for NMDAR autoantibodies, can be helpful to address this issue (17).

Regarding the alternative hypothesis that GFAP autoantibodies are directly pathogenic, a study investigating GFAP autoantibodies in patients with traumatic brain injury found

that these antibodies can enter living astrocytes, indicating a possible pathogenic effect (65).

The discovery of Anti-IgLON5 disease provided an interesting link between autoimmunity and neurodegeneration. The disease course is heterogenic but, in most patients, the disease onset is either subacute or chronic and slowly progressive. In addition to the characteristic parasomnia, typical symptoms include dysautonomia, movement disorder, bulbar syndrome and cognitive decline (67). Interestingly, Anti-IgLON5 disease features both aspects of an antibody mediated autoimmune encephalitis but also of a neurodegenerative disease. Postmortem pathological analysis showed characteristic tau-deposits, typically in the hypothalamus and brainstem, associated with an atypical tauopathy (68). However, inflammatory changes and immune activation are also often seen in early stages of the disease (69), (70). Treatment response to immunotherapy was heterogenous in different studies (67). The antibodies were first thought to be a secondary phenomenon due to the reported neurodegeneration, but further experimental findings supported the hypothesis that the autoantibodies are primary pathogenic themselves. In vitro and in vivo experiments provided evidence that Anti-IgLON5 autoantibodies are pathogenic, e.g. causing cell damage in neuronal cultures, tau-deposition and cognitive impairment in mouse models (71), (72), (73). To date, the exact disease mechanisms and the link between autoantibody-mediated inflammation and tauopathy are not fully understood. The authors of a recent review hypothesized that the IgLON5 autoantibodies are the primary cause of the disease and initiate an inflammation cascade that leads to tau- deposition later in the disease (67). Taken together, the Anti-IgLON5 disease is a prototype for a disease were autoimmunity and neurodegeneration are closely related. This finding is highly relevant when talking about the interaction between other antibodies, in this case GFAP, and neurodegenerative diseases.

Even if autoantibodies, including the ones against GFAP, might not be the primary cause of dementia in this subgroup of patients, they might still be pathogenic and secondarily contribute to disease progression.

Another possibility could be that GFAP autoantibodies in dementia, in analogy to classic GFAP astrocytopathy, are a hallmark of an underlying, possibly T cell-mediated process that causes the disease and might be susceptible to immunosuppressive therapy.

4.3 Strengths and weaknesses of the study

4.3.1 Screening strategy

In the present study, we systematically screened a large cohort of patients with dementia. This strength allowed us to identify a subgroup of patients who were autoantibody-positive and to detect statistically significant differences in autoantibody-positivity and staining pattern between the dementia patients and our control cohorts. We were even able to identify a GFAP as a specific target in a subgroup of 14 dementia patients. Our systematical screening consisted of diverse methods used in a specific order. The decision to perform immunocytochemistry on primary murine embryonic hippocampal/cortical cell cultures as a first, broad screening enabled us to identify patients with diverse, undefined autoantibodies that might have been missed by other methods like specific laboratory assays that could only screen for specific, already known autoantibodies. The following steps of our screening strategy further characterized the previously undefined autoantibodies and lead to the successful identification of GFAP as a specific antigen.

4.3.2 Focus on autoantibodies in serum

The clinical and presentation of our patients was obviously different than in patients with classic GFAP astrocytopathy. Instead of presenting with an acute meningomyeloencephalitis, all our patients had chronic progressive symptoms according to their dementia diagnosis. In most studies, the diagnosis of GFAP astrocytopathy is made based on the presence of autoantibodies in CSF. However, there were patients which had GFAP autoantibodies in serum but not in CSF. In these cases, they were more likely to have an atypical presentation of GFAP astrocytopathy (48). Our study is limited by the fact that we only focused on autoantibodies in serum but not in CSF. Therefore, our results cannot be interpreted analogue to patients with classic, CSF-positive GFAP astrocytopathy. Instead, serum GFAP-positivity might define a subgroup of dementia patients with so far unclear pathophysiological relevance.

4.3.2.1 Autoantibodies against the blood-brain barrier

The occurrence of autoantibodies only in serum, only in the CSF or in both as well as the underlying (patho-)mechanisms behind this finding is highly relevant, not only for our cohort, but also for diverse other autoimmune neurologic disorders. A specific aspect that should be highlighted here concerns autoantibodies against the blood-brain barrier. This

topic is discussed in a study that is part of the present MD/PhD-thesis (22). Here, we investigated the monoclonal autoantibody repertoire from six patients with NMDAR or GABAR autoimmune encephalitis. Besides the known autoantibodies against either NMDAR or GABAR, the patients also had various other autoreactive antibodies, including six autoantibodies that reacted with blood vessels on murine brain sections. Myosin-X was identified as target of one autoantibody. Functional experiments using an in vitro blood-brain barrier model with hCMEC/D3 – cells and in vivo intrathecal antibody injection in mice revealed pathogenic effects. This study showed that patients develop autoantibodies against blood vessels that disrupt the function of the blood-brain barrier and might be a disease mechanism in autoimmune encephalitis (22). Consequently, these autoantibodies might also play a role in autoimmune dementia, causing a leakage of the blood-brain barrier that allows autoantibodies to cross the barrier between serum and CSF.

4.3.3 Clinical and paraclinical data

Patients with GFAP astrocytopathy, as well as patients with autoimmune dementia, as described by Flanagan et al. (7), improve with immunotherapy. Recent case reports also mentioned patients with rapid progressive dementia who tested positive for GFAP autoantibodies and responded to immunotherapy (58). Our patients were diagnosed with a “classic form” of neurodegenerative dementia and had no reported red flags that would have questioned that diagnosis or indicate autoimmune dementia. Therefore, a limitation of our study is that the current knowledge about patients like the ones in our cohort is not enough to justify an immunosuppressive therapy. It is still a challenge to identify dementia patients who could potentially benefit from these therapies.

We found no statistically significant differences in clinical of paraclinical data between GFAP-positive and GFAP-negative dementia patients. These findings might be limited because our sample size was not big enough to detect possible differences.

Serum for follow-up was available for three GFAP-positive patients. All three were still positive for GFAP autoantibodies after 16 to 22 months, indicating that autoantibody-positivity is a persistent phenomenon. Although the three remained positive for GFAP autoantibodies, it would have been interesting to follow-up more patients and investigate other parameters, for example possible changes in the antibody titer and their correlation with the progression in clinical and paraclinical presentation. Studies that follow-up more patients over a longer period would be helpful to further characterize clinical findings in autoantibody-positive patients.

4.4 Implications for clinical practice and further research

In clinical practice, screening for autoantibodies is mostly conducted by standardized laboratories using panels that can detect autoantibodies against specific, already known antigens. So, this method is limited and might produce false negative results in patients that have autoantibodies against antigens that are not known yet and are not covered by the panel. In a research context, like in our study, broader screening methods could be used to identify unknown autoantibodies. Therefore, which diagnostic methods are appropriate in clinical practice need to be discussed. Right now, testing for autoantibodies is not included in the standard diagnostic process for dementia. However, authors recommend testing for autoantibodies in serum and CSF in certain cases in which “red flags” like acute or subacute disease onset, rapid progressing dementia, fever or headache, young age, co-existing autoimmune or oncologic disease, unusual neurologic symptoms e.g. seizures suggest an autoimmune dementia (26), (27).

Our study showed that autoantibodies are also present in a cohort of patients that were diagnosed with various forms of dementia and were not suspected to have autoimmune dementia. Right now, the clinical relevance of these autoantibodies is unclear, and our findings alone cannot justify treatment decisions in clinical practice.

Regardless of their pathogenicity, GFAP autoantibodies, like NMDAR autoantibodies, and even GFAP protein levels in serum of patients with Alzheimer´s disease might be candidates for diagnostic or prognostic markers in patients with dementia (74), (33), (42), (43). However, further research is necessary to ascertain their potential in clinical diagnostics.

Depending on what future research shows, drug trials would also be interesting and could have great impact for a subgroup of dementia patients. However, these trials must respect the fact that, in most cases, dementia is a slowly progressing, chronic disease. Unlike in acute autoimmune encephalitis or classic GFAP astrocytopathy, response to treatment would probably not occur immediately. In addition, patients in all likelihood have suffered from long-term neurodegeneration before the receiving the treatment, which would then be unlikely to completely reverse this long-term neuronal damage. Treatment success would therefore need to be defined as a halt in or even just a slowing down of disease progression. Studies would have to follow patients for a long period of time to detect these treatment effects.

5 Conclusion

In summary, we were able to fulfill the aim of our study; we expanded the current knowledge about autoimmune dementia by systematical screening of a large cohort of patients with dementia for the presence of any autoantibodies against brain structures. We successfully identified GFAP as a target structure and found that these autoantibodies occur statistically significantly more frequently in dementia patients than in our control cohort.

Therefore, we could confirm our hypotheses that autoantibodies against brain structures are present in patients with dementia and that specific antigens can be identified.

Bringing the aspects and the current knowledge about autoimmune encephalitis, autoimmune dementia and GFAP astrocytopathies together, the underlying questions about immunological mechanisms and the pathogenic relevance of autoantibodies in patients with dementia are very complex and cannot be fully answered yet. Although acute, autoimmune encephalitis and autoimmune dementia have many aspects in common, it remains unclear whether autoantibodies in dementia patients may cause a slowly progressing encephalitis, manifesting as autoimmune dementia.

Given the fact that our patients had symptoms according to their diagnosis of a neurodegenerative dementia and CSF autoantibodies could not be investigated, we could not interpret our findings in context of the classic GFAP astrocytopathy with an acute meningomyeloencephalitis phenotype. Rather, the GFAP autoantibodies might define an interesting subgroup of serum autoantibody-positive dementia patients that should be addressed by further research. Factors that may be important are e.g. the role of infections, including COVID-19 as a risk factor, functional in vitro and in vivo experiments with potential pathogenic autoantibodies as shown e.g. for Anti-IgLON5 disease and the role of the blood-brain barrier and associated autoantibodies such as autoantibodies against Myosin-X.

In a clinical perspective, following studies could for example address the role of GFAP autoantibodies as a possible useful diagnostic or prognostic marker, appropriate screening modalities for autoantibodies in dementia patients, as well as long-time follow-up for the course of clinical and paraclinical parameters and the question about the relevance of autoantibodies in serum vs. CSF. More research is needed to unravel the relevance of GFAP autoantibodies in patients with dementia and their implication for clinical practice.

References

1. Nichols E, Steinmetz JD, Vollset SE, Fukutaki K, Chalek J, Abd-Allah F, Abdoli A, Abualhasan A, Abu-Gharbieh E, Akram TT, Al Hamad H, Alahdab F, Alanezi FM, Alipour V, Almustanyir S, Amu H, Ansari I, Arabloo J, Ashraf T, Astell-Burt T, Ayano G, Ayuso-Mateos JL, Baig AA, Barnett A, Barrow A, Baune BT, Béjot Y, Bezabhe WMM, Bezabih YM, Bhagavathula AS, Bhaskar S, Bhattacharyya K, Bijani A, Biswas A, Bolla SR, Boloor A, Brayne C, Brenner H, Burkart K, Burns RA, Cámera LA, Cao C, Carvalho F, Castro-de-Araujo LFS, Catalá-López F, Cerin E, Chavan PP, Cherbuin N, Chu D-T, Costa VM, Couto RAS, Dadras O, Dai X, Dandona L, Dandona R, De la Cruz-Góngora V, Dhamnetiya D, Dias da Silva D, Diaz D, Douiri A, Edvardsson D, Ekholuenetale M, El Sayed I, El-Jaafary SI, Eskandari K, Eskandarieh S, Esmaeilnejad S, Fares J, Faro A, Farooque U, Feigin VL, Feng X, Fereshtehnejad S-M, Fernandes E, Ferrara P, Filip I, Fillit H, Fischer F, Gaidhane S, Galluzzo L, Ghashghaee A, Ghith N, Gialluisi A, Gilani SA, Glavan I-R, Gnedovskaya EV, Golechha M, Gupta R, Gupta VB, Gupta VK, Haider MR, Hall BJ, Hamidi S, Hanif A, Hankey GJ, Haque S, Hartono RK, Hasaballah AI, Hasan MT, Hassan A, Hay SI, Hayat K, Hegazy MI, Heidari G, Heidari-Soureshjani R, Herteliu C, Househ M, Hussain R, Hwang B-F, Iacoviello L, Iavicoli I, Ilesanmi OS, Ilic IM, Ilic MD, Irvani SSN, Iso H, Iwagami M, Jabbarinejad R, Jacob L, Jain V, Jayapal SK, Jayawardena R, Jha RP, Jonas JB, Joseph N, Kalani R, Kandel A, Kandel H, Karch A, Kasa AS, Kassie GM, Keshavarz P, Khan MAB, Khatib MN, Khoja TAM, Khubchandani J, Kim MS, Kim YJ, Kisa A, Kisa S, Kivimäki M, Koroshetz WJ, Koyanagi A, Kumar GA, Kumar M, Lak HM, Leonardi M, Li B, Lim SS, Liu X, Liu Y, Logroscino G, Lorkowski S, Lucchetti G, Lutzky Saute R, Magnani FG, Malik AA, Massano J, Mehndiratta MM, Menezes RG, Meretoja A, Mohajer B, Mohamed Ibrahim N, Mohammad Y, Mohammed A, Mokdad AH, Mondello S, Moni MAA, Moniruzzaman M, Mossie TB, Nagel G, Naveed M, Nayak VC, Neupane Kandel S, Nguyen TH, Oancea B, Otstavnov N, Otstavnov SS, Owolabi MO, Panda-Jonas S, Pashazadeh Kan F, Pasovic M, Patel UK, Pathak M, Peres MFP, Perianayagam A, Peterson CB, Phillips MR, Pinheiro M, Piradov MA, Pond CD, Potashman MH, Pottoo FH, Prada SI, Radfar A, Raggi A, Rahim F, Rahman M, Ram P, Ranasinghe P, Rawaf DL, Rawaf S, Rezaei N, Rezapour A, Robinson SR, Romoli M, Roshandel G, Sahathevan R, Sahebkar A, Sahraian MA, Sathian B, Sattin D, Sawhney M, Saylan M, Schiavolin S, Seylani A, Sha F, Shaikh MA, Shaji KS, Shannawaz M, Shetty JK, Shigematsu M, Shin JI, Shiri R, Silva DAS, Silva JP, Silva R, Singh JA, Skryabin VY, Skryabina AA, Smith AE, Soshnikov S, Spurlock EE, Stein DJ, Sun J, Tabarés-Seisdedos R, Thakur B, Timalsina B, Tovani-Palone MR, Tran BX, Tsegaye GW, Valadan Tahbaz S, Valdez PR, Venketasubramanian N, Vlassov V, Vu GT, Vu LG, Wang Y-P, Wimo A, Winkler AS, Yadav L, Yahyazadeh Jabbari SH, Yamagishi K, Yang L, Yano Y, Yonemoto N, Yu C, Yunusa I, Zadey S, Zastrozhin MS, Zastrozhina A, Zhang Z-J, Murray CJL, Vos T. Estimation of the global prevalence of dementia in 2019 and forecasted prevalence in 2050: an analysis for the Global Burden of Disease Study 2019. The Lancet Public Health. 2022;7(2):e105-e25.

2. Livingston G, Huntley J, Sommerlad A, Ames D, Ballard C, Banerjee S, Brayne C, Burns A, Cohen-Mansfield J, Cooper C, Costafreda SG, Dias A, Fox N, Gitlin LN, Howard R, Kales HC, Kivimäki M, Larson EB, Ogunniyi A, Orgeta V, Ritchie K, Rockwood K, Sampson EL, Samus Q, Schneider LS, Selbæk G, Teri L, Mukadam N. Dementia prevention, intervention, and care: 2020 report of the Lancet Commission. Lancet. 2020;396(10248):413-46.

3. Bello VME, Schultz RR. Prevalence of treatable and reversible dementias: A study in a dementia outpatient clinic. Dement Neuropsychol. 2011;5(1):44-7.
4. Gale SA, Acar D, Daffner KR. Dementia. Am J Med. 2018;131(10):1161-9.
5. Cummings J, Lee G, Nahed P, Kambar M, Zhong K, Fonseca J, Taghva K. Alzheimer's disease drug development pipeline: 2022. Alzheimers Dement (N Y). 2022;8(1):e12295.
6. Halder A, Drummond E. Strategies for translating proteomics discoveries into drug discovery for dementia. Neural Regen Res. 2024;19(1):132-9.
7. Flanagan EP, McKeon A, Lennon VA, Boeve BF, Trenerry MR, Tan KM, Drubach DA, Josephs KA, Britton JW, Mandrekar JN, Lowe V, Parisi JE, Pittock SJ. Autoimmune dementia: clinical course and predictors of immunotherapy response. Mayo Clin Proc. 2010;85(10):881-97.
8. Dalmau J, Tüzün E, Wu HY, Masjuan J, Rossi JE, Voloschin A, Baehring JM, Shimazaki H, Koide R, King D, Mason W, Sansing LH, Dichter MA, Rosenfeld MR, Lynch DR. Paraneoplastic anti-N-methyl-D-aspartate receptor encephalitis associated with ovarian teratoma. Ann Neurol. 2007;61(1):25-36.
9. Bien CG, Vincent A, Barnett MH, Becker AJ, Blümcke I, Graus F, Jellinger KA, Reuss DE, Ribalta T, Schlegel J, Sutton I, Lassmann H, Bauer J. Immunopathology of autoantibody-associated encephalitides: clues for pathogenesis. Brain. 2012;135(Pt 5):1622-38.
10. Mueller SH, Färber A, Prüss H, Melzer N, Golombeck KS, Kümpfel T, Thaler F, Elisak M, Lewerenz J, Kaufmann M, Sühs KW, Ringelstein M, Kellinghaus C, Bien CG, Kraft A, Zettl UK, Ehrlich S, Handreka R, Rostásy K, Then Bergh F, Faiss JH, Lieb W, Franke A, Kuhlenbäumer G, Wandinger KP, Leypoldt F. Genetic predisposition in anti-LGI1 and anti-NMDA receptor encephalitis. Ann Neurol. 2018;83(4):863-9.
11. Duong SL, Prüss H. Paraneoplastic Autoimmune Neurological Syndromes and the Role of Immune Checkpoint Inhibitors. Neurotherapeutics. 2022;19(3):848-63.
12. Prüss H, Finke C, Höltje M, Hofmann J, Klingbeil C, Probst C, Borowski K, Ahnert-Hilger G, Harms L, Schwab JM, Ploner CJ, Komorowski L, Stoecker W, Dalmau J, Wandinger KP. N-methyl-D-aspartate receptor antibodies in herpes simplex encephalitis. Ann Neurol. 2012;72(6):902-11.
13. Leypoldt F, Titulaer MJ, Aguilar E, Walther J, Bönstrup M, Havemeister S, Teegen B, Lütgehetmann M, Rosenkranz M, Magnus T, Dalmau J. Herpes simplex virus-1 encephalitis can trigger anti-NMDA receptor encephalitis: case report. Neurology. 2013;81(18):1637-9.
14. Fatma N, Zakaria S, Mourad Z, Samir B, Samia BS. Atypical anti-NMDA receptor encephalitis associated with varicella zoster virus infection. J Neurovirol. 2022;28(3):456-9.
15. Nabizadeh F, Balabandian M, Sodeifian F, Rezaei N, Rostami MR, Naser Moghadasi A. Autoimmune encephalitis associated with COVID-19: A systematic review. Mult Scler Relat Disord. 2022;62:103795.
16. Franke C, Ferse C, Kreye J, Reincke SM, Sanchez-Sendin E, Rocco A, Steinbrenner M, Angermair S, Treskatsch S, Zickler D, Eckardt KU, Dersch R, Hosp J, Audebert HJ, Endres M, Ploner JC, Prüß H. High frequency of cerebrospinal fluid autoantibodies in COVID-19 patients with neurological symptoms. Brain, behavior, and immunity. 2021;93:415-9.
17. Kreye J, Wenke NK, Chayka M, Leubner J, Murugan R, Maier N, Jurek B, Ly LT, Brandl D, Rost BR, Stumpf A, Schulz P, Radbruch H, Hauser AE, Pache F, Meisel A, Harms L, Paul F, Dirnagl U, Garner C, Schmitz D, Wardemann H, Prüss H. Human

cerebrospinal fluid monoclonal N-methyl-D-aspartate receptor autoantibodies are sufficient for encephalitis pathogenesis. Brain. 2016;139(Pt 10):2641-52.
18. Petit-Pedrol M, Armangue T, Peng X, Bataller L, Cellucci T, Davis R, McCracken L, Martinez-Hernandez E, Mason WP, Kruer MC, Ritacco DG, Grisold W, Meaney BF, Alcalá C, Sillevis-Smitt P, Titulaer MJ, Balice-Gordon R, Graus F, Dalmau J. Encephalitis with refractory seizures, status epilepticus, and antibodies to the GABAA receptor: a case series, characterisation of the antigen, and analysis of the effects of antibodies. Lancet Neurol. 2014;13(3):276-86.
19. Lai M, Hughes EG, Peng X, Zhou L, Gleichman AJ, Shu H, Matà S, Kremens D, Vitaliani R, Geschwind MD, Bataller L, Kalb RG, Davis R, Graus F, Lynch DR, Balice-Gordon R, Dalmau J. AMPA receptor antibodies in limbic encephalitis alter synaptic receptor location. Ann Neurol. 2009;65(4):424-34.
20. Hutchinson M, Waters P, McHugh J, Gorman G, O'Riordan S, Connolly S, Hager H, Yu P, Becker CM, Vincent A. Progressive encephalomyelitis, rigidity, and myoclonus: a novel glycine receptor antibody. Neurology. 2008;71(16):1291-2.
21. Rocchi A, Sacchetti S, De Fusco A, Giovedi S, Parisi B, Cesca F, Höltje M, Ruprecht K, Ahnert-Hilger G, Benfenati F. Autoantibodies to synapsin I sequestrate synapsin I and alter synaptic function. Cell Death Dis. 2019;10(11):864.
22. Li LY, Kreye J, Burek M, Cordero-Gomez C, Barthel PC, Sánchez-Sendín E, Kornau HC, Schmitz D, Scharf M, Meybohm P, Reincke SM, Prüss H, Höltje M. Brain blood vessel autoantibodies in patients with NMDA and GABA(A) receptor encephalitis: identification of unconventional Myosin-X as target antigen. Front Cell Neurosci. 2023;17:1077204.
23. Weinshenker BG, Wingerchuk DM. Neuromyelitis Spectrum Disorders. Mayo Clin Proc. 2017;92(4):663-79.
24. Endres D, Leypoldt F, Bechter K, Hasan A, Steiner J, Domschke K, Wandinger KP, Falkai P, Arolt V, Stich O, Rauer S, Prüss H, van Elst LT. Autoimmune encephalitis as a differential diagnosis of schizophreniform psychosis: clinical symptomatology, pathophysiology, diagnostic approach, and therapeutic considerations. European archives of psychiatry and clinical neuroscience. 2020;270(7):803-18.
25. Prüss H. Autoantibodies in neurological disease. Nat Rev Immunol. 2021:1-16.
26. Banks SA, Sechi E, Flanagan EP. Autoimmune encephalopathies presenting as dementia of subacute onset and rapid progression. Ther Adv Neurol Disord. 2021;14:1756286421998906.
27. Bastiaansen AEM, van Steenhoven RW, de Bruijn M, Crijnen YS, van Sonderen A, van Coevorden-Hameete MH, Nuhn MM, Verbeek MM, Schreurs MWJ, Sillevis Smitt PAE, de Vries JM, Jan de Jong F, Titulaer MJ. Autoimmune Encephalitis Resembling Dementia Syndromes. Neurol Neuroimmunol Neuroinflamm. 2021;8(5).
28. Abe K, Chiba Y. A case of treatable dementia with Lewy bodies remarkably improved by immunotherapy. J Neuroimmunol. 2019;330:35-7.
29. Maat P, de Beukelaar JW, Jansen C, Schuur M, van Duijn CM, van Coevorden MH, de Graaff E, Titulaer M, Rozemuller AJ, Sillevis Smitt P. Pathologically confirmed autoimmune encephalitis in suspected Creutzfeldt-Jakob disease. Neurol Neuroimmunol Neuroinflamm. 2015;2(6):e178.
30. Hansen N, Bartels C, Stöcker W, Wiltfang J, Timäus C. Case Report: Anti-flotillin 1/2 Autoantibody-Associated Atypical Dementia. Front Psychiatry. 2021;12:626121.
31. Li X, Yuan J, Liu L, Hu W. Antibody-LGI 1 autoimmune encephalitis manifesting as rapidly progressive dementia and hyponatremia: a case report and literature review. BMC Neurol. 2019;19(1):19.

32. Younes K, Lepow LA, Estrada C, Schulz PE. Auto-antibodies against P/Q- and N-type voltage-dependent calcium channels mimicking frontotemporal dementia. SAGE open medical case reports. 2018;6:2050313x17750928.
33. Doss S, Wandinger KP, Hyman BT, Panzer JA, Synofzik M, Dickerson B, Mollenhauer B, Scherzer CR, Ivinson AJ, Finke C, Schöls L, Müller Vom Hagen J, Trenkwalder C, Jahn H, Höltje M, Biswal BB, Harms L, Ruprecht K, Buchert R, Höglinger GU, Oertel WH, Unger MM, Körtvélyessy P, Bittner D, Priller J, Spruth EJ, Paul F, Meisel A, Lynch DR, Dirnagl U, Endres M, Teegen B, Probst C, Komorowski L, Stöcker W, Dalmau J, Prüss H. High prevalence of NMDA receptor IgA/IgM antibodies in different dementia types. Ann Clin Transl Neurol. 2014;1(10):822-32.
34. Giannoccaro MP, Gastaldi M, Rizzo G, Jacobson L, Vacchiano V, Perini G, Capellari S, Franciotta D, Costa A, Liguori R, Vincent A. Antibodies to neuronal surface antigens in patients with a clinical diagnosis of neurodegenerative disorder. Brain, behavior, and immunity. 2021;96:106-12.
35. Hansen N, Malchow B, Zerr I, Stöcker W, Wiltfang J, Timäus C. Neural cell-surface and intracellular autoantibodies in patients with cognitive impairment from a memory clinic cohort. Journal of neural transmission (Vienna, Austria : 1996). 2021;128(3):357-69.
36. Meldolesi J. Role of Senescent Astrocytes in Health and Disease. Int J Mol Sci. 2023;24(10).
37. Middeldorp J, Hol EM. GFAP in health and disease. Prog Neurobiol. 2011;93(3):421-43.
38. Blechingberg J, Holm IE, Nielsen KB, Jensen TH, Jørgensen AL, Nielsen AL. Identification and characterization of GFAPkappa, a novel glial fibrillary acidic protein isoform. Glia. 2007;55(5):497-507.
39. Brenner M, Messing A. Regulation of GFAP Expression. ASN Neuro. 2021;13:1759091420981206.
40. Saraste M, Bezukladova S, Matilainen M, Sucksdorff M, Kuhle J, Leppert D, Airas L. Increased serum glial fibrillary acidic protein associates with microstructural white matter damage in multiple sclerosis: GFAP and DTI. Mult Scler Relat Disord. 2021;50:102810.
41. Okonkwo DO, Yue JK, Puccio AM, Panczykowski DM, Inoue T, McMahon PJ, Sorani MD, Yuh EL, Lingsma HF, Maas AI, Valadka AB, Manley GT. GFAP-BDP as an acute diagnostic marker in traumatic brain injury: results from the prospective transforming research and clinical knowledge in traumatic brain injury study. Journal of neurotrauma. 2013;30(17):1490-7.
42. Kim KY, Shin KY, Chang KA. GFAP as a Potential Biomarker for Alzheimer's Disease: A Systematic Review and Meta-Analysis. Cells. 2023;12(9).
43. Cicognola C, Janelidze S, Hertze J, Zetterberg H, Blennow K, Mattsson-Carlgren N, Hansson O. Plasma glial fibrillary acidic protein detects Alzheimer pathology and predicts future conversion to Alzheimer dementia in patients with mild cognitive impairment. Alzheimers Res Ther. 2021;13(1):68.
44. Fang B, McKeon A, Hinson SR, Kryzer TJ, Pittock SJ, Aksamit AJ, Lennon VA. Autoimmune Glial Fibrillary Acidic Protein Astrocytopathy: A Novel Meningoencephalomyelitis. JAMA Neurol. 2016;73(11):1297-307.
45. Yoshikura N, Kimura A, Shimohata T. [Novel Autoantibody-Related Encephalitis: anti-mGluR1 encephalitis, anti-IgLON5 disease, autoimmune GFAP astrocytopathy]. Brain Nerve. 2021;73(5):631-9.
46. Long Y, Liang J, Xu H, Huang Q, Yang J, Gao C, Qiu W, Lin S, Chen X. Autoimmune glial fibrillary acidic protein astrocytopathy in Chinese patients: a retrospective study. Eur J Neurol. 2018;25(3):477-83.

47. Zhu B, Sun M, Yang T, Yu H, Wang L. Clinical, imaging features and outcomes of patients with anti-GFAP antibodies: a retrospective study. Front Immunol. 2023;14:1106490.
48. Xiao J, Chen X, Shang K, Tang Y, Chen M, Deng G, Qin C, Tian DS. Clinical, neuroradiological, diagnostic and prognostic profile of autoimmune glial fibrillary acidic protein astrocytopathy: A pooled analysis of 324 cases from published data and a single-center retrospective study. J Neuroimmunol. 2021;360:577718.
49. Dubey D, Hinson SR, Jolliffe EA, Zekeridou A, Flanagan EP, Pittock SJ, Basal E, Drubach DA, Lachance DH, Lennon VA, McKeon A. Autoimmune GFAP astrocytopathy: Prospective evaluation of 90 patients in 1year. J Neuroimmunol. 2018;321:157-63.
50. Sasaki K, Bean A, Shah S, Schutten E, Huseby PG, Peters B, Shen ZT, Vanguri V, Liggitt D, Huseby ES. Relapsing-remitting central nervous system autoimmunity mediated by GFAP-specific CD8 T cells. Journal of immunology (Baltimore, Md : 1950). 2014;192(7):3029-42.
51. Shu Y, Long Y, Chang Y, Li R, Sun X, Wang Y, Huang Y, Li J, Chen J, Yang Y, Lu Z, Hu X, Kermode AG, Qiu W. Brain Immunohistopathology in a Patient with Autoimmune Glial Fibrillary Acidic Protein Astrocytopathy. Neuroimmunomodulation. 2018;25(1):1-6.
52. Canissario R, Samkoff L, Jean MJ, Williams Z, Diep J. GFAP astrocytopathy presenting with profound intracranial hypertension and vision loss. J Neuroimmunol. 2022;373:577976.
53. Tan C, Zhong M, Yao Z, Hong S, Jiang L, Jiang Y. Anti-GFAP Antibody-Associated Hypertrophic Pachymeningitis. Neuropediatrics. 2022;53(2):143-5.
54. Iwami K, Nomura T, Seo S, Nojima S, Tsuzaka K, Kimura A, Shimohata T, Yabe I. Autoimmune Glial Fibrillary Acidic Protein Astrocytopathy Presenting with Area Postrema Syndrome-Like Symptoms without Medulla Oblongata Lesions. Neuroimmunomodulation. 2022;29(4):433-8.
55. Tomczak A, Su E, Tugizova M, Carlson AM, Kipp LB, Feng H, Han MH. A case of GFAP-astroglial autoimmunity presenting with reversible parkinsonism. Mult Scler Relat Disord. 2019;39:101900.
56. Natori T, Shindo K, Okumura A, Kimura A, Takiyama Y. A treatable case of autoimmune GFAP astrocytopathy presenting chronic progressive cognitive impairment. Neurological Sciences. 2020;41(10):2999-3002.
57. Toledano-Illan C, Esparragosa Vazquez I, Zelaya Huerta MV, Rosales Castillo JJ, Paternain Nuin A, Arbizu Lostao J, Garcia de Eulate MR, Riverol Fernandez M. Autoimmune glial fibrillary acidic protein astrocytopathy: case report of a treatable cause of rapidly progressive dementia. J Neurol. 2021;268(6):2256-8.
58. Friedrich M, Hartig J, Prüss H, Ip CW, Volkmann J. Rapidly progressive dementia: Extending the spectrum of GFAP-astrocytopathies? Ann Clin Transl Neurol. 2022;9(3):410-5.
59. Barthel PC, Staabs F, Li LY, Buthut M, Otto C, Ruprecht K, Prüss H, Höltje M. Immunoreactivity to astrocytes in different forms of dementia: High prevalence of autoantibodies to GFAP. Brain Behav Immun Health. 2023;29:100609.
60. Kreye J, Reincke SM, Kornau HC, Sánchez-Sendin E, Corman VM, Liu H, Yuan M, Wu NC, Zhu X, Lee CD, Trimpert J, Höltje M, Dietert K, Stöffler L, von Wardenburg N, van Hoof S, Homeyer MA, Hoffmann J, Abdelgawad A, Gruber AD, Bertzbach LD, Vladimirova D, Li LY, Barthel PC, Skriner K, Hocke AC, Hippenstiel S, Witzenrath M, Suttorp N, Kurth F, Franke C, Endres M, Schmitz D, Jeworowski LM, Richter A, Schmidt ML, Schwarz T, Müller MA, Drosten C, Wendisch D, Sander LE, Osterrieder N, Wilson IA, Prüss H. A Therapeutic Non-self-reactive SARS-CoV-2 Antibody Protects from Lung Pathology in a COVID-19 Hamster Model. Cell. 2020;183(4):1058-69.e19.

61. Franke C, Boesl F, Goereci Y, Gerhard A, Schweitzer F, Schroeder M, Foverskov-Rasmussen H, Heine J, Quitschau A, Kandil FI, Schild AK, Finke C, Audebert HJ, Endres M, Warnke C, Prüss H. Association of cerebrospinal fluid brain-binding autoantibodies with cognitive impairment in post-COVID-19 syndrome. Brain, behavior, and immunity. 2023;109:139-43.
62. Hansen N, Stöcker W, Wiltfang J, Bartels C, Rentzsch K, Bouter C. Case Report: Semantic Variant of Primary Progressive Aphasia Associated With Anti-Glial Fibrillary Acid Protein Autoantibodies. Front Immunol. 2021;12:760021.
63. Lennon VA, Wingerchuk DM, Kryzer TJ, Pittock SJ, Lucchinetti CF, Fujihara K, Nakashima I, Weinshenker BG. A serum autoantibody marker of neuromyelitis optica: distinction from multiple sclerosis. Lancet. 2004;364(9451):2106-12.
64. Huang TL, Wang JK, Chang PY, Hsu YR, Lin CH, Lin KH, Tsai RK. Neuromyelitis Optica Spectrum Disorder: From Basic Research to Clinical Perspectives. Int J Mol Sci. 2022;23(14).
65. Zhang Z, Zoltewicz JS, Mondello S, Newsom KJ, Yang Z, Yang B, Kobeissy F, Guingab J, Glushakova O, Robicsek S, Heaton S, Buki A, Hannay J, Gold MS, Rubenstein R, Lu XC, Dave JR, Schmid K, Tortella F, Robertson CS, Wang KK. Human traumatic brain injury induces autoantibody response against glial fibrillary acidic protein and its breakdown products. PLoS One. 2014;9(3):e92698.
66. Savas M, Tzartos J, Kucukali CI, Dursun E, Karagiorgou K, Gezen-Ak D, Turkdogan D, Papaconstantinou A, Basoglu S, Hacihafizoglu N, Kutlubay B, Tzartos S, Tuzun E. Glial fibrillary acidic protein (GFAP)-antibody in children with focal seizures of undetermined cause. Acta Neurol Belg. 2021;121(5):1275-80.
67. Zhang YH, Ni Y, Gao YN, Shen DD, He L, Yin D, Meng HY, Zhou QM, Hu J, Chen S. Anti-IgLON5 disease: a novel topic beyond neuroimmunology. Neural Regen Res. 2023;18(5):1017-22.
68. Sabater L, Gaig C, Gelpi E, Bataller L, Lewerenz J, Torres-Vega E, Contreras A, Giometto B, Compta Y, Embid C, Vilaseca I, Iranzo A, Santamaría J, Dalmau J, Graus F. A novel non-rapid-eye movement and rapid-eye-movement parasomnia with sleep breathing disorder associated with antibodies to IgLON5: a case series, characterisation of the antigen, and post-mortem study. The Lancet Neurology. 2014;13(6):575-86.
69. Montagna M, Amir R, De Volder I, Lammens M, Huyskens J, Willekens B. IgLON5-Associated Encephalitis With Atypical Brain Magnetic Resonance Imaging and Cerebrospinal Fluid Changes. Front Neurol. 2018;9:329.
70. Erro ME, Sabater L, Martínez L, Herrera M, Ostolaza A, García de Gurtubay I, Tuñón T, Graus F, Gelpi E. Anti-IGLON5 disease: A new case without neuropathologic evidence of brainstem tauopathy. Neurol Neuroimmunol Neuroinflamm. 2020;7(2).
71. Ryding M, Gamre M, Nissen MS, Nilsson AC, Okarmus J, Poulsen AAE, Meyer M, Blaabjerg M. Neurodegeneration Induced by Anti-IgLON5 Antibodies Studied in Induced Pluripotent Stem Cell-Derived Human Neurons. Cells. 2021;10(4).
72. Ni Y, Feng Y, Shen D, Chen M, Zhu X, Zhou Q, Gao Y, Liu J, Zhang Q, Shen Y, Peng L, Zeng Z, Yin D, Hu J, Chen S. Anti-IgLON5 antibodies cause progressive behavioral and neuropathological changes in mice. J Neuroinflammation. 2022;19(1):140.
73. Landa J, Gaig C, Plagumà J, Saiz A, Antonell A, Sanchez-Valle R, Dalmau J, Graus F, Sabater L. Effects of IgLON5 Antibodies on Neuronal Cytoskeleton: A Link between Autoimmunity and Neurodegeneration. Ann Neurol. 2020;88(5):1023-7.
74. Prüss H, Höltje M, Maier N, Gomez A, Buchert R, Harms L, Ahnert-Hilger G, Schmitz D, Terborg C, Kopp U, Klingbeil C, Probst C, Kohler S, Schwab JM, Stoecker W,

Dalmau J, Wandinger KP. IgA NMDA receptor antibodies are markers of synaptic immunity in slow cognitive impairment. Neurology. 2012;78(22):1743-53.

Statutory Declaration

„Ich, Paula Charlotte Barthel, versichere an Eides statt durch meine eigenhändige Unterschrift, dass ich die vorgelegte Dissertation mit dem Thema: „Analyse zum Vorkommen von Autoantikörpern gegen hirneigene Antigene bei an Demenz Erkrankten - Fokus auf GFAP als Antigen; Analysis of the occurrence of autoantibodies against brain antigens in patients with dementia - Focus on GFAP as antigen“, selbstständig und ohne nicht offengelegte Hilfe Dritter verfasst und keine anderen als die angegebenen Quellen und Hilfsmittel genutzt habe.
Alle Stellen, die wörtlich oder dem Sinne nach auf Publikationen oder Vorträgen anderer Autoren/innen beruhen, sind als solche in korrekter Zitierung kenntlich gemacht. Die Abschnitte zu Methodik (insbesondere praktische Arbeiten, Laborbestimmungen, statistische Aufarbeitung) und Resultaten (insbesondere Abbildungen, Graphiken und Tabellen) werden von mir verantwortet.

Ich versichere ferner, dass ich die in Zusammenarbeit mit anderen Personen generierten Daten, Datenauswertungen und Schlussfolgerungen korrekt gekennzeichnet und meinen eigenen Beitrag sowie die Beiträge anderer Personen korrekt kenntlich gemacht habe (siehe Anteilserklärung). Texte oder Textteile, die gemeinsam mit anderen erstellt oder verwendet wurden, habe ich korrekt kenntlich gemacht.

Meine Anteile an etwaigen Publikationen zu dieser Dissertation entsprechen denen, die in der untenstehenden gemeinsamen Erklärung mit dem/der Erstbetreuer/in, angegeben sind. Für sämtliche im Rahmen der Dissertation entstandenen Publikationen wurden die Richtlinien des ICMJE (International Committee of Medical Journal Editors; www.icmje.og) zur Autorenschaft eingehalten. Ich erkläre ferner, dass ich mich zur Einhaltung der Satzung der Charité – Universitätsmedizin Berlin zur Sicherung Guter Wissenschaftlicher Praxis verpflichte.

Weiterhin versichere ich, dass ich diese Dissertation weder in gleicher noch in ähnlicher Form bereits an einer anderen Fakultät eingereicht habe.

Die Bedeutung dieser eidesstattlichen Versicherung und die strafrechtlichen Folgen einer unwahren eidesstattlichen Versicherung (§§156, 161 des Strafgesetzbuches) sind mir bekannt und bewusst.“

Datum Unterschrift

Detailed declaration of contribution to the publication

Paula Charlotte Barthel hatte folgenden Anteil an den folgenden Publikationen:

Publikation 1: Barthel, P. C., Staabs, F., Li, L. Y., Buthut, M., Otto, C., Ruprecht, K., Prüss, H., Höltje, M., Immunoreactivity to astrocytes in different forms of dementia: High prevalence of autoantibodies to GFAP., Brain, Behavior, & Immunity - Health, 2023

Beitrag im Einzelnen:

- Mitwirkung bei der Konzeptionalisierung der Studie
- Durchführung des Hauptteils der experimentellen Arbeiten: Diverse immunzytochemische und immunhistochemische Färbungen an murinen Zellkulturen und Hirnschnitten, HEK-Zell Transfektionen, Western Blots (s. 2.2; 2.5; 2.6-8; 2.10)
    - Hierfür Verwendung der von Koautor*innen bereits akquirierten Serumproben der Demenz-/Kontrollkohorten
- Mikroskopieren der gefärbten Zellen und Schnitte, Beurteilung der experimentellen Ergebnisse, Erhebung des Bildmaterials und Erstellung der jeweiligen Abbildungen (s. Fig. 1 - 4.)
- Statistische Auswertung der experimentellen Daten, Erstellung der entsprechenden Tabellen (s. Tab. 2)
- Statistische Auswertung der klinischen und paraklinischen Daten, Erstellung der entsprechenden Tabellen und Abbildungen (s.Tab. 1/3; Fig. 4D)
    - Hierfür Verwendung der von Koautor*innen bereits erhobenen, aufbereiteten und selektierten Daten der Demenz-/Kontrollkohorten
- Verfassung des Manuskriptes

Publikation 2: Li, L. Y., Kreye, J., Burek, M., Cordero-Gomez, C., Barthel, P. C., Sánchez-Sendín, E., Kornau, H. C., Schmitz, D., Scharf, M., Meybohm, P., Reincke, S. M., Prüss, H., Höltje, M., Brain blood vessel autoantibodies in patients with NMDA and GABA(A) receptor encephalitis: identification of unconventional Myosin-X as target antigen., Frontiers in Cellular Neuroscience, 2023

Beitrag im Einzelnen:

- Durchführung der HEK-Zell Transfektionen
- Immunzytochemische Färbungen der HEK-Zellen und der primären murinen hippokampalen/kortikalen Zellkulturen, Beurteilung der Färbemuster
- Erhebung des entsprechenden Bildmaterials zur weiteren Verwendung in Abbildungen (Fig.5C-G)
- Überprüfung und Bearbeitung des Manuskriptes

Publikation 3: Kreye J, Reincke SM, Kornau HC, Sánchez-Sendin E, Corman VM, Liu H, Yuan M, Wu NC, Zhu X, Lee CD, Trimpert J, Höltje M, Dietert K, Stöffler L, von Wardenburg N, van Hoof S, Homeyer MA, Hoffmann J, Abdelgawad A, Gruber AD, Bertzbach LD, Vladimirova D, Li LY, Barthel PC, Skriner K, Hocke

AC, Hippenstiel S, Witzenrath M, Suttorp N, Kurth F, Franke C, Endres M, Schmitz D, Jeworowski LM, Richter A, Schmidt ML, Schwarz T, Müller MA, Drosten C, Wendisch D, Sander LE, Osterrieder N, Wilson IA, Prüss H., A Therapeutic Non-self-reactive SARS-CoV-2 Antibody Protects from Lung Pathology in a COVID-19 Hamster Model, Cell, 2020

Beitrag im Einzelnen:

- Untersuchung der monoklonalen Antikörper auf Autoreaktivität gegen hirneigene Antigene (Kap. „Near-Germline SARS-CoV-2 Neutralizing Antibodies Can Bind to Murine Tissue")
- Immunzytochemische Färbungen auf murinen Hirnschnitten und primären murinen hippokampalen/kortikalen Zellkulturen, Beurteilung der Färbemuster (Tab. S3 „Tissue reactivity")
- Erhebung des entsprechenden Bildmaterials (nicht publiziert)
- Überprüfung und Bearbeitung des Manuskriptes

_____

Unterschrift, Datum und Stempel des/der erstbetreuenden Hochschullehrers/in

_____

Unterschrift des Doktoranden/der Doktorandin

Publications

Brain, Behavior, & Immunity - Health 29 (2023) 100609

Contents lists available at ScienceDirect

Brain, Behavior, & Immunity - Health

journal homepage: www.editorialmanager.com/bbih/default.aspx

Immunoreactivity to astrocytes in different forms of dementia: High prevalence of autoantibodies to GFAP

Paula Charlotte Barthel [a], Finja Staabs [b], Lucie Y. Li [a], Maria Buthut [b,c], Carolin Otto [b], Klemens Ruprecht [b], Harald Prüss [b,c], Markus Höltje [a,*]

[a] Institute of Integrative Neuroanatomy Berlin, Charité-Universitätsmedizin Berlin, Freie Universität Berlin and Humboldt-Universität zu Berlin, Berlin, Germany
[b] Department of Neurology, Charité-Universitätsmedizin Berlin, Freie Universität Berlin and Humboldt-Universität zu Berlin, Berlin, Germany
[c] German Center for Neurodegenerative Diseases (DZNE) Berlin, Berlin, Germany

ARTICLE INFO

Keywords:
Dementia
GFAP
Autoimmunity
Astrocytes

ABSTRACT

Objective: To study the prevalence of autoantibodies to glial and neuronal antigens with a focus on glial acidic fibrillary protein (GFAP) in patients with dementia.
Methods: Sera of 127 patients with different forms of dementia and sera of 82 age-matched patients with various neurological diseases except for dementia, as well as sera from 15 age-matched healthy controls were analyzed for anti-glial or anti-neuronal IgG using 1) primary murine embryonic hippocampus cell cultures, 2) murine brain sections, 3) immunoblotting on mouse brain homogenates and 4) astrocyte cultures. Sera reacting with astrocytes in hippocampus cell cultures were further analyzed using HEK293 cells transfected with human GFAP.
Results: IgG in serum from 45 of 127 (35.5%) patients with dementia but only 8 of 97 (8.2%, $p \leq 0.001$) controls bound to either glial or neuronal structures in cultured murine hippocampus cells. In these cultures antibodies to astrocytes were detected in 35 of 127 (27.5%) of the dementia patients, whereas in controls antibodies to astrocytes were detected in 4 sera only (4.1%, $p \leq 0.001$). Among the sera exhibiting reactivity to astrocytes, 14 of 35 (40%) showed immunoreaction to HEK293 cells transfected with GFAP in dementia patients, representing 11% of all sera. Within the 4 immunoreactive control sera reacting with astrocytes one reacted with GFAP (1.0% of total immunoreactivity, $p = 0.003$).
Conclusions: Autoantibodies to glial epitopes in general and to GFAP in particular are more frequent in patients with dementia than in age-matched controls without dementia, thus indicating the need for further investigations regarding the potential pathophysiological relevance of these antibodies.

1. Introduction

Autoimmune brain diseases caused by pathogenic antibodies gained increasing attention and became one of today's most relevant and growing research fields in neurology and psychiatry. Antibodies are mostly directed against neuronal cell-surface antigens eg. NMDA-, AMPA- and GABA-receptors (Dalmau et al., 2007; Kreye et al., 2016; Lai et al., 2009; Lancaster et al., 2010; Petit-Pedrol et al., 2014) or ion-channel subunits like LGI1 or CASPR2 (Irani et al., 2010). In addition, antibodies against intracellular proteins like synapsin (Piepgras et al., 2015; Höltje et al., 2017), amphiphysin (Folli et al., 1993) or GAD65 (Meinck et al., 2001) have been described. Due to the highly variable clinical presentation, diagnosis can be difficult, especially in cases when autoantibodies known to normally cause acute autoimmune encephalitis mimic neurodegenerative diseases such as atypical dementia (Hansen et al., 2021), Creutzfeldt-Jakob-Disease (Yoo and Hirsch, 2014), rapidly progressive dementia (Li et al., 2019), or frontotemporal dementia (Younes et al., 2018). In 2010, Flanagan et al. established the term "autoimmune dementia" for a subgroup of dementia patients with suspected autoimmune etiology, which improved with immunotherapy (Flanagan et al., 2010). Remarkably, autoantibodies against brain structures also occur in a large number of patients with a correctly diagnosed classic neurodegenerative disorder. The relevance of these antibodies, whether they are a primary cause of the disease or a secondary phenomenon, is unclear (Doss et al., 2014; Giannoccaro et al., 2021; Hansen et al., 2021). We aim to further explore

* Corresponding author. Charité –Universitätsmedizin Berlin, Freie Universität Berlin and Humboldt-Universität zu Berlin, Institut für Integrative Neuroanatomie Philippstr. 12, 10115, Berlin, Germany.
E-mail address: markus.hoeltje@charite.de (M. Höltje).

https://doi.org/10.1016/j.bbih.2023.100609
Received 25 October 2022; Received in revised form 21 February 2023; Accepted 25 February 2023
Available online 2 March 2023

Table 1
A) Demographic and dementia type data of the 127 patients analyzed in this study. Data are given in absolute numbers and proportions. AD = Alzheimer's disease; MCI = mild cognitive impairment; FTD = frontotemporal dementia; SAE = subcortical arteriosclerotic encephalopathy; LBD = Lewy body dementia; PD=Parkinson's disease dementia; CAA = cerebral amyloid angiopathy B, C) Demographic data of the two age-matched cohorts used for control. Neuropsychological testing was available for the 15 healthy subjects.

A) Dementia cohort.							
Mean ± SD age at blood draw N = 127		Sex		Sex %	Type of dementia		Type of dementia %
73,8 ± 9,4		female	56	44	AD	59	46
female	male	male	71	56	MCI	24	19
73,0 ± 9,3	74,6 ± 9,6				FTD	13	10
					SAE	11	9
					SAE/AD	10	8
					LBD/PD	6	5
					CAA	4	3

B) Charité CSF/serum biobank cohort					C) Healthy subjects				
Mean ± SD age at blood draw N = 82		Sex		Sex %	Mean ± SD age at blood draw N = 15		Sex		Sex %
70, 8 ± 7,7		female	44	53,7	75,8 ± 5,1		female	9	60
female	male	male	38	46,3	female	male	male	6	40
70,8 ± 7,0	70,9 ± 8,5				75,9 ± 5,4	75,7 ± 4,6	Mean MMST ± SD 29 ± 0,6/30		

Table 2
Summary of staining results.

	Dementia cohort	Charité-Biobank cohort	Age-matched control cohort	P-value
number	127	82	15	
Immunoreactivity in primary hippocampal cell culture				
Neurons, n (%)	10 (8)	4 (4.9)	0 (0)	$p = 0.40$ dementia vs. Biobank $p = 0.25$ dementia vs. total controls
Neurons and astrocytes, n (%)	7 (5.5)	1 (1.6)	0 (0)	$p \leq 0.001$ dementia vs. Biobank $p \leq 0.001$ dementia vs. total controls
Astrocytes, n (%)	28 (22)	3 (4.7)	0 (0)	$p \leq 0.001$ dementia vs. Biobank $p \leq 0.001$ dementia vs. total controls
Immunoreactivity with HEK293 cells expressing GFAP, n (%)	14 (11)	1 (1.6)	0 (0)	$p = 0.007$ dementia vs. Biobank $p = 0.003$ dementia vs. total controls

Immunocytochemical findings obtained from stainings of mixed neuronal and glial hippocampal/cortical primary cultures as well as GFAP-transfected HEK293 cells at a dilution of 1:200 (n = 127 dementia patient sera, n = 97 sera from age-matched patients or healthy subjects). Data are presented as absolute numbers and proportions. Statistical significance was verified using Chi-square test.

the hypothesis that autoantibodies against brain structures may also play a role in dementia and associate with a less acute form of autoimmune encephalitis with slowly progressing damage to the brain that could manifest as autoimmune dementia. These autoantibodies may not only target neuronal structures but also antigens in glial cells like astrocytes that are crucial for a healthy and functioning CNS.

Glial fibrillary acidic protein (GFAP) is an intracellular intermediate filament protein that is highly expressed in the cytoskeleton of astrocytes. Autoantibodies to GFAP are already known to occur in serum and/or CSF in humans with GFAP astrocytopathy, a disease first described in 2016 as an acute or subacute meningoencephalomyelitis. The diagnosis is made based on the presence of GFAP autoantibodies in CSF/serum (Fang et al., 2016). Main symptoms of the meningoencephalomyelitis include headache, fever, movement disorders, abnormal vision and dysautonomia (Flanagan et al., 2017; Dubey et al., 2018; Kimura et al., 2019; Xiao et al., 2021). The pathogenic role of the GFAP autoantibodies is still not fully understood. GFAP-autoantibodies with unknown relevance were also found in patients with other neurologic diseases, for example traumatic brain injury, glioma or epilepsy (Zhang et al., 2014; Wei et al., 2013; Savas et al., 2021).

Little is known about GFAP-autoantibodies in dementia. In a study investigating clinical characteristics of 19 patients with GFAP-astrocytopathy, 15.8% had symptoms of dementia but together with other more typical symptoms (Long et al., 2018). More research is needed to find out if there is a link between autoantibodies against brain structures and dementia. This led us to the question if specific antigens could be identified in these cases, manifesting in subtypes of autoimmune dementia. Therefore, we screened a cohort of 127 dementia patients for any autoimmune reaction against brain structures, with a special focus on autoantibodies against astrocytes and GFAP.

2. Material and methods

2.1. Patients

Serum samples from 127 patients diagnosed with MCI and various forms of dementia including Alzheimer's disease, frontotemporal dementia, subcortical arteriosclerotic encephalopathy, Lewy body dementia, Parkinson's disease dementia and cerebral amyloid angiopathy based on clinical examination, neuropsychological testing and imaging studies were obtained from the memory clinic of the department of Neurology, Charité – Universitätsmedizin Berlin, and German Center for Neurodegenerative Diseases (DZNE) Berlin, from January 2018 until April 2021 and stored at −80 °C. All patients, irrespective of the form of dementia, were included in the study without any additional exclusion criteria. We used two cohorts of patients as an age-matched control group. The first cohort included 82 patients, older than 60 years with various neurologic diseases. A diagnosis of any form of mild cognitive impairment (MCI) or dementia as well as a diagnosis of neurological

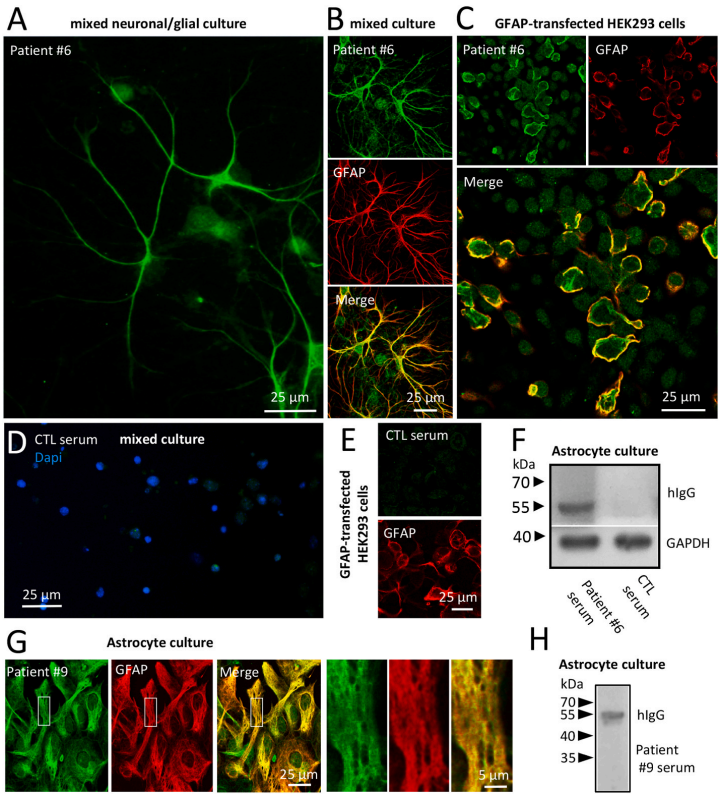

Fig. 1. Serum autoantibodies against glial fibrillary acidic protein (GFAP) in two patients with Alzheimer's disease. A) Patient serum #6 intensely stained large, branched cells that morphologically appeared like astrocytes in mixed embryonic hippocampal/cortical cultures. B) Patient serum antibodies co-localize with GFAP in cultured astrocytes. Cultures were double stained for human IgG and commercial monoclonal GFAP antibody. Both signals stained filament-like structures in stellate astrocytes and showed a high degree of overlap in the soma and astrocytic processes. Confocal imaging C) Patient serum antibodies react with GFAP-transfected HEK293 cells. HEK293 cells were transfected with a human GFAP plasmid. Only transfected cells reacted with patient IgG and signals showed a high degree of overlap with commercial GFAP staining. Confocal imaging D) Mixed embryonic hippocampal/cortical cultures were incubated with a serum from a 73-year old healthy control. No staining occurred. E) Likewise, control serum did not show any immunoreactivity to GFAP-transfected HEK cells. F) Purified astrocyte cultures were subjected to Western blotting and probed with patient serum and an age-matched control serum. For loading control, glyceraldehyde 3-phosphate dehydrogenase (GAPDH) was used. Incubation with patient serum resulted in a single immunoreactive band at around 55 kDa, corresponding to the expected molecular weight of GFAP. Control serum yielded no staining. G) Purified astrocyte cultures were fixed and double stained for binding of IgG from another patient (patient #9) and GFAP, thereby showing a high degree of overlap (see insets). H) In line with this, autoantibodies of patient #9 show a major immunoreactive band at around 55 kDa in Western blots. Reactivity to GFAP was verified using HEK293 cells transfected with human GFAP (not shown).

diseases known to be associated with dementia were used as exclusion criteria. Sera were obtained from the Charité CSF/serum biobank. The second cohort includes sera of 15 individuals, who accompanied patients to the memory clinic. They had no history of any neurologic or psychiatric disease.

The study was approved by the ethics committee of Charité – Universitätsmedizin Berlin. All participants provided written informed consent.

2.2. Immunostaining strategy

The general screening strategy based on the detection of serum autoantibodies by immunostaining on murine neuronal hippocampal/cortical cultures as the primary detection assay. Additionally, purified astrocyte cultures or brain slices were incubated with immunopositive sera. Further characterization involved co-staining with commercial primary and secondary antibodies to identify specific cell types and targeted antigenes. Sera that stained astrocytes, which are also present in primary murine hippocampal culture, indicate the presence of autoantibodies against astrocyte proteins, and were further tested on GFAP-transfected HEK cells.

2.3. Primary murine hippocampal cell culture

We prepared primary cultures of murine primary hippocampal and cortical neurons. First, pregnant SWISS-mice were killed by cervical dislocation to remove the embryos at day E16-17. Embryonic brains were dissected and transferred into a 0.6% PBS-glucose solution. We then isolated the hippocampi and parts of the cortex and collected them in NB-medium containing 10 ml B27, 5 ml penicillin/streptomycin (pen/strep), 1.25 ml L-glutamine and 485 ml Neurobasal Medium. We added N-medium composed of 50 ml fetal calf serum (FCS), 5 ml pen/strep; 5 ml L-glutamine; 10 mM HEPES, 1 mg/ml insulin, 44 mM glucose, 5 ml collagen G, filled up to 500 ml with Dulbecco's Modified Eagle Medium (DMEM), centrifuged at 800 rpm for 2 min at 4 °C, resuspended the pellet in N-medium without collagen, centrifuged again at 800 rpm for 2 min at 4 °C and diluted the cells in NB-starter medium (25 µL Na-glutamate (100 mM)/100 ml NB-media). Coverslips in 24-well plates were incubated with poly-L-lysine solution in PBS (1:20) overnight and then coated with N-medium with collagen. Finally, we removed the medium and added the cell-solution (8×10^4/ml). The cells were incubated for 10–14 days at 37 °C and then used for immunostaining.

2.4. Purified astrocyte culture

For astrocyte cultures, brains from SWISS-mice were dissected between postnatal days P2 and P3. We removed the meninges, transferred the brains into Hank's balanced salt solution (HBSS, Sigma) and suspended them. After centrifugation at 300×*g* for 3 min, the astrocytes were resuspended in HBSS. This step was repeated two more times with smaller pipette diameters. 6-well plates were pretreated with poly-L-lysine (100 µg/ml in PBS) and the cell suspension was added. Astrocytes from ½ whole brain were seeded per single well. We incubated the

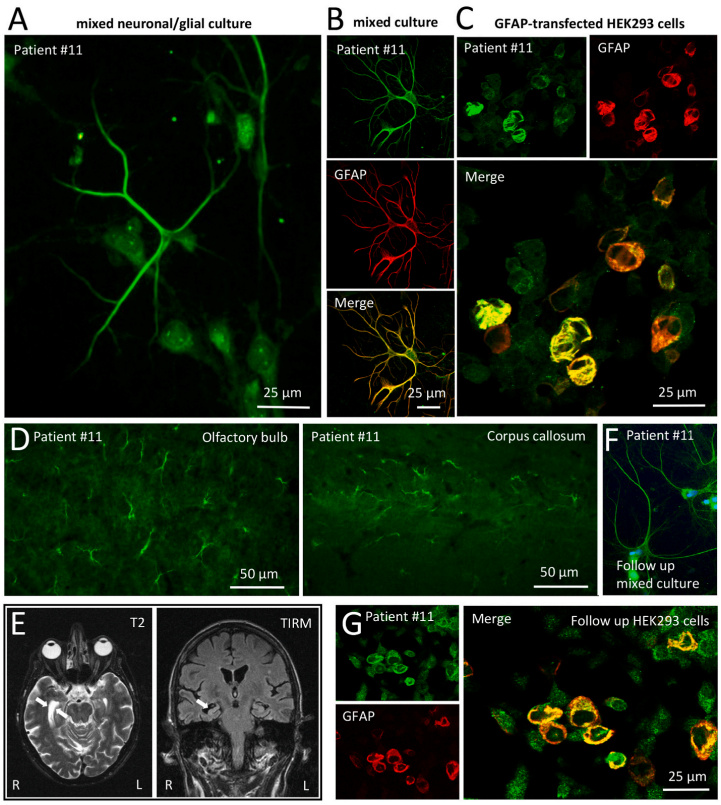

Fig. 2. Follow-up evaluation of serum autoantibodies against glial fibrillary acidic protein (GFAP) in a patient with Alzheimer's disease. A) Patient serum #11 intensely stained large, branched cells that morphologically appeared like astrocytes in mixed embryonic hippocampal/cortical primary cultures. B) Patient serum antibodies co-localize with GFAP in cultured astrocytes. Cultures were double stained for human IgG and GFAP. Both signals stained filament-like structures in stellate astrocytes and showed a high degree of overlap in the soma and astrocytic processes. Confocal imaging C) Patient serum antibodies react with GFAP-transfected HEK293 cells. Only transfected cells reacted with patient IgG and signals showed a high degree of overlap with commercial GFAP staining. Confocal imaging D) Astrocyte staining by patient autoantibodies in brain sections. Patient serum #11 stained astrocytes in various brain areas, being most prominent in the olfactory bulb and *Corpus callosum*. E) Axial and coronal MRIs (T2 and turbo inversion recovery magnitude sequence) of patient #11 demonstrate moderate decrease in brain volume with right mesiotemporal emphasis (arrows). F) Follow up test for the presence of autoantibodies to GFAP in mixed cortical/hippocampal cultures and transfected HEK293 cells. Patient serum was collected again 18 months after first testing and used in the described detection assays. Recurrently, stellate astrocytes were stained in the primary culture and only GFAP-transfected cells HEK293 reacted with patient IgG and both signals showed a high degree of overlap.

cells for 7 days at 37 °C, at 5% CO_2 in DMEM, supplemented with 10% FCS, 100U/ml pen/strep and 2 mM L-glutamine. During this time, the medium was replaced two times and the microglial cells were removed from the astrocytes by shaking the plates. For immunostaining, the cells were collected after 7 days and seeded at a density of 4×10^4 cells per well to 24-well plates which were previously treated with poly-L-lysine (100 µg/ml in PBS). Cells for Western blots remained in culture for 12–14 days.

2.5. GFAP transfected HEK cells

HEK293 cells were transfected with a plasmid encoding for human glial fibrillary acidic protein (GFAP alpha (I), based on a VB900131-8024ppx plasmid backbone, Vector Builder, Chicago, IL, USA) using established transfection procedures applying polyethyleneimine (PEI) as transfection reagent. After a transfection time of 24 h cells were fixed with 4% PFA for 20 min and processed for immunofluorescence as described below. To verify transfection efficiency and for double staining experiments with serum samples, a monoclonal anti-GFAP antibody was used (see 2.7).

2.6. Staining of cultured cells

2.6.1. Hippocampal cell cultures and purified astrocyte cultures

Fixed cells: We removed the medium from the wells, washed the cells with PBS (10%), fixed them with ice-cold methanol at 80% on coverslips for 20 min and incubated them with blocking-solution (0.1% Triton; 5% NGS; 2,0% BSA; PBS) for 1 h at room temperature. We diluted the samples (serum dilution at 1:200) in blocking-solution and incubated the cells with the patient's serum for 24 h at 4 °C. After that, cells were washed with PBS and incubated with the secondary antibody (FITC-conj. goat-a-human IgG, Dianova, #109095003, dilution: 1:100) in secondary-antibody-solution (2% BSA in PBS) for 90 min at room temperature. Again, cells were washed with PBS, stained with DAPI (4′, 6-diamidino-2-phenylindole) for 10 min and mounted with Immu-Mount (Thermo Fisher Scientific, Waltham, MA).

Live cells: Cultured cells were incubated overnight with patient serum at a dilution of 1:200 in culture medium. After removal of the medium and washing with PBS, cells were fixed and treated with secondary antibody as above.

2.6.2. HEK cells

GFAP transfected HEK cells were fixed with 4% PFA dissolved in PBS but otherwise treated as described above.

2.7. Staining of murine brain slices

Perfusion-fixed brains from adult SWISS-mice were dissected, cryoprotected and frozen at −80 °C prior to cutting into 20 µm coronar and sagittal sections including cortex, hippocampus and cerebellum. The slices were washed with PBS and incubated in blocking solution (10% NGS in PBS; 0.3% Triton-X-100) for 30 min at room temperature. The serum samples were diluted (serum dilution at 1:200) in primary-antibody-solution (10% NGS in PBS; 0.3% Triton-X-100; 0.1% NaN_3),

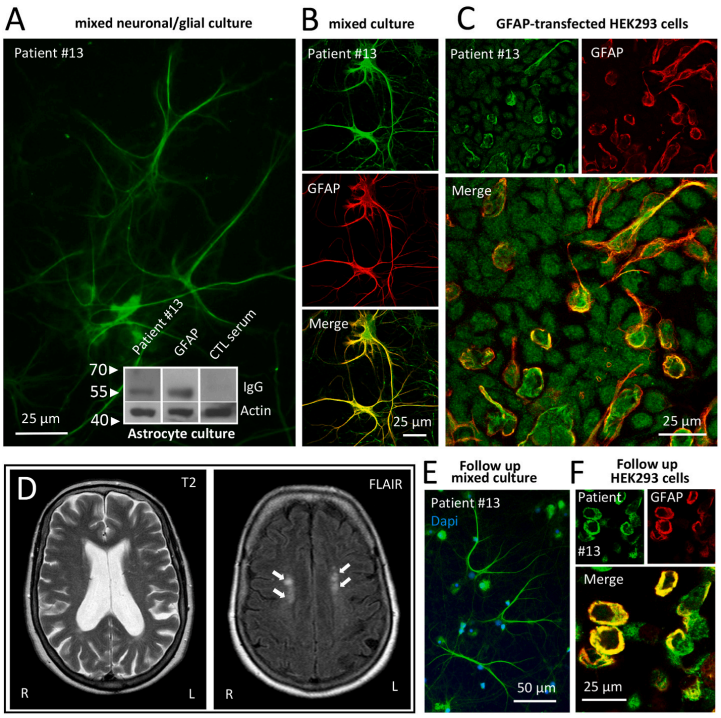

Fig. 3. Follow-up evaluation of serum autoantibodies against glial fibrillary acidic protein (GFAP) in another patient with Alzheimer's disease. A) Patient serum #13 intensely stained large, branched cells that morphologically appeared like astrocytes in mixed embryonic hippocampal/cortical cultures. Inset: Biochemical evaluation showed that incubation with patient serum resulted in a single immunoreactive band at around 55 kDa in purified astrocyte culture corresponding to commercial GFAP staining. Control serum yielded no staining. B) Patient serum antibodies co-localize with GFAP in astrocytes of mixed cultures. Cultures were double stained for human IgG and GFAP. Both signals stained filament-like structures in stellate astrocytes and showed a high degree of overlap in the soma and astrocytic processes. Confocal imaging C) Patient serum antibodies react with GFAP-transfected HEK293 cells. Only transfected cells reacted with patient IgG and signals showed a high degree of overlap with commercial GFAP staining. Confocal imaging D) Axial MRIs (T2 and fluid-attenuated inversion recovery sequence) of patient #13 demonstrate mild to moderate frontoparietal atrophy with corresponding enlargement of the lateral ventricles and periventricular white matter lesions (arrows). E) Follow up test for the presence of autoantibodies to GFAP in mixed cortical/hippocampal cultures and transfected HEK293 cells. Patient serum was collected again 22 months after first testing and used in the described detection assays. Recurrently, stellate astrocytes were stained in the primary culture and only GFAP-transfected cells HEK293 reacted with patient IgG and both signals showed a high degree of overlap.

added to the brain slices and incubated for 24 h at 4 °C. After incubating the slices, we washed them with PBS and incubated them with the secondary antibody (FITC-conj. goat-a-human IgG, Dianova, #109095003, dilution: 1:100) in secondary-antibody-solution (5% NGS in PBS; 0.1% Triton-x-100) for 1 h at room temperature in the dark. The slices were washed with PBS and mounted to the slides.

2.8. Co-staining with commercial antibodies

Co-staining against GFAP was performed on cells and brain slices, following the same protocols as used for staining without commercial antibodies. A commercial primary monoclonal mouse anti-GFAP antibody (Synaptic Systems, Göttingen, Germany, #173011, dilution 1:1000) was applied to cells or brain slices, together with the serum sample. Both secondary antibodies (FITC-conj. goat-a-human IgG, see above) and Alexa-red goat-anti-mouse 594 (MoBiTec, #A11032, dilution 1:1000) were also applied together.

2.9. Screening for co-existing antibodies

Of the sera tested positive for GFAP antibodies 12 were also routinely tested for co-existing antibodies using the standard and research autoimmune diagnostic panels by the Euroimmun AG (Lübeck, Germany). The following antigens were included: Hu, Ri, ANNA-3, Yo, Tr/DNER, Ma/Ta, GAD65, Amphiphysin, Aquaporin4, MOG, NMDA-R, AMPA-R, $GABA_B$-R, LGl1, CASPR2, IGLON5, ZIC4, DPPX, Myelin, CARPVIII, Glycine-R, mGlu-R1, mGlu-R5, $GABA_A$-R, RHO activating GTPase 26, Recoverin, Glu-RD2, Flotillin 1/2, ITPR1, Homer3, Neurochondrin, Neurexin-3-alpha, ERC1, Sez6I2, AP3B2, Contactin1, Neurofascin 155, Neurofascin 186, AT1A3, KCNA2, Dopamin-R2.

2.10. Immunoblots

For immunoblotting, whole brains from adult SWISS-mice or astrocyte cultures grown for 14 days *in vitro* were homogenized (tissue and cells were processed in PBS using a glass-Teflon homogenizer applying 10 strokes at 900 rpm with protease inhibitors added). Homogenates were spun down at 1500×*g* for 10 min, and the resulting supernatant devoid of cell nuclei was diluted in Laemmli buffer and submitted to SDS-PAGE. The membranes containing the transferred proteins were then incubated with patient or control serum at a dilution of 1:200. A mouse monoclonal antibody against GFAP (the same as used for immunofluorescence) served as a positive control. A mouse monoclonal antibody against glyceraldehyde-3-phosphate dehydrogenase (GAPDH, Merck Millipore, Darmstadt, Germany; #MAB374) or a rabbit polyclonal antibody to Actin (Sigma-Aldrich, St. Louis, MO, USA, #A5060) was used as loading control. Horseradish peroxidase coupled goat anti-human kappa light chain secondary IgG (Life Technologies, Carlsbad, CA, USA; #A18859), horse anti-mouse IgG as well as goat anti-rabbit IgG (Vector Laboratories, Burlingame, CA, USA; #PI-2000 and #PI-1000) served as secondary antibodies. Immunoreactivity was visualized by using enhanced chemiluminescence (GE Healthcare Europe GmbH, Freiburg, Germany).

2.11. Image acquisition

Images were acquired using either an upright Leica DMLB epifluorescence microscope or a Leica SL confocal microscope.

2.12. Statistics

Statistical significance of differences of frequencies of glial and GFAP

Table 3
Demographical data, dementia type, secondary diagnoses, neuropsychological testing and laboratory findings of 14 GFAP-positive patients verified by transfected HEK293 cells. Means are given and compared to GFAP-negative patients. Laboratory findings were available for 8 GFAP-positive and 53–69 (parameter-depending) GFAP-negative patients.

Patient ID	Age at blood draw	Sex	Type of dementia	Secondary diagnosis	Co-existing Autoantibodies	MMSE	pTau (181)	Total-Tau	Aβ (1–40) [pg/ml]	Aβ (1–42) [pg/ml]	Aβ Ratio	TPC (mg/l)
1	54	m	FTD		negative							
2	73	m	CAA	s/p ICH (2018)	anti-Rho GTPase-activating protein	25/30	91	839.18	11245	502	0.45	608.3
3	79	m	AD	Suspicion of NPH (2017)	negative		62	297.42	29962	537	0.18	809.5
4	61	f	AD	APP gene mutation (c2149 G > A); Epilepsy	negative							301
5	78	m	AD	s/p CRC	negative	7/30	136	1200.97	13213	483	0.37	525.8
6	67	m	AD		anti-myelin	4/30						
7	78	m	AD/SAE	s/p AIS (2012)	n.d.	17/30	31	227.34	7904	557	0.71	410.7
8	79	m	AD	s/p TIA (2017); s/p SAH (2017); RA	negative							
9	82	m	AD	Movement disorder; Lung tumor	negative		136	949	13485	699	0.52	389
10	74	m	AD	HBP, nicotine abuse; T2D	negative	21/30						593.7
11	75	f	AD		n.d.	18/30	73	535.29	17751	575	0.32	306.6
12	78	f	MCI	Suspicion of NPH (2016); organic depression disorder DDX anxiety disorder; s/p CRC	negative	27/30	100	519.8	23683	987	0.42	448.2
13	76	f	AD		negative		54	527	10467	539	0.51	504.6
14	54	f	FTD		unknown surface antigen (this study)							
Mean GFAP +	72±9					17/30 ±8.0	85 ±35	637 ±311	15963 ±6981	610 ±155	0.44 ±0.14	489,7 ±146,9
Mean GFAP –	74±9,4					22/30 ±6.3	81 ±40	617 ±422	15566 ±7682	756 ±361	0.72 ±1.1	508,07 ±211,47

AD = Alzheimer's disease; AIS = androgen insensity syndrome; CAA = cerebral amyloid angiopathy; CRC = colorectal cancer; FTD = frontotemporal dementia; HBP = high blood pressure; ICH = intracerebral hemorrhage; MCI = mild cognitive impairment; NPH = normal pressure hydrocephalus; RA = rheumatoid arthritis; SAE = subcortical arteriosclerotic encephalopathy; SAH = subarachnoid hemorrhage; TIA = transient ischemic attack; T2D = type 2 diabetes; TPC = total protein count.

antibodies between cohorts was assessed using the Chi-square test. P-values ≤ 0.05 were considered significant.

3. Results

3.1. Frequency of immunoreactivity against glial and neuronal epitopes

Sera from 127 patients diagnosed with different forms of dementia based on clinical examination, neuropsychological testing, and imaging studies (Table 1) were used for initial immunostaining on mixed murine neuronal/glial primary hippocampal/cortical cell culture to screen for antibodies directed against CNS epitopes. The majority of patients were diagnosed with Alzheimer's disease (AD, 46%), followed by mild cognitive impairment (MCI, 19%) and frontotemporal dementia (FTD, 10%). Besides various types of neurons, these cultures always contain a growing population of astrocytes co-cultured with the neurons. Based on previous studies, a serum dilution of 1:200 was applied to fixed and permeabilized cells yielding an optimized signal-to-background ratio. At the chosen experimental conditions, 45 of 127 (35.5%) sera tested positive for IgG autoantibodies, showing various glial or neuronal staining patterns (Table 2). Reactivity was mainly directed against astrocytes (35/127; 27.5%) whereas neuron staining was less frequent (17/127; 13.5%). In addition to the approach using fixed cells we also tested all 127 patient sera on live cultures. However, only 3 sera yielded a signal that was clearly above the background signal (Supplemental Figure 1). Due to this low frequency we decided to focus on fixed cells. To exclude that the observed occurrence of antibodies against CNS epitopes represents the normal proportion found in aged patients a total of 97 serum samples consisting of two cohorts was used as an age-matched control group. Immunostaining results of both control cohorts are given (Table 2). Clinical diagnoses for patients of the control cohort obtained from the Charité CSF/serum biobank (cohort 1) are shown in supplemental Table 1. Age-matched healthy controls had no autoimmune reaction at all, whereas some sera of control cohort 1 were tested positive on hippocampal cell culture. In detail, immunoreactivity was detected in 8 of 97 serum samples (8.2%, p-value of ≤ 0.001 for dementia cohort vs. total age-matched controls). Of these 8 sera, 3 samples had antibodies against astrocytes only, and 4 samples had anti-neuronal antibodies. One of the samples exhibited immunoreactivity to both astrocytes and neurons (p-value of ≤ 0.001 for antibodies to astrocytes in dementia cohort vs. total age-matched controls).

In the following, we decided to focus our further investigations on the subgroup of 35 sera obtained from dementia patients that showed autoimmune reactivity against astrocytes in our culture system.

3.2. Frequency of autoantibodies to GFAP

In order to identify targeted antigens, we tested for reactivity against GFAP, a highly abundant intermediate filament protein of the astrocyte cytoskeleton. To this end, HEK293 cells were transfected with cDNA coding for human GFAP and incubated with the 35 patient sera which reacted with astrocytes. Immunocytochemical staining revealed reactivity against GFAP in 14 samples, representing 11% of the total 127 sera, indicating the presence of IgG autoantibodies against this specific antigen. In the control group, only one patient, diagnosed with motor neuron disease, had GFAP autoantibodies, representing 1.0% of the 97 control sera (p-value of 0.003 for antibodies to GFAP in dementia cohort vs. total age-matched controls).

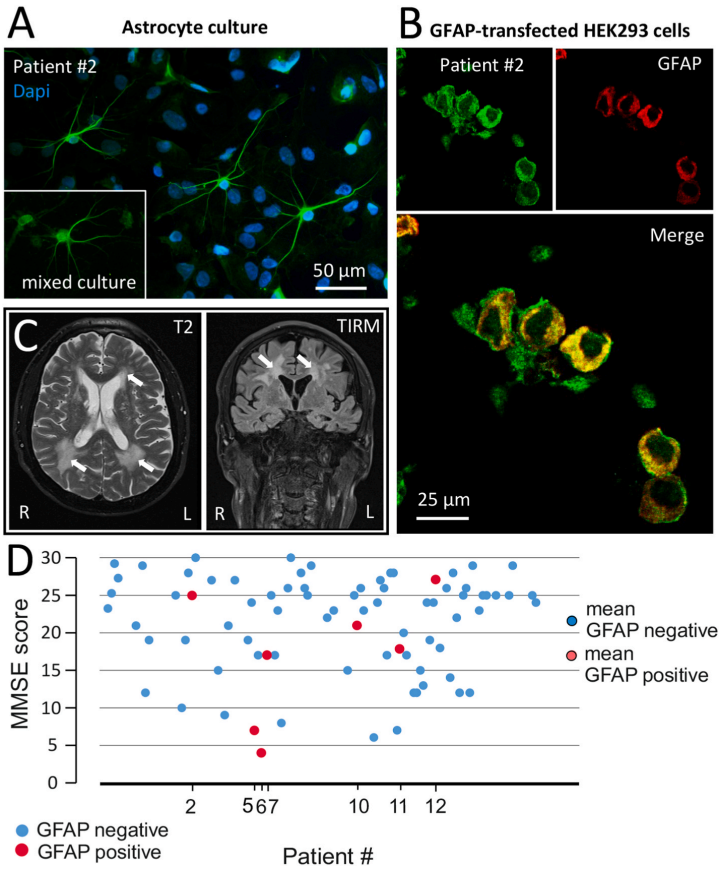

Fig. 4. Serum autoantibodies against glial fibrillary acidic protein (GFAP) in a patient with Cerebral Amyloid Angiopathy. A) Patient serum #2 intensely stained mainly large stellate astrocytes in purified astrocyte cultures. Polygonal flattened cells were only weakly stained. Inset: Patient serum also recognized astrocytes in mixed neuronal/glial cultures. B) Patient serum antibodies react with GFAP-transfected HEK293 cells. Only transfected cells reacted with patient IgG and signals showed a high degree of overlap with commercial GFAP staining. Confocal imaging C) Axial and coronal MRIs (T2 and turbo inversion recovery magnitude sequence) of patient #2 demonstrate marked ubiquitously occurring white matter gliosis (arrows). D) Cognitive screening by Mini-Mental State Examination (MMSE) was available for a total of 79 dementia patients. Blue dots indicate GFAP-negative patient sera, red dots indicate 7 screening scores available for GFAP-positive patients. Mean values are indicated on the right. (For interpretation of the references to color in this figure legend, the reader is referred to the Web version of this article.)

Follow-up after 16–22 months was possible for three dementia patients. All three of the sera were still positive for anti-GFAP autoantibodies in HEK cell assays and hippocampal cell culture.

We performed additional experiments, including 1.) Immunoblotting and 2.) Immunohistochemistry to refine our results. Biochemical analysis was performed using Western Blots on purified murine astrocyte cultures and whole brain homogenates to investigate whether serum GFAP antibodies also recognize linear epitopes. Seven of the 14 GFAP-positive sera (#1; #3; #4; #6; #9; #13; #14, all 35 sera that exhibited immunoreactivity to astrocytes were tested) exhibited immunoreactive bands in both or either one of the preparations between 50 and 55 kDa, corresponding to the molecular weight of GFAP. Representative Western blots are shown (Figs. 1 and 3). While all 14 GFAP-positive sera reacted with the typical ramified astrocyte type found when co-cultured with neurons (resembling the *in vivo* morphology) serum #8 also co-localized with GFAP in an intense filamentous staining pattern in flattened, polygonal astrocytes that usually express lower levels of GFAP (Fig. 1G). Two of the 14 sera (#11 and #13) also showed a clear astrocyte staining in fixed murine brain slices, being especially pronounced in the olfactory bulb and *Corpus callosum* (Fig. 2, serum #11). Other immunohistochemical staining procedures, such as the use of unfixed brain sections, were not in the focus of this study.

3.3. Clinical and paraclinical findings

Results for the laboratory testing on serum and CSF are given for GFAP-positive patients and compared with available data from GFAP-negative dementia patients (Table 3). The tests focused on parameters that are part of the standard protocol for the evaluation of a possible dementia diagnosis. Here we highlight the laboratory values for Amyloid-beta and Tau, which usually reach abnormal values in dementia patients. It became evident that most GFAP-positive patients had abnormal values for the majority of investigated parameters. Consequently, all mean values for Tau and Amyloid-beta were abnormal, which means that the values for pTau(181), total tau and total protein count (TPC) were increased and the values for Amyloid-beta (1–42) and beta-Amyloid ratio 42/40 were decreased. In comparison with the GFAP-negative dementia patients, most results were similar in both groups, although Amyloid-beta (1–42) and beta-Amyloid ratio 42/40 were lowered in GFAP-positive patients without reaching statistical significance. Screening for co-existing autoantibodies was performed for 12 of the 14 GFAP positive sera (EUROIMMUN Medizinische Labordiagnostik AG Lübeck, Germany). In two sera (#2 and #6) concomitant autoantibodies were detected against anti-Rho GTPase activating protein and Myelin, respectively (Table 3).

Brain MRIs were available for 11 GFAP positive patients, revealing different findings accompanying the respective diagnosis. Frequently

found pathologies associated with dementia were atrophy (seven patients) and medullary gliosis (six patients). Representative images are given for three patients (Figs. 2–4). Results of neuropsychological testing were available for 7 GFAP-positive patients by Mini-Mental State Examination (MMSE). This test is a relatively broad screening, used to examine a patient's cognitive abilities. A score of 24/30 or higher is considered as normal cognitive function, whereas a lower score suggests any kind of cognitive impairment. The GFAP positive patients had an average score of 17, compared to an average MMSE score of 22 for 72 GFAP negative dementia patients (Fig. 4D).

An illustration of the results for five exemplary patients, their experimental findings and MRI images are presented in Figs. 1–4. Demographic data and clinical characteristics of all GFAP-positive patients are shown in Table 3.

Taken together, our data provide evidence for a higher prevalence of autoantibodies to GFAP in dementia patients compared to age-matched neurological patients without dementia or healthy subjects.

4. Discussion

In the current study, we report on the prevalence of GFAP autoantibodies in dementia patients. We were able to identify GFAP as antibody target in 11% of these patients. The occurrence of these autoantibodies in a significantly higher number than in age-matched healthy controls or patients with various neurologic diseases without dementia raises questions about the relevance of these antibodies. The underlying causes for the generation of autoantibodies to brain antigens are probably not based on a single mechanism but are most likely due to a combination of events. Amongst the factors contributing to the development of autoimmunity are infections, neoplasms, genetic predisposition, or lifestyle factors. Putting the focus on dementia patients, it is assumable that also neurodegeneration plays a major role in the development of autoimmunity in the brain. On the other hand, autoimmunity might be one of many aspects that contribute to dementia. For example, the presence of preexisting or coexisting autoimmune diseases is associated with an increased risk for developing dementia as shown for patients with autoimmune rheumatic diseases (Lin et al., 2018). According to our findings, GFAP antibodies seem to be a hallmark in dementia patients. The obvious question is whether these autoantibodies are pathogenic and might contribute to the course of the disease or represent a secondary phenomenon due to the neurodegeneration. Nevertheless, this might just as well contribute to the disease development. Evidence for the association of autoantibodies to GFAP with dementia exist in the literature. ELISA-testing of sera from patients with Alzheimer's dementia and vascular dementia showed a higher rate of GFAP-autoantibodies in these patients, compared with healthy controls (Tanaka et al., 1989; Mecocci et al., 1992). A few case reports mention patients with GFAP-autoantibodies, presenting with atypical symptoms such as chronic cognitive impairment, rapid progressive dementia or parkinsonism (Natori et al., 2020; Toledano-Illan et al., 2021; Tomczak et al., 2019). Clinical symptoms improved in all patients reported in these studies following immunotherapy. Recently, a case study reported on the association of GFAP autoantibodies in serum with primary progressive aphasia, thereby extending the disease spectrum for these antibodies (Hansen et al., 2022). Mechanistically, animal studies revealed that GFAP astrocytopathy may be caused by GFAP-specific cytotoxic T-cells (Sasaki et al., 2014). Pathologic studies in humans found that CD8(+) T-cells are predominant, but also B-cells, plasma cells and macrophages are involved in the disease (Shu et al., 2018; Yuan et al., 2021; Long et al., 2018). A pooled analysis of 324 cases of classical GFAP astrocytopathy published until 2021 summarizes the clinical features, radiological findings and treatment regimes. The median age of disease onset was 45 years with no sex predominance. 19.8% had neoplasms, most commonly ovarian teratoma. 25.5% had coexisting neuronal autoantibodies, most commonly anti NMDA-R autoantibodies. MRI imaging showed characteristic linear radial enhancement in 43.7%. Treatment consisted of high-dose corticosteroids, intravenous immunoglobulins and plasma exchange. Most patients (86.5%) responded well to acute immunotherapy (Xiao et al., 2021).

Most of the previously described antineuronal autoantibodies that occur in classic autoimmune encephalitis are directed against extracellular antigens. This enables them to directly bind to living cells rendering them more likely pathogenic (Kreye et al., 2016). When focusing on autoimmune gliopathies, there are also known pathogenic autoantibodies that target extracellular proteins, for example anti-Aquaporin 4 or anti-Myelin Oligodendrocyte Glycoprotein autoantibodies in patients with Neuromyelitis optica spectrum disorder (Weinshenker and Wingerchuk, 2017). In contrast to these findings, GFAP is an intracellular antigen. Studies that investigated the pathomechanisms behind GFAP astrocytopathy stated that the disease might be T-cell mediated and the occurring anti-GFAP autoantibodies represent a secondary phenomenon still making them suitable as a disease marker (Fang et al., 2016; Yuan et al., 2021). Nevertheless, the pathomechanisms behind different autoantibodies against intracellular antigens are not fully understood. In fact, there are autoantibodies against intracellular antigens, for example synapsin, that can enter non-permeabilized, living neurons via Fcγ II/III receptor-mediated endocytosis to affect synaptic transmission (Rocchi et al., 2019). A study about GFAP autoantibodies in sera from patients with traumatic brain injury showed that these autoantibodies could enter living astrocytes in rat primary astrocyte culture and cause cell death (Zhang et al., 2014). In vitro-investigations about the pathogenicity of well-known onconeuronal autoantibodies such as Anti-Hu and Anti-Yo which occur in paraneoplastic encephalitis, showed inconsistent results. Some studies revealed that these autoantibodies are able to enter living cells and cause neurotoxicity, whereas others found no evidence or just little evidence for this hypothesis (Greenlee et al., 1993, 2010; Zaborowski and Michalak, 2013). To sum up, considering the existing literature, the pathogenicity of intracellular autoantibodies remains unclear, but the fact that autoantibodies target intracellular antigens does not make it unlikely that they could enter living cells to cause pathogenic effects.

More research is needed to find out whether the detected anti-GFAP antibodies are pathogenic, cause damage *in vivo* and, and if this is the case, contribute to the symptoms of dementia in patients who developed these autoantibodies. Regardless of its pathogenicity, it would also be intriguing to investigate the question whether the GFAP-autoantibodies could serve as a useful clinical marker for the severity and progression of the dementia symptoms as described for anti-NMDA-R autoantibodies in patients with progressive cognitive impairment (Doss et al., 2014). Another aspect that comes along with our finding of GFAP autoantibodies in dementia patients is the question of its relevance for clinical practice. Autoimmune dementia, as described before, is a relatively broad term that is not very well defined. It is generally used for a heterogenic subgroup of dementia patients in which the disease is most likely autoimmune rather than neurodegenerative. Currently, the screening for autoantibodies is not a part of the standard diagnostic process for dementia. However, it has been stated that there are "red flags", for example young age, acute or subacute onset, rapid progressing symptoms, seizures and headaches indicate a possible autoimmune dementia and should lead to testing for autoantibodies (Flanagan et al., 2017). Other features indicating an autoimmune pathogenesis are a fluctuating disease course, early psychosis, known cancer or family history of cancer and autoimmunity. Some symptoms are even strongly suggestive for certain autoantibodies for example Facio-brachial dystonic seizures in patients with LGI1-mediated autoimmune dementia. Taken together, atypical clinical or paraclinical presentation that cannot be attributed to classic causes of dementia, e.g. Alzheimer's disease, vascular dementia, Lewy-body-dementia, frontotemporal dementia or dementia in typical or atypical Parkinson's disease, should raise awareness for a possible autoimmune pathogenesis rather than a primary neurodegenerative process. It is important to improve the clinical diagnostics to identify these patients early on since some of them

improve with immunotherapy (Bastiaansen et al., 2021; Banks et al., 2021). It also needs to be discussed which methods are appropriate to diagnose single patients or even investigate larger cohorts of dementia patients for the presence of autoantibodies, since most of the previously mentioned studies only looked for various specific, already known autoantibodies using standardized screening methods. That is also the case in clinical practice, where samples are sent to specialized laboratories that detect common autoantibodies.

5. Limitations

In our study, there was no phenotype in clinical or paraclinical data specific to GFAP positive patients. This could be due to the relatively small cohort of GFAP positive patients identified. Also, a limitation of our study lies in the fact that no CSF samples were available for testing of autoantibodies to GFAP in this compartment. In classical GFAP encephalopathy, autoantibodies in CSF show higher diagnostic value compared with isolated serum GFAP autoantibodies (Friedrich et al., 2022; Xiao et al., 2021). Therefore, our data cannot be directly interpreted in the context of the classical GFAP encephalopathy manifesting as meningoencephalomyelitis. Rather, GFAP seropositive patients in our cohort did not show characteristic signs in brain imaging such as linear, radial perivascular pattern of enhancement.

In conclusion, given the clinical presentation and age of disease onset our study suggests a different phenotype associated with serum antibodies to GFAP. Altogether, GFAP seropositive patients might represent a subgroup of autoimmune dementia with anti-GFAP antibodies as a hallmark. Further studies will be needed to ascertain the pathogenicity and clinical utility of anti-GFAP antibodies.

Declaration of competing interest

All authors of the manuscript “Immunoreactivity to astrocytes in different forms of dementia: high prevalence of autoantibodies to GFAP” report no conflicts of interest.

Data availability

Data will be made available on request.

Acknowledgements

This work was supported by grants from the German Research Foundation (DFG) (grants FOR3004, PR1274/3-1, PR1274/5-1 and PR1274/9-1), by the Helmholtz Association (HIL-A03 BaoBab) and by the German Federal Ministry of Education and Research (Connect-Generate 01GM1908D) to H.P.

We thank Birgit Metze, Marion Möbes, Antje Dräger for technical assistance.

This research has been conducted using samples obtained from the Charité CSF/serum Biobank at the Central Biobank Charité (ZeBanC) whose support is acknowledged.

Appendix A. Supplementary data

Supplementary data to this article can be found online at https://doi.org/10.1016/j.bbih.2023.100609.

References

Banks, S.A., Sechi, E., Flanagan, E.P., 2021. Autoimmune encephalopathies presenting as dementia of subacute onset and rapid progression. Ther Adv Neurol Disord 14, 1756286421998906.

Bastiaansen, A.E.M., van Steenhoven, R.W., de Bruijn, M., Crijnen, Y.S., van Sonderen, A., van Coevorden-Hameete, M.H., et al., 2021. Autoimmune encephalitis resembling dementia syndromes. Neurol Neuroimmunol Neuroinflamm 8 (5).

Dalmau, J., Tüzün, E., Wu, H.Y., Masjuan, J., Rossi, J.E., Voloschin, A., et al., 2007. Paraneoplastic anti-N-methyl-D-aspartate receptor encephalitis associated with ovarian teratoma. Ann. Neurol. 61 (1), 25–36.

Doss, S., Wandinger, K.P., Hyman, B.T., Panzer, J.A., Synofzik, M., Dickerson, B., et al., 2014. High prevalence of NMDA receptor IgA/IgM antibodies in different dementia types. Ann. Clin. Trans. Neurol. 1 (10), 822–832.

Dubey, D., Hinson, S.R., Jolliffe, E.A., Zekeridou, A., Flanagan, E.P., Pittock, S.J., et al., 2018. Autoimmune GFAP astrocytopathy: prospective evaluation of 90 patients in 1year. J. Neuroimmunol. 321, 157–163.

Fang, B., McKeon, A., Hinson, S.R., Kryzer, T.J., Pittock, S.J., Aksamit, A.J., et al., 2016. Autoimmune glial fibrillary acidic protein astrocytopathy: a novel meningoencephalomyelitis. JAMA Neurol. 73 (11), 1297–1307.

Flanagan, E.P., McKeon, A., Lennon, V.A., Boeve, B.F., Trenerry, M.R., Tan, K.M., et al., 2010. Autoimmune dementia: clinical course and predictors of immunotherapy response. Mayo Clin. Proc. 85 (10), 881–897.

Flanagan, E.P., Hinson, S.R., Lennon, V.A., Fang, B., Aksamit, A.J., Morris, P.P., et al., 2017. Glial fibrillary acidic protein immunoglobulin G as biomarker of autoimmune astrocytopathy: analysis of 102 patients. Ann. Neurol. 81 (2), 298–309.

Folli, F., Solimena, M., Cofiell, R., Austoni, M., Tallini, G., Fassetta, G., et al., 1993. Autoantibodies to a 128-kd synaptic protein in three women with the stiff-man syndrome and breast cancer. N. Engl. J. Med. 328 (8), 546–551.

Friedrich, M., Hartig, J., Prüss, H., Ip, C.W., Volkmann, J., 2022. Rapidly progressive dementia: extending the spectrum of GFAP-astrocytopathies? Ann Clin Transl Neurol 9 (3), 410–415.

Giannoccaro, M.P., Gastaldi, M., Rizzo, G., Jacobson, L., Vacchiano, V., Perini, G., et al., 2021. Antibodies to neuronal surface antigens in patients with a clinical diagnosis of neurodegenerative disorder. Brain Behav. Immun. 96, 106–112.

Greenlee, J.E., Parks, T.N., Jaeckle, K.A., 1993. Type IIa (‘anti-Hu’) antineuronal antibodies produce destruction of rat cerebellar granule neurons in vitro. Neurology 43 (10), 2049–2054.

Greenlee, J.E., Clawson, S.A., Hill, K.E., Wood, B.L., Tsunoda, I., Carlson, N.G., 2010. Purkinje cell death after uptake of anti-Yo antibodies in cerebellar slice cultures. J. Neuropathol. Exp. Neurol. 69 (10), 997–1007.

Hansen, N., Bartels, C., Stöcker, W., Wiltfang, J., Timäus, C., 2021. Case report: anti-flotillin 1/2 autoantibody-associated atypical dementia. Front. Psychiatr. 12, 626121.

Hansen, N., Stöcker, W., Wiltfang, J., Bartels, C., Rentzsch, K., Bouter, C., 2022. Case report: semantic variant of primary progressive aphasia associated with anti-glial fibrillary acid protein autoantibodies. Front. Immunol. 12, 760021.

Höltje, M., Mertens, R., Schou, M.B., Saether, S.G., Kochova, E., Jarius, S., et al., 2017. Synapsin-antibodies in psychiatric and neurological disorders: prevalence and clinical findings. Brain Behav. Immun. 66, 125–134.

Irani, S.R., Alexander, S., Waters, P., Kleopa, K.A., Pettingill, P., Zuliani, L., et al., 2010. Antibodies to Kv1 potassium channel-complex proteins leucine-rich, glioma inactivated 1 protein and contactin-associated protein-2 in limbic encephalitis, Morvan’s syndrome and acquired neuromyotonia. Brain : J. Neurol. 133 (9), 2734–2748.

Kimura, A., Takekoshi, A., Yoshikura, N., Hayashi, Y., Shimohata, T., 2019. Clinical characteristics of autoimmune GFAP astrocytopathy. J. Neuroimmunol. 332, 91–98.

Kreye, J., Wenke, N.K., Chayka, M., Leubner, J., Murugan, R., Maier, N., et al., 2016. Human cerebrospinal fluid monoclonal N-methyl-D-aspartate receptor autoantibodies are sufficient for encephalitis pathogenesis. Brain : J. Neurol. 139 (Pt 10), 2641–2652.

Lai, M., Hughes, E.G., Peng, X., Zhou, L., Gleichman, A.J., Shu, H., et al., 2009. AMPA receptor antibodies in limbic encephalitis alter synaptic receptor location. Ann. Neurol. 65 (4), 424–434.

Lancaster, E., Lai, M., Peng, X., Hughes, E., Constantinescu, R., Raizer, J., et al., 2010. Antibodies to the GABA(B) receptor in limbic encephalitis with seizures: case series and characterisation of the antigen. Lancet Neurol. 9 (1), 67–76.

Li, X., Yuan, J., Liu, L., Hu, W., 2019. Antibody-LGI 1 autoimmune encephalitis manifesting as rapidly progressive dementia and hyponatremia: a case report and literature review. BMC Neurol. 19 (1), 19.

Lin, T.M., Chen, W.S., Sheu, J.J., Chen, Y.H., Chen, J.H., Chang, C.C., 2018. Autoimmune rheumatic diseases increase dementia risk in middle-aged patients: a nationwide cohort study. PLoS One 13 (1), e0186475.

Long, Y., Liang, J., Xu, H., Huang, Q., Yang, J., Gao, C., et al., 2018. Autoimmune glial fibrillary acidic protein astrocytopathy in Chinese patients: a retrospective study. Eur. J. Neurol. 25 (3), 477–483.

Mecocci, P., Parnetti, L., Donato, R., Santucci, C., Santucci, A., Cadini, D., et al., 1992. Serum autoantibodies against glial fibrillary acidic protein in brain aging and senile dementias. Brain Behav. Immun. 6 (3), 286–292.

Meinck, H.M., Faber, L., Morgenthaler, N., Seissler, J., Maile, S., Butler, M., et al., 2001. Antibodies against glutamic acid decarboxylase: prevalence in neurological diseases. J. Neurol. Neurosurg. Psychiatry 71 (1), 100–103.

Natori, T., Shindo, K., Okumura, A., Kimura, A., Takiyama, Y., 2020. A treatable case of autoimmune GFAP astrocytopathy presenting chronic progressive cognitive impairment. Neurol. Sci. 41 (10), 2999–3002.

Petit-Pedrol, M., Armangue, T., Peng, X., Bataller, L., Cellucci, T., Davis, R., et al., 2014. Encephalitis with refractory seizures, status epilepticus, and antibodies to the GABAA receptor: a case series, characterisation of the antigen, and analysis of the effects of antibodies. Lancet Neurol. 13 (3), 276–286.

Piepgras, J., Höltje, M., Otto, C., Harms, H., Satapathy, A., Cesca, F., et al., 2015. Intrathecal immunoglobulin A and G antibodies to synapsin in a patient with limbic encephalitis. Neurol Neuroimmunol Neuroinflamm 2 (6), e169.

Rocchi, A., Sacchetti, S., De Fusco, A., Giovedi, S., Parisi, B., Cesca, F., Höltje, M., Ruprecht, K., Ahnert-Hilger, G., Benfenati, F., 2019. Autoantibodies to synapsin I sequestrate synapsin I and alter synaptic function. Cell Death Dis. 10 (11), 864.
Sasaki, K., Bean, A., Shah, S., Schutten, E., Huseby, P.G., Peters, B., et al., 2014. Relapsing-remitting central nervous system autoimmunity mediated by GFAP-specific CD8 T cells. J.Immunol. (Baltimore, Md. 192 (7), 3029–3042, 1950.
Savas, M., Tzartos, J., Kucukali, C.I., Dursun, E., Karagiorgou, K., Gezen-Ak, D., et al., 2021. Glial fibrillary acidic protein (GFAP)-antibody in children with focal seizures of undetermined cause. Acta Neurol. Belg. 121 (5), 1275–1280.
Shu, Y., Long, Y., Chang, Y., Li, R., Sun, X., Wang, Y., et al., 2018. Brain immunohistopathology in a patient with autoimmune glial fibrillary acidic protein astrocytopathy. Neuroimmunomodulation 25 (1), 1–6.
Tanaka, J., Nakamura, K., Takeda, M., Tada, K., Suzuki, H., Morita, H., et al., 1989. Enzyme-linked immunosorbent assay for human autoantibody to glial fibrillary acidic protein: higher titer of the antibody is detected in serum of patients with Alzheimer's disease. Acta Neurol. Scand. 80 (6), 554–560.
Toledano-Illan, C., Esparragosa Vazquez, I., Zelaya Huerta, M.V., Rosales Castillo, J.J., Paternain Nuin, A., Arbizu Lostao, J., et al., 2021. Autoimmune glial fibrillary acidic protein astrocytopathy: case report of a treatable cause of rapidly progressive dementia. J. Neurol. 268 (6), 2256–2258.
Tomczak, A., Su, E., Tugizova, M., Carlson, A.M., Kipp, L.B., Feng, H., et al., 2019. A case of GFAP-astroglial autoimmunity presenting with reversible parkinsonism. Mult Scler Relat Disord 39, 101900.
Wei, P., Zhang, W., Yang, L.S., Zhang, H.S., Xu, X.E., Jiang, Y.H., et al., 2013. Serum GFAP autoantibody as an ELISA-detectable glioma marker. Tumour biology : J. Int. Soc. Oncodev. Biol. Med. 34 (4), 2283–2292.
Weinshenker, B.G., Wingerchuk, D.M., 2017. Neuromyelitis spectrum disorders. Mayo Clin. Proc. 92 (4), 663–679.
Xiao, J., Chen, X., Shang, K., Tang, Y., Chen, M., Deng, G., et al., 2021. Clinical, neuroradiological, diagnostic and prognostic profile of autoimmune glial fibrillary acidic protein astrocytopathy: a pooled analysis of 324 cases from published data and a single-center retrospective study. J. Neuroimmunol. 360, 577718.
Yoo, J.Y., Hirsch, L.J., 2014. Limbic encephalitis associated with anti-voltage-gated potassium channel complex antibodies mimicking Creutzfeldt-Jakob disease. JAMA Neurol. 71 (1), 79–82.
Younes, K., Lepow, L.A., Estrada, C., Schulz, P.E., 2018. Auto-antibodies against P/Q- and N-type Voltage-dependent Calcium Channels Mimicking Frontotemporal Dementia, vol. 6. SAGE open medical case reports, 2050313x17750928.
Yuan, Z., Li, H., Huang, L., Fu, C., Chen, Y., Zhi, C., et al., 2021. CD8(+) T-cell predominance in autoimmune glial fibrillary acidic protein astrocytopathy. Eur. J. Neurol. 28 (6), 2121–2125.
Zaborowski, M.P., Michalak, S., 2013. Cell-mediated immune responses in paraneoplastic neurological syndromes. Clin. Dev. Immunol. 2013, 630602.
Zhang, Z., Zoltewicz, J.S., Mondello, S., Newsom, K.J., Yang, Z., Yang, B., et al., 2014. Human traumatic brain injury induces autoantibody response against glial fibrillary acidic protein and its breakdown products. PLoS One 9 (3), e92698.

frontiers | Frontiers in Cellular Neuroscience

TYPE Original Research
PUBLISHED 30 January 2023
DOI 10.3389/fncel.2023.1077204

OPEN ACCESS

EDITED BY
Michael Fleischer,
Essen University Hospital, Germany

REVIEWED BY
Zhilin Li,
University of Helsinki, Finland
Ashutosh Kumar,
All India Institute of Medical Sciences (Patna), India
Anuska V. Andjelkovic,
University of Michigan, United States

*CORRESPONDENCE
Markus Höltje
markus.hoeltje@charite.de

SPECIALTY SECTION
This article was submitted to Cellular Neuropathology, a section of the journal Frontiers in Cellular Neuroscience

RECEIVED 22 October 2022
ACCEPTED 09 January 2023
PUBLISHED 30 January 2023

CITATION
Li LY, Kreye J, Burek M, Cordero-Gomez C, Barthel PC, Sánchez-Sendín E, Kornau H-C, Schmitz D, Scharf M, Meybohm P, Reincke SM, Prüss H and Höltje M (2023) Brain blood vessel autoantibodies in patients with NMDA and $GABA_A$ receptor encephalitis: identification of unconventional Myosin-X as target antigen. Front. Cell. Neurosci. 17:1077204. doi: 10.3389/fncel.2023.1077204

Brain blood vessel autoantibodies in patients with NMDA and $GABA_A$ receptor encephalitis: identification of unconventional Myosin-X as target antigen

Lucie Y. Li[1], Jakob Kreye[2,3,4], Malgorzata Burek[5], César Cordero-Gomez[2,3], Paula C. Barthel[1], Elisa Sánchez-Sendín[2,3], Hans-Christian Kornau[2,6], Dietmar Schmitz[2,6,7,8,9], Madeleine Scharf[10], Patrick Meybohm[5], S. Momsen Reincke[2,3], Harald Prüss[2,3] and Markus Höltje[1]*

[1]Institute of Integrative Neuroanatomy Berlin, Charité-Universitätsmedizin Berlin, corporate member of Freie Universität Berlin, Humboldt-Universität zu Berlin and Berlin Institute of Health, Berlin, Germany, [2]German Center for Neurodegenerative Diseases (DZNE) Berlin, Berlin, Germany, [3]Department of Neurology and Experimental Neurology, Charité-Universitätsmedizin Berlin, corporate member of Freie Universität Berlin, Humboldt-Universität Berlin and Berlin Institute of Health, Berlin, Germany, [4]Department of Pediatric Neurology, Charité-Universitätsmedizin Berlin, corporate member of Freie Universität Berlin and Humboldt-Universität zu Berlin and Berlin Institute of Health, Berlin, Germany, [5]Department of Anaesthesiology, Intensive Care, Emergency and Pain Medicine, University Hospital Würzburg, Würzburg, Germany, [6]Charité-Universitätsmedizin Berlin, corporate member of Freie Universität Berlin, Humboldt-Universität zu Berlin and Berlin Institute of Health, Neuroscience Research Center, Berlin, Germany, [7]Max Delbrück Center for Molecular Medicine in the Helmholtz Association, Berlin, Germany, [8]Einstein Center for Neurosciences Berlin, Berlin, Germany, [9]Bernstein Center for Computational Neuroscience Berlin, Berlin, Germany, [10]Institute of Experimental Immunology, EUROIMMUN AG, Lübeck, Germany

Introduction: The antibody repertoire from CSF-derived antibody-secreting cells and memory B-cells in patients with encephalitis contains a considerable number of antibodies that do not target the disease-defining autoantigen such as the GABA or NMDA receptors. This study focuses on the functional relevance of autoantibodies to brain blood vessels in patients with $GABA_A$ and NMDA receptor encephalitis.

Methods: We tested 149 human monoclonal IgG antibodies from the cerebrospinal fluid of six patients with different forms of autoimmune encephalitis on murine brain sections for reactivity to blood vessels using immunohistochemistry. Positive candidates were tested for reactivity with purified brain blood vessels, effects on transendothelial electrical resistance (TEER), and expression of tight junction proteins as well as gene regulation using human brain microvascular endothelial hCMEC/D3 cells as *in vitro* blood-brain barrier model. One blood-vessel reactive antibody was infused intrathecally by pump injection in mice to study *in vivo* binding and effects on tight junction proteins such as Occludin. Target protein identification was addressed using transfected HEK293 cells.

Results: Six antibodies reacted with brain blood vessels, three were from the same patient with $GABA_A$R encephalitis, and the other three were from different patients with NMDAR encephalitis. One antibody from an NMDAR encephalitis patient, mAb 011-138, also reacted with cerebellar Purkinje cells. In this case, treatment of hCMEC/D3 cells resulted in decreased TEER, reduced Occludin expression, and mRNA levels. Functional relevance *in vivo* was confirmed as Occludin downregulation was observed in mAb 011-138-infused animals. Unconventional Myosin-X was identified as a novel autoimmune target for this antibody.

10.3389/fncel.2023.1077204

Discussion: We conclude that autoantibodies to blood vessels occur in autoimmune encephalitis patients and might contribute to a disruption of the blood-brain barrier thereby suggesting a potential pathophysiological relevance of these antibodies.

KEYWORDS

blood-brain barrier, autoimmunity, encephalitis, occludin, Myosin-X

Introduction

Autoantibodies associated with neurological diseases have deeply changed the clinical landscape and our understanding of immunological processes in the nervous system. Especially antibodies against neuronal surface receptors turned out to be directly pathogenic, hallmarking previously unclassified disease entities. In anti-N-methyl-D-aspartate receptor (NMDAR) encephalitis, antibodies targeting the NR1 subunit reduce surface NMDA receptor clusters and disrupt synaptic currents (Hughes et al., 2010; Kreye et al., 2016). Patients develop psychiatric symptoms typically involving behavioral changes, catatonia, hallucination as well as autonomic fluctuations and seizures in the course of the disease (Dalmau et al., 2007). The more recently discovered anti-γ-aminobutyric acid A receptor ($GABA_AR$) encephalitis is characterized by antibodies reducing the synaptic and extra-synaptic density of $GABA_A$ receptors and exerting electrophysiological changes in cultured neurons (Ohkawa et al., 2014; Petit-Pedrol et al., 2014; Pettingill et al., 2015). Patients characteristically present with catatonia, seizures, refractory status epilepticus, cognitive impairment, and MRI abnormalities (Ohkawa et al., 2014; Petit-Pedrol et al., 2014; Pettingill et al., 2015; Spatola et al., 2017).

Despite the advances in unraveling the molecular mechanisms of anti-NMDAR and anti-$GABA_AR$ antibodies, knowledge about how they gain access to central nervous system (CNS) targets is still lacking. Possible mechanisms of immune system components transmigrating the blood-brain barrier (BBB) have been investigated in other inflammatory autoimmune disorders. In neuropsychiatric systemic lupus erythematodes (NPSLE), BBB disruption has been demonstrated to be a crucial step in disease development (Kowal et al., 2004; Huerta et al., 2006; Hirohata et al., 2014). This process is fueled by endothelial antibody binding and upregulating the expression of proinflammatory cytokines and leukocyte adhesion molecules (Meroni et al., 2003; Armitage et al., 2004; Yoshio et al., 2013). Furthermore, for neuromyelitis optica (NMO) it has been shown that BBB disruption correlates with disease severity (Tomizawa et al., 2012). Findings in NMO have uncovered monoclonal antibodies targeting Glucose-regulated protein 78 (GRP78), which after repeated administration, caused extravasation of serum albumin, IgG, and fibrinogen in mouse brains (Shimizu et al., 2017). Shortly after, GRP78 antibodies were also discovered to impair the BBB in patients with paraneoplastic cerebellar degeneration with Lambert-Eaton myasthenic syndrome (PCD-LEMS), thereby potentially allowing access of pathogenic autoantibodies (Shimizu et al., 2019). Thus, antibodies targeting blood vessels can be directly pathogenic by inducing an endothelial pro-inflammatory phenotype, can cause BBB dysfunction, and possibly even promote the transition of macromolecules through the BBB.

Additionally, studies of recombinant human monoclonal antibodies (mAbs) have demonstrated that recombinant mAbs from CSF-derived antibody-secreting cells and memory B-cells especially in patients with NMDAR encephalitis do not only target the disease-defining autoantigen (Kreye et al., 2016, 2021). Rather, the majority of antibodies strongly react with further brain epitopes. Their possible involvement in the disease pathomechanism remains unclear. Hence, with our non-biased approach using recombinant production of CSF-derived mAbs (Kreye et al., 2016, 2021), we aimed to further investigate the intrathecal human monoclonal antibody repertoire. Using immunofluorescence methods on murine brain tissue we identified a subgroup of blood vessel reactive mAbs to a similar extent in patients diagnosed with NMDAR encephalitis and $GABA_AR$ encephalitis.

To our knowledge, this is the first characterization of autoantibodies to brain blood vessels in NMDAR encephalitis and $GABA_AR$ encephalitis patients. We illustrate binding to brain blood vessels *in vitro* and replicate characteristic binding *in vivo*. Furthermore, in this qualitative study, we identified Myosin-X as the target antigen for one selected mAb and showed its functional effects *in vitro* and *in vivo*. Collectively, we provide the first evidence for a putative contribution of brain blood vessel reactive mAbs to disease development.

Materials and methods

Immunohistochemistry on mouse brain sections

For tissue sections of unfixed mice brains, animals were sacrificed, brains were removed and snap-frozen in −50°C cold 2-methyl butane. Twenty micrometer sagittal sections were cut and processed as described previously (Kreye et al., 2016, 2021).

Indirect immunofluorescence assay on monkey and rat brain sections

Stainings were performed using slides with a biochip screening array of brain tissue cryosections (cerebellum of rat and *Macaca mulatta*). Each biochip mosaic was incubated with 35 µl of PBS-diluted sample at 4°C for 16 h in a humidity chamber. In the second step, Alexa488-labelled goat anti-human IgG (Jackson Research, Suffolk, United Kingdom), was applied and incubated at RT for 2 h. Results were evaluated independently by two observers using a fluorescence microscope (EUROStar II, Euroimmun AG, Lübeck, Germany).

Generation of human monoclonal antibodies

Human monoclonal antibodies were previously generated as recombinant proteins from patients with NMDA receptor encephalitis or $GABA_A$ receptor encephalitis (Kreye et al., 2016, 2021; Nikolaus et al., 2018). The diagnosis was confirmed by: (i) the presence of autoantibodies against the respective autoantigen in the patient's cerebrospinal fluid as detected in a commercial cell-based assay (EUROIMMUN, Lübeck Germany); and by (ii) typical neurological symptoms. For monoclonal antibody isolation, we used established methods (Kreye et al., 2016, 2020, 2021; Reincke et al., 2020). In brief, from patients' cerebrospinal fluid, single antibody-secreting cells and B cells were isolated using fluorescence-activated cell sorting. From single-cell cDNA variable immunoglobulin encoding genes were amplified, sequenced, and cloned into expression vectors. Pairs of functional heavy and light chain vectors were used to transfect human embryonic kidney (HEK293T) cells using Polyethylenimine (Polysciences, Inc., Warrington, USA). On day three/four and day seven after transfection cell culture supernatants were harvested, then centrifuged at 2,000× *g* for 5 min at 4°C to remove cell debris before sodium acid was added to a concentration of 0.05% to prevent bacterial growth. The human IgG concentration in cell culture supernatants was determined using a commercial ELISA kit (Mabtech, Nacka Strand, Sweden) following the provider's instructions. For functional assays, mAbs were purified from supernatants using Protein G Sepharose beads (GE Healthcare), then dialyzed against PBS and sterile-filtered using 0.2 μm filter units (GE Healthcare). Recombinant mGO53 antibody served as a control antibody in *in vitro* and *in vivo* experiments.

Commercial antibodies

A monoclonal anti-Myosin-X antibody was purchased from Santa Cruz Biotechnology (# sc-166720, St. Cruz, USA). A monoclonal anti-smooth muscle actin (SMA) antibody was from Agilent Dako (#M0851, Santa Clara, USA). A rat monoclonal anti-CD31 antibody was from BD Biosciences (#553708, Franklin Lakes, NJ, USA). A monoclonal anti-CD34 antibody was from Arigo Biolaboratories (#ARG52756, Hsinchu City, Taiwan). A polyclonal anti-Collagen IV antibody was purchased from Abcam (#ab6586, Cambridge, UK). Polyclonal anti-Occludin and anti-Claudin5 antibodies were from Thermo Fisher Scientific (#71-1500 and #34-1600; Waltham, USA). A monoclonal anti-VE-cadherin antibody was from Cell Signaling (#2500, Danvers, USA). A mouse monoclonal anti-ZO-1 antibody was from Thermo Fisher Scientific (#33-9100).

Cell culture of human cerebral endothelial cells

Immortalized human cerebral microvascular endothelial cells hCMEC/D3 (Weksler et al., 2005) obtained from CELLutions Biosystems Inc. (#CLU512, Burlington, Ontario, Canada) were grown to confluence on coverslips. Cells were then used for either immunofluorescence staining on fixed cells or live incubation. For the fixed approach, endothelial cells were incubated with 4% PFA for 10 min and subsequently washed twice with PBS. Primary human antibodies (5 μg/ml) remained on the coverslips overnight at 4°C. For live incubation, a patient antibody was added to the medium at 5 μg/ml overnight at 36°C and 5% CO_2. After fixation with 4% PFA for 20 min cells were incubated with a secondary antibody for 2 h at RT in the dark.

Transfection

Human embryonic kidney (HEK) 293 cells were cultured in 24-well multiplates to 70% confluency and transfected with 1 μg plasmid cDNA coding for eGFPC1-hMyoX (Addgene, #47608) per well for 24 h using Polyethylenimine as transfection reagent. Transfected cells were fixed with 4% paraformaldehyde for 20 min at 4°C. Cells were subsequently permeabilized with 0.1% Triton X-100. Thereafter, cells were incubated with commercial antibodies at indicated concentrations or human monoclonal antibodies at 5 μg/ml.

Purification of mouse brain vessels

Purification of mouse brain vessels was performed following a previously described protocol (Boulay et al., 2015). In brief, myelin was removed from adult mice brain homogenate using an 18% dextran solution and density gradient centrifugation. From the resulting suspension brain blood vessels between 30 and 100 μm and >100 μm were collected by a sequence of filtering steps and directly used for immunohistochemistry or lysed for further analysis.

Measurement of TEER (transendothelial electrical resistance)

Human hCMEC/D3 cells were seeded onto Matrigel-coated trans-well inserts (0.4 μm pore size, Corning) at a density of 40×10^3 in ECM Medium (PELOBiotech, Martinsried, Germany) supplemented with 5% FCS. After 5 days ECM was depleted of growth factors and FCS was reduced to 0.5% for differentiation. Subsequently, endothelial cells were treated with patient antibodies at the indicated concentrations or left untreated for an additional 24 or 48 h. TEER measurements across each trans-well were conducted using chopstick electrodes (STX-PLUS, WPI, Sarasota, Fl, USA) and an Epithelial-Volt/Ohm-Meter (EVOM3, WPI). The TEER values of blank filters were subtracted from the measured values before calculations. Values were measured in triplicates.

Real-time PCR

RNA was isolated using the NucleoSpin® RNA Isolation Kit (Machery-Nagel, Düren, Germany) according to the manufacturer's instructions. Total RNA (1 μg) was reverse transcribed using the High Capacity cDNA Reverse Transcription Kit (Thermo Fisher Scientific). The following TaqMan probes (Thermo Fisher Scientific) were used: Hs00901465_m1 (CDH5, VE-cadherin), Hs01558409_m1 (CANX, Calnexin), Hs00533949_s1 (CLDN5,

Claudin5), Hs00202485_m1 (MYO10, Myosin-X), Hs00170162_m1 (OCLN, Occludin), Hs01551861_m1 (TJP1, ZO-1) with the TaqMan® Fast Advanced Master Mix in the QuantStudio™ 7 Flex Real-Time PCR System (Thermo Fisher Scientific). CANX was used as an endogenous control. The relative expression was calculated using the comparative Ct method with QuantStudio™ Real-Time PCR Software v1.7.1.

Membrane preparations

hCMEC/D3 cells were grown to confluency, seeded in 6-well plates, and cultured for 48 h with the respective antibodies as indicated. Following the removal of medium, the cells were washed with PBS, harvested, homogenized, and lysed in a glass/teflon homogenizer under hypoosmotic conditions. Homogenates were centrifuged at 1,043× *g* for 10 min to obtain a postnuclear supernatant. The resulting supernatant was centrifuged at 267,008× *g* for 30 min to obtain highly enriched cellular membranes. Membrane fractions were subjected to immunoblot analysis.

Immunoprecipitation

Triton-X100 (1%) lysate from monkey (*Macaca mulatta)* cerebella was centrifuged at 21,000× *g* at 4°C for 15 min and clear supernatants were incubated with the patient's serum (diluted 1:33) at 4°C for 3 h. The samples were then incubated with Protein G Dynabeads (ThermoFisher Scientific, Dreieich, Germany) at 4°C overnight to capture immunocomplexes. The beads were washed 3 times with PBS and eluted with NuPage LDS sample buffer (ThermoFisher Scientific) containing 25 mmol/L dithiothreitol at 70°C for 10 min. Carbamidomethylation with 59 mM iodoacetamide (Bio-Rad, Hamburg, Germany) was performed prior to SDS-PAGE (NuPAGE, ThermoFisher Scientific). Separated proteins were visualized with Coomassie Brillant Blue (G-250; Merck), and identified by mass spectrometric analysis or were applied for Western Blot.

Intrathecal antibody infusion

Experimental animals were randomized for the different treatment groups by an independent investigator. 10–12 weeks old C57BL6/J mice received either mAb 011-138 or control mAb mGO53 (100 μg over 7 days, 200 μg over 14 days, 1 μg/h). Antibody cerebroventricular infusion was performed using osmotic pumps (model 1002, Alzet, Cupertino, CA). Pump characteristics included: volume 100 μl and flow rate 0.25 μl/h. For pump implantation, mice were placed in a stereotaxic frame and a cannula was inserted into the right ventricle (coordinates: 0.2 mm posterior and ± 1.00 mm lateral from bregma, depth 2.2 mm). The cannula was connected to a pump, which was subcutaneously implanted in the interscapular space of the animals. After pump implantation, the animals were daily monitored to assess clinical symptoms and weight variations. Mice were sacrificed either on day 7 or day 14, brains were removed and snap-frozen in 2-methylbutan for immunohistochemistry. In addition, blood samples were collected for serum preparation (2,000× *g* for 15 min, RT). Unfixed sections from mouse brains were either incubated with FITC-coupled anti-human IgG secondary antibody alone or serum from treated mice prior to the application of secondary antibody.

Fluorescence intensity measurements

To analyze the intensity of IgG binding to the brain blood vessel images were taken at 40× magnification using a Leica DMLB epifluorescence microscope. Image areas attributed to vessel walls were cropped and average gray scale brightness values were calculated by the histogram function of Adobe Photoshop CS6 software.

Results

Autoimmunity to brain blood vessels and Purkinje cells

We have previously reported that the CSF antibody repertoire from patients with NMDAR encephalitis and $GABA_AR$ encephalitis does not only include mAbs that are autoreactive to the disease-defining antigen. Besides neuronal and glial binding, several CSF antibodies exhibit autoreactivity to brain blood vessels with yet unknown functional relevance. Here, we systematically screened 149 CSF-derived mAbs from six autoimmune encephalitis patients, including 67 from $GABA_AR$ encephalitis, 61 from NMDAR encephalitis, and 21 from non-$GABA_AR$/non-NMDAR encephalitis patients for blood vessel autoreactivity in murine brain tissue. We identified six mAbs with prominent brain blood vessel reactivity, of which three (113-109, 113-111, 113-126) had been isolated from a $GABA_AR$ encephalitis patient (Nikolaus et al., 2018; Kreye et al., 2021) and three (080-221, 003-151, 011-138) from NMDAR encephalitis patients (Kreye et al., 2016). Patient details can be obtained from these previous publications.

Among the three blood vessel reactive antibodies obtained from one young patient with $GABA_AR$ encephalitis, mAb 113–109 provided remarkably strong staining of vessels of all diameters throughout the entire brain (**Figure 1A**). The homogeneous staining of mAb 113–109 throughout brain blood vessels of all sizes suggested an epitope structure present up to the capillary level. Blood vessel staining was further confirmed using co-stainings against the basal membrane constituent Collagen IV and the blood vessel endothelial cell marker CD31 and is shown exemplarily (**Figure 1B**). In contrast, mAbs 113-111 and 113-126 obtained from the same patient stained primarily large-sized vessels (**Figures 1C,D**, see also **Supplementary Figure 1** for co-stainings with CD31). Additionally, in blood vessels isolated from adult mouse brains, all three antibodies showed clear staining on the 30–100 μm fraction of brain blood vessels (**Figure 1E**).

An additional three blood vessel reactive mAbs were detected among the recombinant mAbs derived from the CSF of anti-NMDAR encephalitis patients. These include mAb 080-221 which showed prominent staining of vessels of all sizes including the capillaries (**Figure 2A**, for capillary staining, see inset a, see also **Supplementary Figure 1**). In contrast, the other two mAbs predominantly stained mid to large-size blood vessels. Vessels stained by mAb 003–151 showed a less homogeneous and more speckled pattern (**Figure 2B** and **Supplementary Figure 1**). In addition to the strong reactivity

10.3389/fncel.2023.1077204

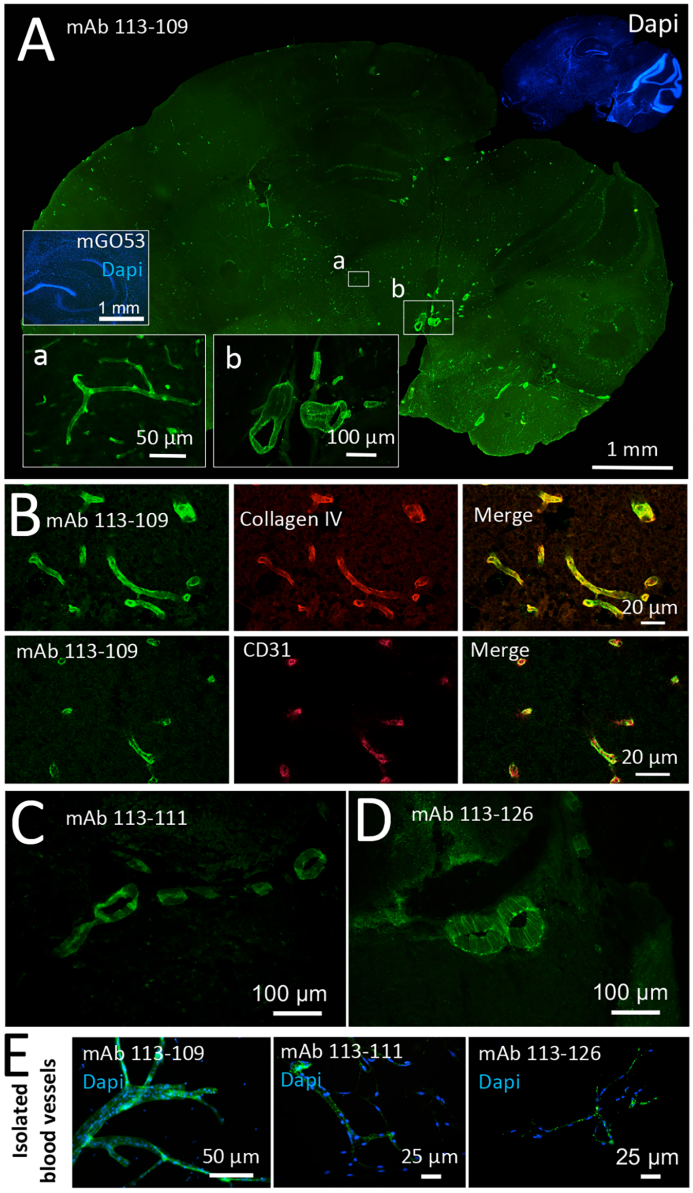

FIGURE 1
Recombinant monoclonal antibodies from a $GABA_AR$ encephalitis patient bind to brain blood vessels. Sections from unfixed and unpermeabilized adult mouse brains were incubated with 5 µg/ml of the respective monoclonal antibodies obtained from a patient diagnosed with $GABA_AR$ encephalitis. Visualization of tissue binding was performed using a FITC-coupled anti-human IgG secondary antibody. **(A)** Sagittal brain section incubated with human monoclonal antibody (mAb) 113-109. Prominent staining of blood vessels of all diameters in all brain regions was obtained (see insets a and b). Incubation with control mAb mGO53 yielded no tissue staining (inset). **(B)** Double stainings against Collagen IV (upper panel) and CD31 (lower panel) confirm immunoreactivity of mAb 113-109 to blood vessels. **(C)** Sagittal brain section incubated with mAb 113-111. Prominent staining of large blood vessels was obtained in all brain regions (the area between the cerebellum and midbrain is shown). **(D)** Sagittal brain section incubated with mAb 113-126. Again, prominent staining of large blood vessels in all brain regions was obtained (the area between the cerebellum and midbrain is shown). **(E)** Stainings of isolated brain blood vessels. Blood vessels were obtained from homogenized mouse brains by combinatory centrifugation and filtering steps. A 30-100 µm filter size fraction incubation with all three antibodies resulted in clear staining of the vessels within this fraction. Note that the diameter of mounted blood vessels is subject to shrinking artifacts during the staining procedure.

to brain blood vessels (Figure 2C), mAb 011-138 reacted with cerebellar Purkinje cells, leading to pronounced somatic staining (Figure 2C, inset d). To further characterize mAb 011-138 reactivity, we double-stained with smooth muscle actin (SMA) on murine brain slices (Figure 2D). The mAb 011-138 signal exhibited a high degree of overlap with SMA-positive smooth muscle cells of the vessels supporting our previous observation that the patient mAb predominantly recognizes large to mid-size vessels. Again, Collagen IV and CD31 stainings were applied to mark blood vessels (Figure 2E). Additionally, reactivity to brain blood vessels was confirmed using purified murine brain vessels sized 30–100 μm (Figure 2F).

In this cohort of mAbs, antibody 011-138 stood out due to its combinatory reactivity to brain blood vessels and a defined group of neuronal cells—cerebellar Purkinje cells, making mAb 011-138 a particularly interesting candidate for further investigation in terms of target identification as well as possible mechanistic effects.

Monoclonal antibody 011-138 reduces TEER in an *in vitro* BBB model and decreases the expression of cell junction protein occludin

To test for putative pathophysiological effects on blood vessels we applied an *in vitro* model for the analysis of BBB disruption. Human cerebral microvascular endothelial cells (hCMEC/D3; Weksler et al., 2005) represent an established model to mimic the *in vivo* phenotype of the BBB and are commonly used to investigate pathomechanisms and transport processes (Helms et al., 2016). Functional evaluation of endothelial monolayer integrity in response to antibody treatment was quantified with transendothelial electrical resistance (TEER) measurements. For our purposes, hCMEC/D3 cells were grown to confluency as exemplarily shown by fluorescent staining of adherens junction protein VE-Cadherin and endothelial cell marker CD34 (Figures 3A,B). We assessed TEER changes in response to 24 h and 48 h of treatment with patient mAbs in comparison to non-reactive control mAb mGO53 (Figures 3C–E). When hCMEC/D3 cells were exposed to mAbs obtained from the patient with $GABA_AR$ encephalitis as well as mAbs 080-221 and 003-151 from patients with NMDAR encephalitis, TEER values did not significantly decrease, and barrier breakdown could not be observed. For 24 h treatment with mAb 080-221 an increase in TEER was seen (Figure 3C). Conversely, the results showed that treatment with mAb 011-138 led to a significant reduction of TEER after 48 h but not after 24 h (Figure 3E). A significant reduction of TEER after 48 h was achieved using 5 μg/ml and was slightly stronger with a concentration of 10 μg/ml.

In the following, we investigated the fluorescent binding pattern of mAb 011-138 in hCMEC/D3 cells. Incubation of fixed and permeabilized cells revealed a stress fiber-like filamentous staining pattern that included the plasma membrane region not observed with control mGO53 (Figures 3F,G). Incubation of live cells with 5 μg/ml mAb 011-138 resulted in a plasma membrane-like staining of the cell periphery (Figure 3H). The reactiveness of antibody 011-138 to hCMEC/D3 cells was also tested using Western Blot analysis. Blotted cell lysates were incubated with 5 μg/ml of either mAb 011-138 or mGO53 for control (Figure 3I). Incubation with antibody 011-138 yielded a major immunoreactive band slightly above 200 kDa and a few lower bands around the 130 kDa marker. Incubation with control mAb mGO53 yielded no bands.

To investigate the underlying mechanisms of BBB disruption, the expression of barrier-constituting junctional proteins was evaluated after treatment with mAb 011-138 for 48 h in comparison to the control antibody (Figure 3J). Resulting Western blots yielded a significant decrease of Occludin expression in hCMEC/D3 cells. The decreased expression of Occludin was confirmed on the mRNA level using qPCR (Figure 3L). Downregulation of Occludin by mAb 011-138 treatment was not only observed in whole cell homogenates but was also evident for plasma membrane-enriched cell fractions (Figure 3K). VE-Cadherin, Claudin5, and Zonula occludens protein-1 (ZO-1) expression was not significantly altered. Concordantly, qPCR experiments did not show significant genetic changes (Figure 3L).

As an integral component of tight junctions, Occludin may therefore contribute to the decreased TEER.

In vivo reactivity of mAb 011-138 to brain blood vessels and decreased expression of occludin

To first confirm the detectable presence of recombinant mAb 011-138 in patients CSF, we stained CSF-011 on unfixed murine brain sections. This showed simultaneous reactivity in vessels and Purkinje cells as well in addition to the typical NMDAR distribution (Figure 4A). Prompted by these findings and to investigate the effects of mAb 011-138 *in vivo*, mice were intrathecally infused with mAb 011-138 or isotype control using an osmotic pump system for continuous delivery into the CNS (Figure 4B). Detection of human IgG after 7 and 14 days of infusion (100 μg for 7 days and 200 μg for 14 days were administered) showed mid to large-size blood vessels staining throughout different brain regions in mAb 011-138 infused animals (exemplary vessel staining of 14-day infusion: Figure 4C). In contrast, sections of animals that received the control antibody mGO53 for infusion did not show any staining (Figures 4D,F), whilst the presence of vessels containing the target vessel wall structures was ensured by SMA-staining. From the same animals, serum was collected to check for the access of antibodies to the bloodstream to provide a source of blood vessel reactive antibodies. Staining of unfixed wild-type murine brain slices with sera from mAb 011-138 treated animals showed the same staining pattern of large to mid-size blood vessels as the previously described secondary antibody treated brain sections from animals that received mAb 011-138 intrathecally (Figures 4E,G). These findings demonstrate the capacity of antibody 011-138 to bind to its target structure *in vivo* and suggest access to the blood system from the CSF compartment in our experimental paradigm. This could represent an antibody effect as well as a lesion-induced phenomenon or be due to a physiologically occurring FcRn-mediated process.

Additionally, we conducted Western blot experiments to assess the expression of Occludin in brain tissue of animals intrathecally infused with mAb 011-138 compared to the control antibody. We found Occludin expression to be significantly decreased, matching our *in vitro* findings using hCMEC/D3 cells (Figure 4H). As already observed *in vitro*, other tight junction proteins such as VE-Cadherin,

10.3389/fncel.2023.1077204

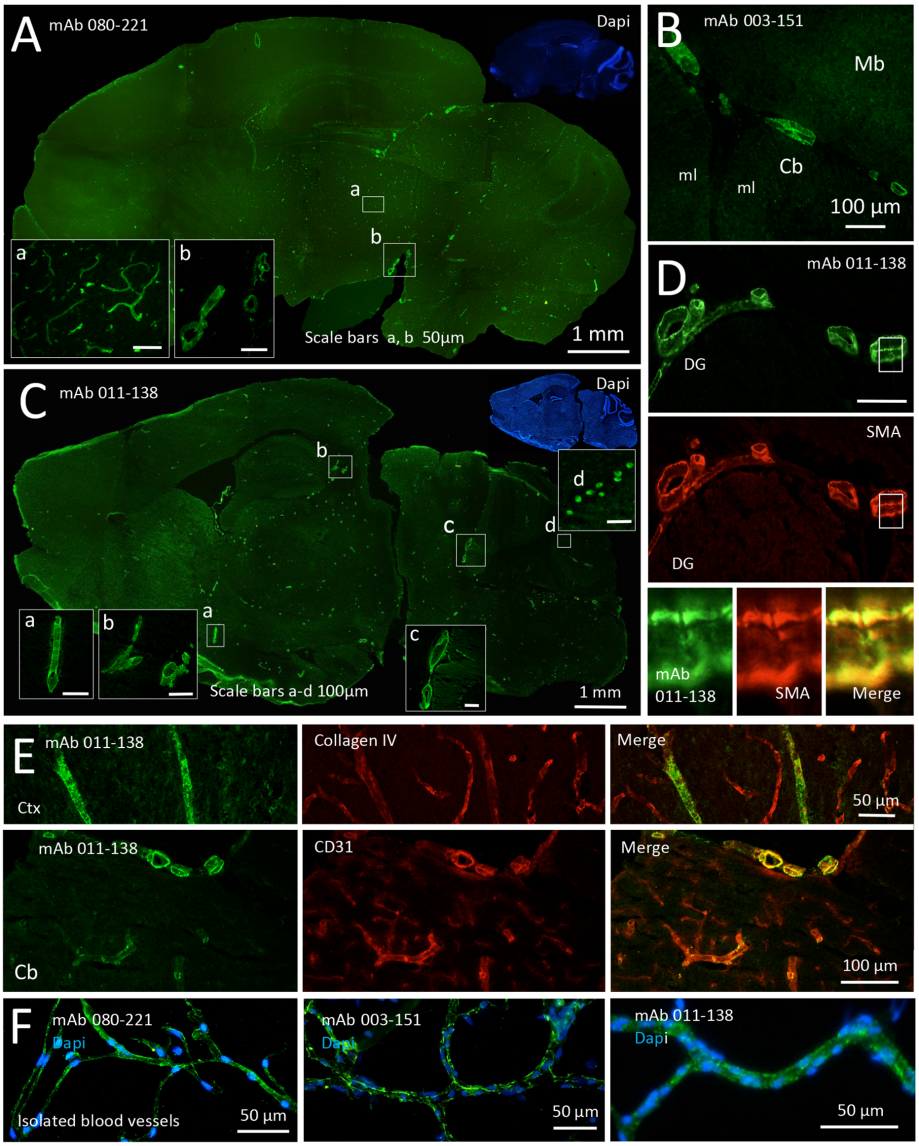

FIGURE 2
Recombinant monoclonal antibodies from NMDAR encephalitis patients bind to brain blood vessels and Purkinje cells. Unfixed and unpermeabilized sections from adult mouse brains were incubated with 5 µg/ml of the respective human monoclonal antibodies (mAbs) obtained from three different patients diagnosed with NMDAR encephalitis. Visualization of tissue binding was performed using a FITC-coupled anti-human IgG secondary antibody. **(A)** Sagittal brain section incubated with mAb 080-221. Prominent staining of large to small blood vessels including capillaries was obtained in all brain regions (see insets a and b). **(B)** Sagittal brain section incubated with mAb 003-151. Prominent staining of large to mid-size blood vessels in all brain regions was obtained (a section of cerebellum, *Cb*, and midbrain, *Mb*, is shown; *ml* molecular layer). **(C)** Sagittal brain section incubated with mAb 011-138. Prominent staining of large to mid-size blood vessels in all brain regions was obtained (see insets a, b, and c). In addition to blood vessel staining cerebellar Purkinje cells showed marked somatic staining (see inset d). **(D)** Double staining against human IgG and SMA (smooth muscle actin) in a brain section adjacent to the dentate gyrus (*DG*) of the hippocampus formation. Bound human IgG was mainly detected within the SMA-positive muscle layer of the vessels. **(E)** Double stainings against Collagen IV (upper panel) and CD31 (lower panel) confirm immunoreactivity of mAb 011-138 to blood vessels. *Ctx Cortex* **(F)** Staining of isolated brain blood vessels. Blood vessels were obtained from homogenized mouse brains by combinatory centrifugation and filtering steps. A 30–100 µm filter size fraction incubation with all three antibodies resulted in clear staining of the vessels within this fraction. Note that the diameter of mounted blood vessels is subject to shrinking artifacts during the staining procedure.

10.3389/fncel.2023.1077204

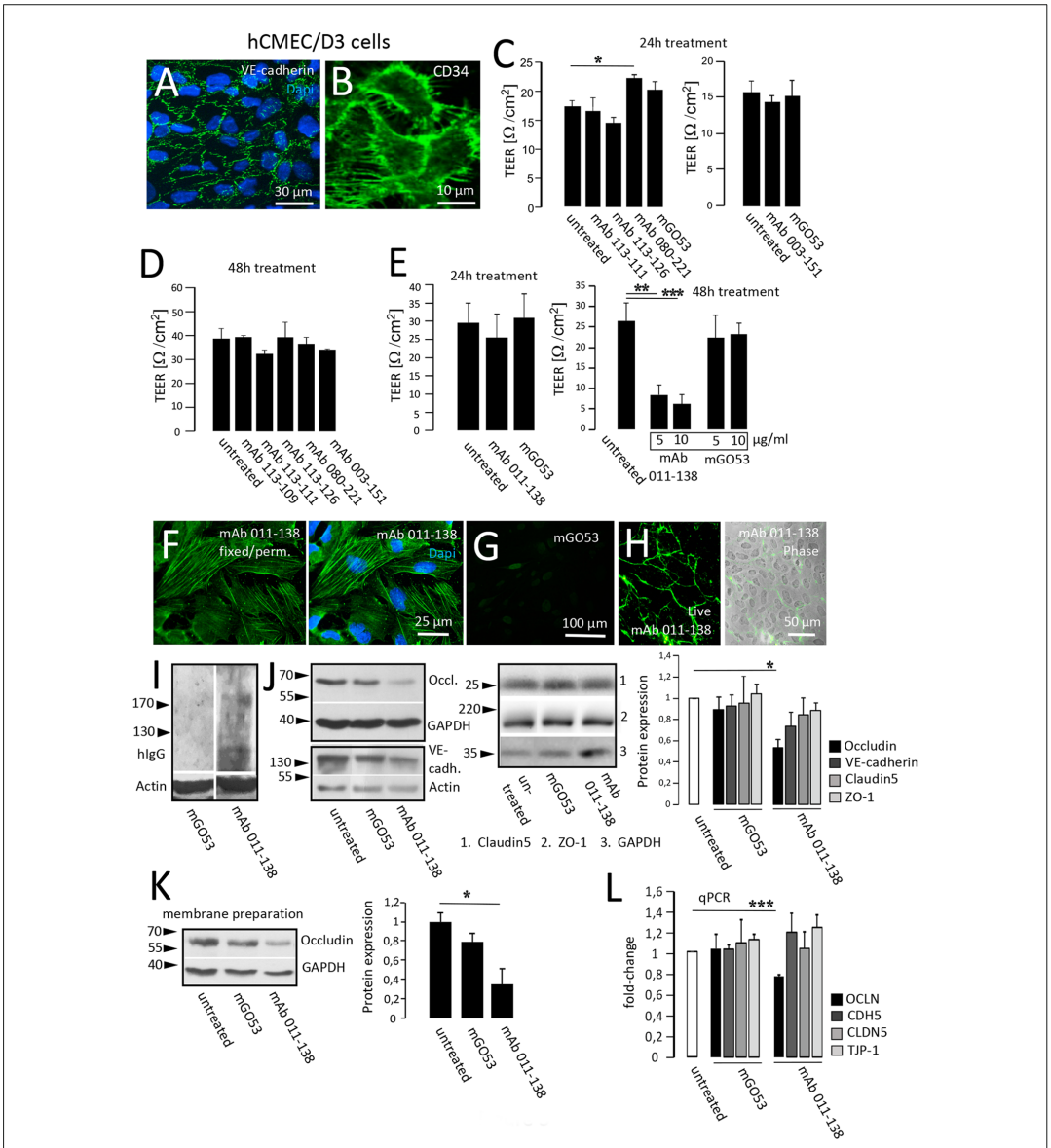

FIGURE 3
Antibody 011-138 decreases transendothelial electrical resistance and downregulates tight junctional Occludin. **(A,B)** Human cerebral microvascular endothelial cells (hCMEC/D3) were used as an *in vitro* blood-brain barrier model. Tight junction protein VE-cadherin and the endothelial cell marker CD34 were clearly expressed and depicted adjacent cell boundaries. The following functional experiments were carried out on live cells grown to confluence. **(C)** After 24 h of antibody treatment at 5 µg/ml, none of the human monoclonal antibodies (mAb) decreased TEER, only mAb 080-221 increased TEER. **(D)** No effects on TEER were observed after incubation for 48 h with 5 µg/ml with the respective antibodies. **(E)** Incubation with 5 µg/ml mAb 011-138 for 24 h had no significant effects on TEER. Conversely, incubation for 48 h resulted in a highly significant reduction of electrical resistance by mAb 011-138, but not mGO53, used as control Ab. Values analyzed in triplicates are expressed as means ± SEM from a representative experiment that was at least repeated once per condition **(C–D)** or from three independent experiments **(E)**. **(F–H)** Immunofluorescence detection of mAb 011-138 binding (5 µg/ml) to either live or fixed and permeabilized hCMEC/D3 cells. Fixed cells revealed a filamentous signal of mAb 011-138, and live cells showed a rather surface localized signal. Incubation with mGO53 resulted in no signal under either condition (**G**, shown for fixed cells). **(I)** Western blotting of hCMEC/D3 cell homogenates with either mAb 011-138 or control mGo53. Bound monoclonal 011-138 expressed higher molecular weight bands with a prominent signal at or above 200 kDa, mGO53 revealed no immune signal. **(J)** Confluent hCMEC/D3 cells were incubated for 48 h
(*Continued*)

FIGURE 3 (Continued)
with 5 μg/ml mAb 011-138 or mGO53. Western blotting for detection of Occludin, VE-cadherin, Claudin5, and ZO-1 expression. GAPDH or Actin were used as loading control. Incubation with mAb 011-138 resulted in a significant downregulation of Occludin expression exclusively. Values adjusted to loading are expressed as means ± SEM from 4–5 independent experiments. **(K)** Membrane preparations were performed from hCMEC/D3 cells following incubation with 5 μg/ml mAb 011-138 or mGO53. Western blot analysis revealed a significant removal of Occludin from the membrane compartment largely consisting of plasma membrane fractions following incubation with mAb 011-138. Western blot values adjusted to loading are expressed as normalized means ± SEM from three independent experiments. **(L)** Additionally, quantitative RT-PCR was performed to check for alterations in gene regulation of tight junction proteins. Calnexin (CANX) was used as endogenous control. Significantly decreased mRNA levels were found for Occludin (OCLN), the other genes (CDH5 VE-cadherin; CLDN5 Claudin5, and TJP-1 ZO-1) remained unchanged. Quantitative PCR values are expressed as means ± SEM from three independent experiments. $*p \leq 0.05$, $**p \leq 0.01$, $***p \leq 0.001$.

Claudin5, and ZO-1 were not significantly altered by the injection of mAb 011-138 (**Supplementary Figure 2**), thereby confirming the specificity of the effects on Occludin.

Unconventional Myosin-X represents a target epitope of mAb 011-138

In brain biochip tissues of monkey and rat cerebellum, mAb 011-138 yielded a very similar staining pattern to the one observed in mouse brain (**Figure 5A**). To identify the target of mAb 011-138 we performed immunoprecipitation studies with rodent aorta lysates, purified mouse brain vessels, and monkey brain lysates as antigen-providing tissues and repeatedly received various conventional and unconventional myosins. Exemplarily, a Western blot is shown for an immunoprecipitation experiment using monkey brain lysate (**Figure 5B**). Incubation of the precipitated protein fraction with mAb 011-138 showed a distinct band around 240 kDa corresponding to the molecular weight of many myosin isoforms, together with a lower band around 80 kDa. Reactivity to the precipitating heavy chain around 55 kDa was shared also by other precipitating human monoclonal antibodies used for control. We were aware of the fact that myosins tend to be "sticky" and, therefore, are often pulled down unspecifically during immunoprecipitation. However, the combined occurrence of strong immunoreactivity in brain blood vessels together with the reactivity to cerebellar Purkinje cells matched the published brain distribution of unconventional Myosin-X (Sousa et al., 2006) and therefore prompted us to test for reactivity of mAb 011-138 to Myosin-X.

The binding of mAb 011-138 to Myosin-X was first investigated in a cell-based assay. Expression of eGFP-tagged Myosin-X in HEK cells was verified using a commercial anti-Myo-X antibody (**Figure 5C**). Incubation with mAb 011-138 resulted in specific binding to transfected cells with a high degree of signal overlap between eGFP-MyoX and patient antibody signals (**Figures 5D–F**). Furthermore, confirmation of CSF immunoreactivity to Myo-X was received by prominent staining of transfected cells with CSF of patient 011 (**Figure 5G**). Further supporting our finding, patient antibody 011-138 and a commercial Myosin-X antibody stained mouse brain Purkinje cells and blood vessels in a very similar fashion with a high degree of signal overlap between both antibodies (**Figures 6A,B**). Incubation of hCMEC/D3 cells with commercial anti-Myo-X antibody revealed a similar, although not fully identical staining pattern (**Figure 6C**). Double staining with mAb 011-138 revealed a partial overlap of both signals being most prominent at the cell periphery (**Figure 6C** insets a and b). Expression of Myosin-X protein in hCMEC/D3 cells was verified by Western blotting (**Figure 6D**). Furthermore, while mRNA levels remained unchanged, we detected a decrease in Myosin-X expression at the protein level in mAb 011-138 treated cells (**Figure 6D**).

Discussion

This qualitative study is the first to characterize a subgroup of brain blood vessel reactive autoantibodies in autoimmune encephalitis patients. Our data shows a range of binding patterns which point towards a bandwidth of possible target antigens. Results from our *in vivo* experiments suggest that blood vessel reactive autoantibodies are capable of binding to brain vessel epitopes when administered to the CSF. Furthermore, our results indicate –though still limited to a small number of cases- ways of potential principal contribution from blood vessel reactive antibodies to the pathomechanisms of autoimmune encephalitis as a setscrew in BBB disruption.

The growing interest in the pathomechanisms of autoimmune encephalitis has strongly fueled research efforts and thereby improved our understanding—especially of disease-defining autoantibodies targeting extracellular proteins. However, studies have shown that additional antibodies coexist in patients' CSF. In fact, non-disease-defining autoantibodies make up the majority of the antibodies generated (Kreye et al., 2016). Furthermore, antibody-associated neurological diseases typically present with a wide range of clinical symptoms (Titulaer et al., 2013), with the result that variable clinical pictures can be associated with the same antibody. Since antibody titers only partially correlate with the clinical course (Gresa-Arribas et al., 2014), other contributing factors are suspected. Such as differential epitope specificity, strong differences in affinity, and contribution of low-affinity antibodies currently eluding diagnostic observation (Ly et al., 2018; Wagner et al., 2020). The contribution of coexisting non-disease-defining antibodies remains unresolved. Utilizing recombinant human monoclonal antibodies allowed for this study to vastly eliminate unspecific effects of serological components and attribute observed binding patterns and functional effects to single mAbs. This unbiased approach of screening mAbs on murine unfixed brain sections has proven useful in previous exploratory antibody studies (Kreye et al., 2016, 2021).

In this study, we focused on CSF-derived mAbs with reactivity against blood vessels from patients with autoimmune encephalitis. $GABA_AR$ and NMDAR encephalitis patient-derived mAbs exhibited diverse binding to brain blood vessels, suggesting that mAbs likely target several different antigens on the brain vasculature. Interestingly, even within the same $GABA_A$ receptor encephalitis patient (113) blood vessel reactive antibodies showed differing binding patterns. This is in line with the observed variability of non-$GABA_A$ receptor reactive neuronal antibodies, shown previously on murine brain tissue (Kreye et al., 2021). However, overall blood vessel reactive mAbs can be roughly divided into two "pattern groups". One comprised of mAbs with reactivity to mid- to large size vessels,

10.3389/fncel.2023.1077204

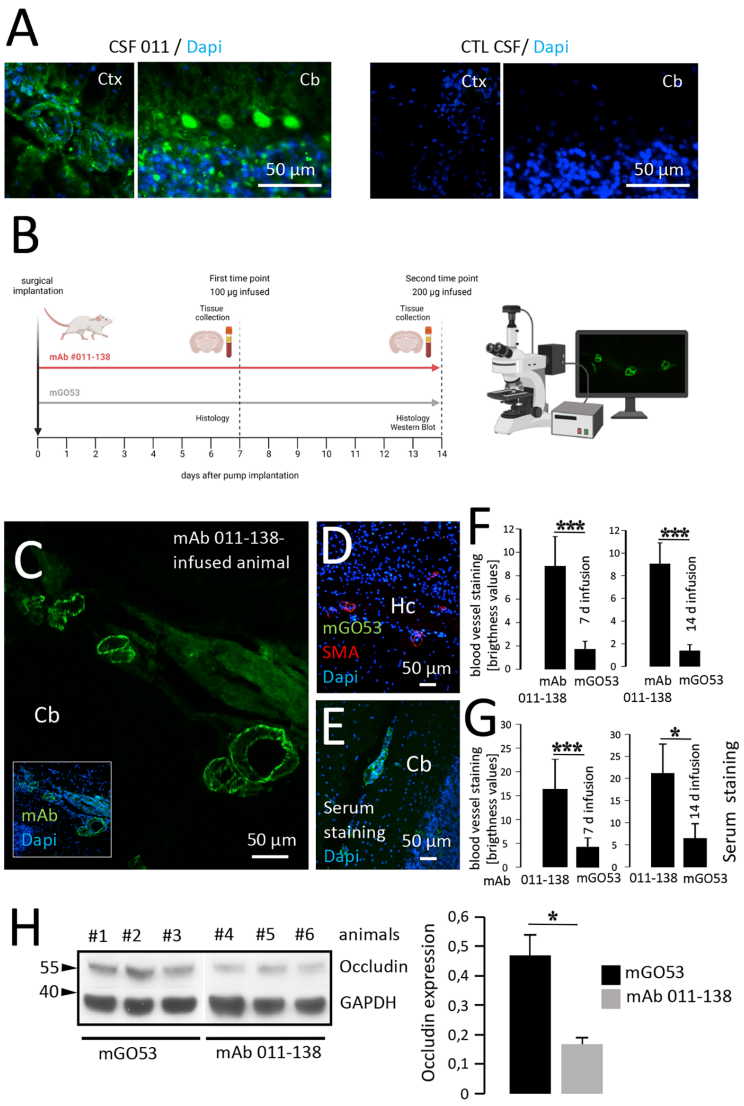

FIGURE 4
Intrathecal application of antibody 011-138 leads to *in vivo* blood vessel binding and Occludin downregulation. **(A)** Sections from unfixed adult mouse brains were incubated with CSF of patient 011 and an age-matched control patient at a dilution of 1:2. Incubation with 011 CSF resulted in IgG staining of blood vessels and cerebellar Purkinje cells. Incubation with control CSF yielded no staining. **(B)** Adult mice were either administered a dose of 100 µg of human monoclonal antibody (mAb) 011-138 into the right lateral ventricle for 7 days or 200 µg for 14 days. Animals were sacrificed, brains were removed, and immediately frozen for immunohistochemistry. In addition, blood was collected to obtain serum. **(C)** Representative sagittal brain section from an animal treated for 14 days with mAb 011-138 was incubated with FITC-coupled anti-human IgG. Clear staining of large to mid-size blood vessels in all brain regions was visible (shown for the cerebellum, *Cb*). **(D)** Sagittal brain section from one animal treated with control antibody mGO53 for 14 days. Incubation with a secondary antibody revealed no staining *Hc = hippocampus*. **(E)** Sagittal unfixed brain section from an untreated adult mouse was incubated with serum (dilution 1:200) from an animal that had received mAb 011-138 for 14 days. Visualization with secondary antibody revealed staining of larger to mid-size blood vessels by the mouse serum. **(F)** Quantification of blood vessel IgG immunoreactivity. Data are given as means ± SEM from three animals per condition. Per condition, between 38 and 43 blood vessel sections were analyzed. ***$p \leq 0.001$. **(G)** Quantification of serum blood vessel IgG immunoreactivity on naive brain sections. Data are given as means ± SEM from three animals per condition. Per condition, between 22 and 45 blood vessel sections were analyzed. *$p \leq 0.05$, ***$p \leq 0.001$. Brightness levels of mGO53 staining were within the background range. **(H)** Downregulation of Occludin by mAb 011-138. In brains of mice treated with mAb 011-138 for 14 days protein expression was strongly reduced by 65% compared to animals that had received mGO53. Data are given as means ± SEM adjusted to loading from seven animals per condition from two independent experiments. *$p \leq 0.05$. Three animals per condition from one experiment are exemplarily shown.

10.3389/fncel.2023.1077204

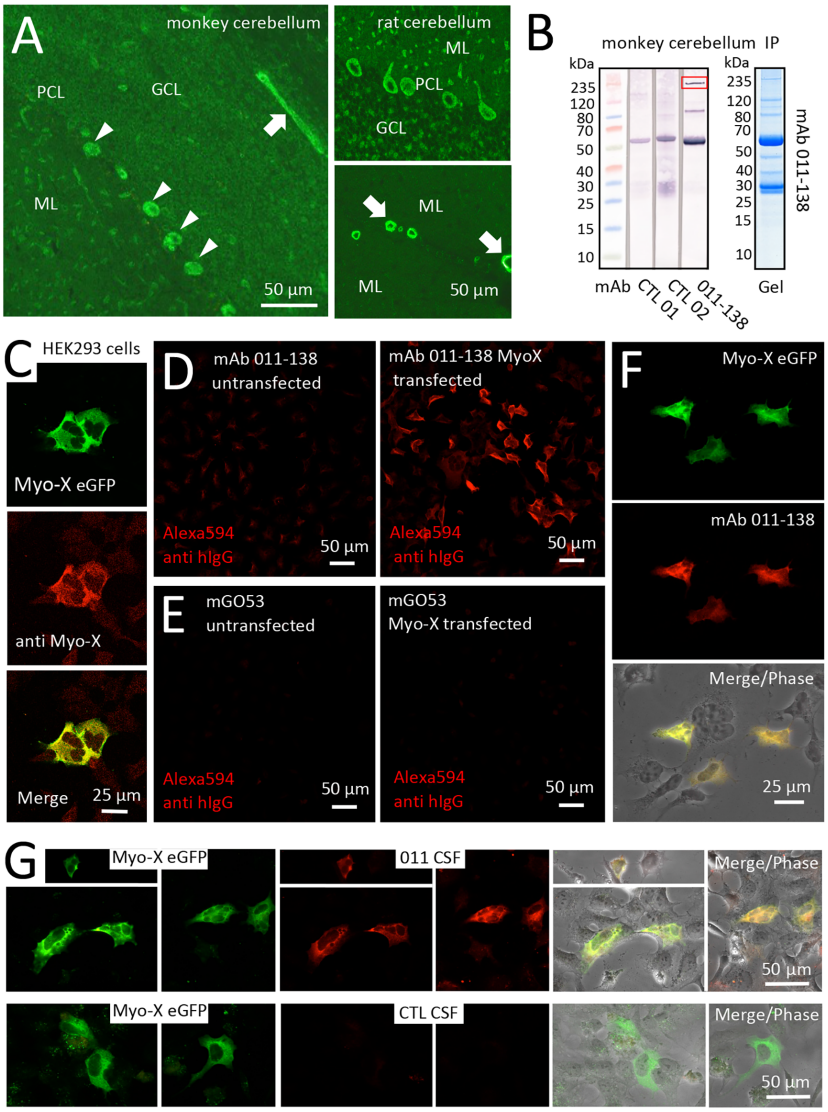

FIGURE 5
Antibody 011-138 targets Myosin-X in transfected HEK cells. **(A)** Monkey and rat brain biochip cryosections (EUROIMMUN AG) were incubated with human monoclonal antibody (mAb) 011-138 (1:100) and exhibited pronounced staining of blood vessels (left panel and lower right panel arrows) and Purkinje cells (left panel arrowheads and upper right panel). **(B)** Immunoprecipitation analysis using monkey brain lysates. Lysates were incubated with either mAb 011-138 or two other non-vessel reactive human monoclonal antibodies for control. Dynabeads were used to precipitate antibodies together with bound antigens. Elute fractions were again incubated with the precipitating antibody followed by Western blotting. The marked band at 55 kDa in all three lanes presumably resulted from detection of the precipitating heavy chain by the detecting secondary anti-human IgG conjugate. In addition, mAb 011-138 showed two distinct bands at 80 and 240 kDa (boxed), respectively. The corresponding Coomassie gel is shown for mAb 011-138. **(C)** HEK 293 cells were transfected with an eGFP construct of human Myosin-X (Myo-X) plasmid DNA for 24 h. Expression of Myo-X was verified in fixed cells using a commercial monoclonal anti-Myo-X antibody showing a very high degree of signal overlap (confocal imaging). **(D)** Incubation of Myo-X-transfected cells with 5 µg/ml of 011-138 antibody showed binding to fixed transfected cells that were absent in untransfected cells. A secondary anti-human IgG antibody coupled to Alexa594 was used for detection. **(E)** For negative control untransfected and Myo-X-transfected cells were incubated with 5 µg/ml of mGo53 antibody. No staining was observed under either condition. **(F)** In transfected cells incubated with 011-138 antibody the human IgG signal showed a very high degree of overlap with eGFP-Myo-X signal. **(G)** HEK 293 cells were transfected with an eGFP construct of human Myo-X plasmid DNA for 24 h. Incubation of Myo-X-transfected cells with patient-CSF 011 showed binding that was absent after incubation with control-CSF. The right panel shows a high degree of overlap of patient-CSF 011 signal with eGFP-Myo-X signal.

10.3389/fncel.2023.1077204

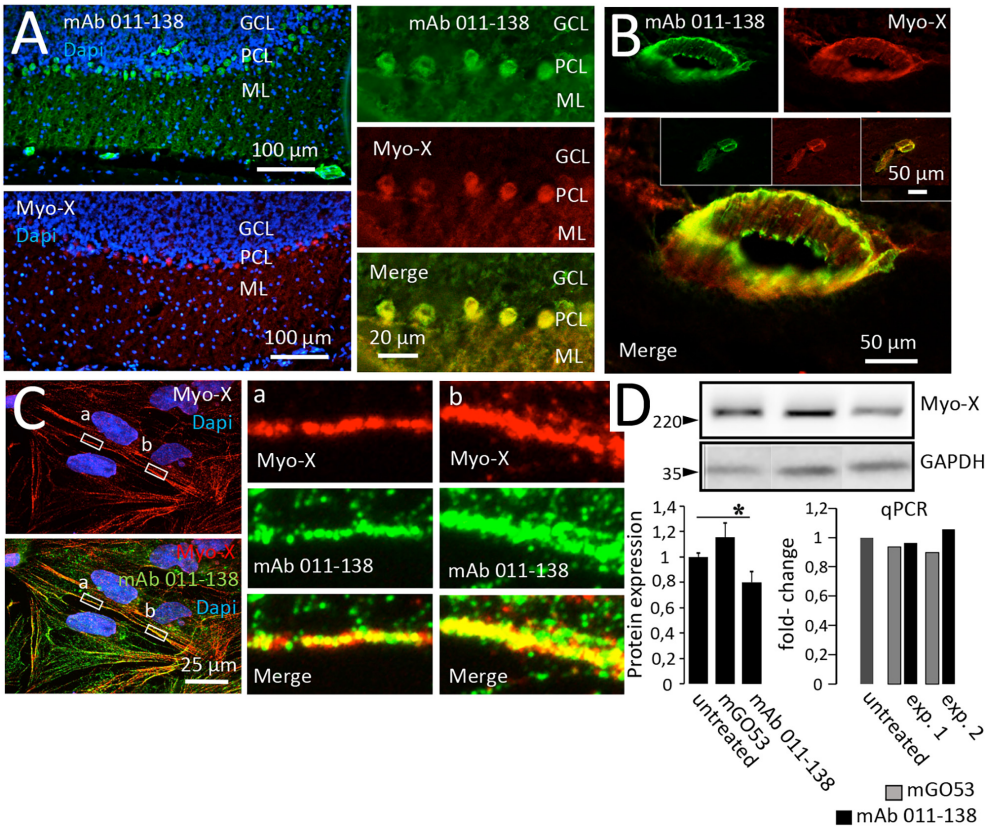

FIGURE 6
Antibody 011-138 colocalizes with commercial anti-Myosin-X antibodies in brain sections and hCMEC/D3 cells and downregulates Myosin-X. **(A)** Unfixed and unpermeabilized sections from adult mouse brains were incubated with 5 µg/ml of human monoclonal antibody (mAb) 011-138 and a commercial monoclonal mouse antibody directed against unconventional Myosin-X (Myo-X). Shown is the 3-layer cerebellar cortex consisting of the granule cell layer (GCL), Purkinje cell layer (PCL), and outermost molecular layer (ML). Incubation with mAb 011-138 resulted in staining of the Purkinje cell somata and larger blood vessels (upper panel). Staining with commercial anti-Myo-X antibody showed a comparable pattern (lower panel, no larger vessels present). Double staining revealed a high degree of signal overlap between patient 011-138 and commercial MyoX antibodies in Purkinje cells. **(B)** Likewise, double staining revealed a high degree of signal overlap between patient 011-138 and commercial Myo-X antibodies in mid-size (insets) to larger blood vessels. **(C)** Double incubation of fixed hCMEC/D3 cells with antibody 011-138 and commercial anti-Myosin-X IgG. Both stainings yielded a similar staining pattern with partially overlapping signals (see insets). **(D)** Incubation of hCMEC/D3 cells with mAb 011-38 results in the downregulation of Myo-X. Following incubation of hCMEC/D3 cells with 5 µg/ml of mAb 011-138 or mGO53 as control for 48 h cells were homogenized and subjected to Western blotting and quantitative PCR to check for protein expression and gene regulation. Incubation with mAb 011-138 decreased protein expression of Myo-X by 20% (left chart), gene regulation was unaltered (right chart). Data are given as normalized means ± SEM adjusted to loading from two individual experiments analyzed in duplicates (Western blot) and as two individual experiments (qPCR). *$p \leq 0.05$.

while the second group mAbs reacted to vessels of all sizes including capillaries. The binding pattern in the second group points towards a potential target that is present throughout the entire vascular tree. Since this study had an exploratory approach and investigated only a small number of patients, the frequency of blood vessel reactive antibodies in autoimmune encephalitis remains to be ascertained in future studies targeting exactly this subgroup of antibodies in larger patient cohorts.

The BBB represents a critical gatekeeper between blood circulation and brain tissue. Its function is maintained mainly by an endothelial cell layer tightly sealed by Claudins, Occludin, and junction adhesion proteins like VE-cadherin (Rubin et al., 1991; Corada et al., 1999; Vorbrodt and Dobrogowska, 2003). Human hCMEC/D3 cells are among the most commonly used and best characterized *in vitro* BBB models (Helms et al., 2016). The integrity of the endothelial cell layer was measured through transendothelial electrical resistance (TEER), which is a widely used and accepted method (Srinivasan et al., 2015; Burek et al., 2019). We found mAb 011-138 to significantly decrease TEER values in the hCMEC/D3 BBB model after treatment for 48 h in comparison to the control antibody, indicating a disruption in the BBB integrity, which was not observed when other antibodies were applied. Mab 011-138 treated cells also showed a significant decrease in Occludin expression. No significant changes were observed for other junctional proteins, amongst them

VE-cadherin, which represents the main player at adherens junctions (Corada et al., 1999). Occludin is a tight junction specific protein with regulatory functions at the BBB. Among other mechanisms, altered expression of VE-cadherin and Occludin has been found to influence TEER and to associate with increased permeability of brain endothelial cells (Wang et al., 2001; Xu et al., 2012; Hebda et al., 2013; Mishra and Singh, 2013).

Our investigations *in vivo* show that intrathecally applied mAb 011-138 can reach its target in brain blood vessels. We replicated the mAb 011-138 characteristic binding pattern using patient CSF on unfixed murine brain sections. This ensures that the patient's CSF indeed contains mAb 011-138. Our *in vivo* experiments thus replicated our *in vitro* findings and support the concept of antibody-antigen binding of mAb 011-138 to brain blood vessel targets when present in patient CSF. Moreover, in line with previous *in vitro* findings, we detected decreased Occludin expression in brain lysates of mAb 011-138 treated animals. This undermines the involvement of Occludin in the effects of antibody treatment to endothelial layer integrity. Considering this ability of mAbs to decrease electrical resistance and change the expression of junction components it could be further speculated that they might also enhance the permeability of larger molecules, although this needs to be assessed in future studies. Specifically utilizing monoclonal antibodies in the future will allow for the attribution of effects to certain mAbs.

We provide conclusive evidence to propose Myosin-X as a target of blood vessel reactive patient mAb 011-138. Myosin-X is currently the first and only known representative of unconventional myosin class X (Berg et al., 2000). It is expressed in most tissues, although at low levels, including brain cerebellar Purkinje cells (Berg et al., 2000; Sousa et al., 2006). MAb 011-138 predominantly stained mid- to large sized blood vessels in unfixed unpermeablized tissue, which initially showed binding to vascular smooth muscle cell layer rather than to endothelial cells. However, previous studies have shown Myosin-X expression and function in endothelial cells (Almagro et al., 2010). This was also reflected in our detection of Myosin-X in hCMEC/D3 cells using Western blot and qPCR analysis. Since Myosin-X is expressed at low levels, it may have evaded indirect immunofluorescence staining by patient mAb 011-138 in unpermeabilized endothelial cells. In permeabilized hCMEC/D3 cells we were able to detect a distinct staining pattern with commercially available Myosin-X antibody, resembling filamentous structures. There remains the possibility that mAb 011-138 binds to multiple types of myosin. We are aware of the fact that intracellular targets such as Myosin-X intuitively appear to be shielded from antibody binding at first glance. Nevertheless, some naturally occurring antibodies such as anti-DNA antibodies in SLE possess the ability to penetrate living cells (Noble et al., 2016). Among the diverse mechanisms by which cell-penetrating antibodies enter the cell, antibodies targeting intracellularly located synapsin in patients presenting with limbic encephalitis (Piepgras et al., 2015) were identified that utilize Fcy II/III receptor mediated endocytosis to reach their cytosolic target (Rocchi et al., 2019). Moreover, further intracellular autoimmune targets have been identified such as glutamate decarboxylase 65 (GAD65) and Amphiphysin in patients with the brainstem, extrapyramidal and spinal cord dysfunction, and in stiff-person syndrome respectively (Pittock et al., 2006; Geis et al., 2010).

Consistent with other classes of myosins, Myosin-X acts as an actin-based molecular motor. Nevertheless, it is presumed to have further functions including actin-membrane interaction due to its unique domain composition (Berg et al., 2000). Myosin-X is present at regions of highly dynamic actin such as the tips of filopodia (Berg et al., 2000; Berg and Cheney, 2002) and has been proposed as a candidate for trafficking VE-cadherin (Almagro et al., 2010). Knockdown of Myosin-X in developing kidney epithelial cells leads to delayed recruitment of junction proteins E-cadherin and ZO-1 reflected by a delayed peak transepithelial electrical resistance (Liu et al., 2012). The same study found that even after maturing, the epithelial monolayers showed a higher paracellular permeability. These findings together with our observation of reduced TEER and downregulation of Occludin and Myosin-X by antibody treatment support the concept of Myosin-X playing an important role in the dynamics and kinetics in polarized cells such as endothelial cells. As a player in cytoskeleton trafficking and membrane interactions, Myosin-X represents an exciting target structure for further investigations in the context of antibody-mediated diseases. In addition to blood vessel binding, cerebellar Purkinje cells were also targeted by mAb 011-138. This cell type exhibits a marked Myosin-X expression throughout development (Sousa et al., 2006). Functional implications, however, were not addressed in this study and are subject to further investigations.

The involvement of BBB disruption in autoimmune encephalitis has been proposed previously (Dalmau et al., 2007; Kreye et al., 2021). In other antibody-mediated neurological diseases such as NPSLE breakdown of the BBB has been verified as a key feature (Kowal et al., 2004; Huerta et al., 2006; Hirohata et al., 2014). Additionally, recent findings of anti-GRP78 antibodies in NMO and PCD-LEMS have revealed that endothelial targeting antibodies enhance the transmigration of pathogenic IgG (Shimizu et al., 2017, 2019). A proceeding endothelial activation as part of an inflammatory response as shown in these studies is a conceivable mechanism in our patient cohort, although this needs to be further investigated. Studying vessel targeting antibodies is therefore particularly interesting, as they potentially unfold new perspectives on the development, progression, and variability of autoimmune encephalitis.

In conclusion, we have identified vessel-targeting antibodies in autoimmune encephalitis patients, identified a corresponding antigenic structure and demonstrated the potential cause of the observed endothelial disruption. Therefore, our findings provide additional qualitative evidence for the concept of antibody-mediated BBB disruption as a further identified mechanism in neuroinflammatory diseases.

Data availability statement

The original contributions presented in the study are included in the article/**Supplementary material**, further inquiries can be directed to the corresponding author.

Ethics statement

The studies involving human participants were reviewed and approved by Institutional review board Charité-Universitätsmedizin Berlin (EA1/096/12). The patients/participants provided their written informed consent to participate in this study. The animal study was

reviewed and approved by the Landesamt für Gesundheit und Soziales in Berlin, Germany (approval number 0078/19) and performed in compliance with relevant national and international guidelines for care and humane use of animals.

Author contributions

LL, JK, MB, CC-G, SR, HP, and MH: contributed to the conception and design of the study. LL, JK, MB, CC-G, PB, ES-S, H-CK, DS, MS, PM, HP, and MH: contributed to the acquisition and analysis of data. LL, JK, MB, CC-G, PB, HP, and MH: contributed to drafting the text and preparing the figures. All authors contributed to the article and approved the submitted version.

Funding

This work was supported by grants from the German Research Foundation (DFG; grants FOR3004, PR1274/3-1, PR1274/5-1, and PR1274/9-1), by the Helmholtz Association (HIL-A03 BaoBab), and by the German Federal Ministry of Education and Research (Connect-Generate 01GM1908D) to HP. We acknowledge financial support from the Open Access Publication Fund of Charitè—Universitätsmedizin Berlin and the German Research Foundation (DFG).

Acknowledgments

We thank Birgit Metze, Marion Möbes, Antje Dräger for technical assistance, Kinga Blecharz-Lang for supporting us with BBB measurements.

Conflict of interest

MS was employed by the company EUROIMMUN AG, Lübeck, Germany.

The remaining authors declare that the research was conducted in the absence of any commercial or financial relationships that could be construed as a potential conflict of interest.

Publisher's note

Supplementary material

The Supplementary Material for this article can be found online at: https://www.frontiersin.org/articles/10.3389/fncel.2023.1077204/full#supplementary-material.

SUPPLEMENTARY FIGURE 1
Co-stainings of monoclonal patient antibodies and CD31. Double stainings of mAbs 113-111, 113-126, 080-221, and 003-151 (5 μg/ml) with CD31 on unfixed murine brain sections confirm immunoreactivity of all four monoclonal antibodies to cerebral blood vessels.

SUPPLEMENTARY FIGURE 2
Tight junction proteins VE-cadherin, Claudin5, and ZO-1 are not downregulated *in vivo* by treatment with mAb 011-138. In brains from mice treated with mAb 011-138 or mGO53 (5 μg/ml) for control for 14 days, protein expression of VE-cadherin, Claudin5, and ZO-1 were unaltered. Data are given as means ± SEM adjusted to loading from four animals per condition. Immune signals from one animal per condition are exemplarily shown.

References

Almagro, S., Durmort, C., Chervin-Petinot, A., Heyraud, S., Dubois, M., Lambert, O., et al. (2010). The motor protein myosin-X transports VE-cadherin along filopodia to allow the formation of early endothelial cell-cell contacts. *Mol. Cell. Biol.* 30, 1703–1717. doi: 10.1128/MCB.01226-09

Armitage, J. D., Homer-Vanniasinkam, S., and Lindsey, N. J. (2004). The role of endothelial cell reactive antibodies in peripheral vascular disease. *Autoimmun. Rev.* 3, 39–44. doi: 10.1016/S1568-9972(03)00087-9

Berg, J. S., and Cheney, R. E. (2002). Myosin-X is an unconventional myosin that undergoes intrafilopodial motility. *Nat. Cell Biol.* 4, 246–250. doi: 10.1038/ncb762

Berg, J. S., Derfler, B. H., Pennisi, C. M., Corey, D. P., and Cheney, R. E. (2000). Myosin-X, a novel myosin with pleckstrin homology domains, associates with regions of dynamic actin. *J. Cell Sci.* 113, 3439–3451. doi: 10.1242/jcs.113.19.3439

Boulay, A. C., Saubamea, B., Decleves, X., and Cohen-Salmon, M. (2015). Purification of mouse brain vessels. *J. Vis. Exp.* 113:e53208. doi: 10.3791/53208

Burek, M., König, A., Lang, M., Fiedler, J., Oerter, S., Roewer, N., et al. (2019). Hypoxia-induced microRNA-212/132 alter blood-brain barrier integrity through inhibition of tight junction-associated proteins in human and mouse brain microvascular endothelial cells. *Transl. Stroke Res.* 10, 672–683. doi: 10.1007/s12975-018-0683-2

Corada, M., Mariotti, M., Thurston, G., Smith, K., Kunkel, R., Brockhaus, M., et al. (1999). Vascular endothelial-cadherin is an important determinant of microvascular integrity in vivo. *Proc. Natl. Acad. Sci. U S A* 96, 9815–9820. doi: 10.1073/pnas.96.17.9815

Dalmau, J., Tüzün, E., Wu, H., Masjuan, J., Rossi, J. E., Voloschin, A., et al. (2007). Paraneoplastic anti-N-methyl-D-aspartate receptor encephalitis associated with ovarian teratoma. *Ann. Neurol.* 61, 25–36. doi: 10.1002/ana.21050

Geis, C., Weishaupt, A., Hallermann, S., Grünewald, B., Wessig, C., Wultsch, T., et al. (2010). Stiff person syndrome-associated autoantibodies to amphiphysin mediate reduced GABAergic inhibition. *Brain* 133, 3166–3180. doi: 10.1093/brain/awq253

Gresa-Arribas, N., Titulaer, M. J., Torrents, A., Aguilar, E., McCracken, L., Leypoldt, F., et al. (2014). Antibody titres at diagnosis and during follow-up of anti-NMDA receptor encephalitis: a retrospective study. *Lancet Neurol.* 13, 167–177. doi: 10.1016/S1474-4422(13)70282-5

Hebda, J. K., Leclair, H. M., Azzi, S., Roussel, C., Scott, M. G., Bidère, N., et al. (2013). The C-terminus region of β-arrestin1 modulates VE-cadherin expression and endothelial cell permeability. *Cell Commun. Signal.* 11:37. doi: 10.1186/1478-811X-11-37

Helms, H. C., Abbott, N. J., Burek, M., Cecchelli, R., Couraud, P. O., Deli, M. A., et al. (2016). in vitro models of the blood-brain barrier: an overview of commonly used brain endothelial cell culture models and guidelines for their use. *J. Cereb. Blood Flow Metab.* 36, 862–890. doi: 10.1177/0271678X16630991

Hirohata, S., Arinuma, Y., Yanagida, T., and Yoshio, T. (2014). Blood-brain barrier damages and intrathecal synthesis of anti-N-methyl-D-aspartate receptor NR2 antibodies in diffuse psychiatric/neuropsychological syndromes in systemic lupus erythematosus. *Arthritis Res. Ther.* 16:R77. doi: 10.1186/ar4518

Huerta, P. T., Kowal, C., DeGiorgio, L. A., Volpe, B. T., and Diamond, B. (2006). Immunity and behavior: antibodies alter emotion. *Proc. Natl. Acad. Sci. U S A* 103, 678–683. doi: 10.1073/pnas.0510055103

Hughes, E. G., Peng, X., Gleichman, A. J., Lai, M., Zhou, L., Tsou, R., et al. (2010). Cellular and synaptic mechanisms of anti-NMDA receptor encephalitis. *J. Neurosci.* 30, 5866–5875. doi: 10.1523/JNEUROSCI.0167-10.2010

Kowal, C., DeGiorgio, L. A., Nakaoka, T., Hetherington, H., Huerta, P. T., Diamond, B., et al. (2004). Cognition and immunity; antibody impairs memory. *Immunity* 21, 179–188. doi: 10.1016/j.immuni.2004.07.011

Kreye, J., Reincke, S. M., Kornau, H.-C., Sánchez-Sendin, E., Corman, V. M., Liu, H., et al. (2020). A therapeutic non-self-reactive SARS-CoV-2 antibody protects from lung pathology in a COVID-19 hamster model. *Cell* 183, 1058–1069.e19. doi: 10.1016/j.cell.2020.09.049

Kreye, J., Wenke, N. K., Chayka, M., Leubner, J., Murugan, R., Maier, N., et al. (2016). Human cerebrospinal fluid monoclonal N-methyl-D-aspartate receptor autoantibodies are sufficient for encephalitis pathogenesis. *Brain* 139, 2641–2652. doi: 10.1093/brain/aww208

Kreye, J., Wright, S. K., van Casteren, A., Stöffler, L., Machule, M.-L., Reincke, S. M., et al. (2021). Encephalitis patient-derived monoclonal GABAA receptor antibodies cause epileptic seizures. *J. Exp. Med.* 218:e20210012. doi: 10.1084/jem.20210012

Liu, K. C., Jacobs, D. T., Dunn, B. D., Fanning, A. S., and Cheney, R. E. (2012). Myosin-X functions in polarized epithelial cells. *Mol. Biol. Cell* 23, 1675–1687. doi: 10.1091/mbc.E11-04-0358

Ly, L.-T., Kreye, J., Jurek, B., Leubner, J., Scheibe, F., Lemcke, J., et al. (2018). Affinities of human NMDA receptor autoantibodies: implications for disease mechanisms and clinical diagnostics. *J. Neurol.* 265, 2625–2632. doi: 10.1007/s00415-018-9042-1

Meroni, P. L., Tincani, A., Sepp, N., Raschi, E., Testoni, C., Corsini, E., et al. (2003). Endothelium and the brain in CNS lupus. *Lupus* 12, 919–928. doi: 10.1191/0961203303lu503oa

Mishra, R., and Singh, S. K. (2013). HIV-1 Tat C modulates expression of miRNA-101 to suppress VE-cadherin in human brain microvascular endothelial cells. *J. Neurosci.* 33, 5992–6000. doi: 10.1523/JNEUROSCI.4796-12.2013

Nikolaus, M., Knierim, E., Meisel, C., Kreye, J., Prüss, H., Schnabel, D., et al. (2018). Severe GABAA receptor encephalitis without seizures: a paediatric case successfully treated with early immunomodulation. *Eur. J. Paediatr. Neurol.* 22, 558–562. doi: 10.1016/j.ejpn.2018.01.002

Noble, P. W., Bernatsky, S., Clarke, A. E., Isenberg, D. A., Ramsey-Goldman, R., and Hansen, J. E. (2016). DNA-damaging autoantibodies and cancer: the lupus butterfly theory. *Nat. Rev. Rheumatol.* 12, 429–434. doi: 10.1038/nrrheum.2016.23

Ohkawa, T., Satake, S., Yokoi, N., Miyazaki, Y., Ohshita, T., Sobue, G., et al. (2014). Identification and characterization of $GABA_A$ receptor autoantibodies in autoimmune encephalitis. *J. Neurosci.* 34, 8151–8163. doi: 10.1523/JNEUROSCI.4415-13.2014

Petit-Pedrol, M., Armangue, T., Peng, X., Bataller, L., Cellucci, T., Davis, R., et al. (2014). Encephalitis with refractory seizures, status epilepticus and antibodies to the GABAA receptor: a case series, characterisation of the antigen and analysis of the effects of antibodies. *Lancet Neurol.* 13, 276–286. doi: 10.1016/S1474-4422(13)70299-0

Pettingill, P., Kramer, H. B., Coebergh, J. A., Pettingill, R., Maxwell, S., Nibber, A., et al. (2015). Antibodies to GABAA receptor α1 and γ2 subunits: clinical and serologic characterization. *Neurology* 84, 1233–1241. doi: 10.1212/WNL.0000000000001326

Piepgras, J., Holtje, M., Otto, C., Harms, H., Satapathy, A., Cesca, F., et al. (2015). Intrathecal immunoglobulin A and G antibodies to synapsin in a patient with limbic encephalitis. *Neurol. Neuroimmunol. Neuroinflamm.* 2:e169. doi: 10.1212/NXI.0000000000000169

Pittock, S. J., Yoshikawa, H., Ahlskog, J. E., Tisch, S. H., Benarroch, E. E., Kryzer, T. J., et al. (2006). Glutamic acid decarboxylase autoimmunity with brainstem, extrapyramidal and spinal cord dysfunction. *Mayo Clin. Proc.* 81, 1207–1214. doi: 10.4065/81.9.1207

Reincke, S. M., Prüss, H., and Kreye, J. (2020). Brain antibody sequence evaluation (BASE): an easy-to-use software for complete data analysis in single cell immunoglobulin cloning. *BMC Bioinform.* 21:446. doi: 10.1186/s12859-020-03741-w

Rocchi, A., Sacchetti, S., Fusco, A. de., Giovedi, S., Parisi, B., Cesca, F., et al. (2019). Autoantibodies to synapsin I sequestrate synapsin I and alter synaptic function. *Cell Death Dis.* 10:864. doi: 10.1038/s41419-019-2106-z

Rubin, L. L., Hall, D. E., Porter, S., Barbu, K., Cannon, C., Horner, H. C., et al. (1991). A cell culture model of the blood-brain barrier. *J. Cell Biol.* 115, 1725–1735. doi: 10.1083/jcb.115.6.1725

Shimizu, F., Schaller, K. L., Owens, G. P., Cotleur, A. C., Kellner, D., Takeshita, Y., et al. (2017). Glucose-regulated protein 78 autoantibody associates with blood-brain barrier disruption in neuromyelitis optica. *Sci. Transl. Med.* 9:eaai9111. doi: 10.1126/scitranslmed.aai9111

Shimizu, F., Takeshita, Y., Sano, Y., Hamamoto, Y., Shiraishi, H., Sato, T., et al. (2019). GRP78 antibodies damage the blood-brain barrier and relate to cerebellar degeneration in Lambert-Eaton myasthenic syndrome. *Brain* 142, 2253–2264. doi: 10.1093/brain/awz168

Sousa, A. D., Berg, J. S., Robertson, B. W., Meeker, R. B., and Cheney, R. E. (2006). Myo10 in brain: developmental regulation, identification of a headless isoform and dynamics in neurons. *J. Cell Sci.* 119, 184–194. doi: 10.1242/jcs.02726

Spatola, M., Petit-Pedrol, M., Simabukuro, M. M., Armangue, T., Castro, F. J., Barcelo Artigues, M. I., et al. (2017). Investigations in GABAA receptor antibody-associated encephalitis. *Neurology* 88, 1012–1020. doi: 10.1212/WNL.0000000000003713

Srinivasan, B., Kolli, A. R., Esch, M. B., Abaci, H. E., Shuler, M. L., and Hickman, J. J. (2015). TEER measurement techniques for in vitro barrier model systems. *J. Lab. Automation* 20, 107–126. doi: 10.1177/2211068214561025

Titulaer, M. J., McCracken, L., Gabilondo, I., Armangué, T., Glaser, C., Iizuka, T., et al. (2013). Treatment and prognostic factors for long-term outcome in patients with anti-N-Methyl-D-Aspartate (NMDA) receptor encephalitis: a cohort study. *Lancet Neurol.* 12, 157–165. doi: 10.1016/S1474-4422(12)70310-1

Tomizawa, Y., Yokoyama, K., Saiki, S., Takahashi, T., Matsuoka, J., and Hattori, N. (2012). Blood-brain barrier disruption is more severe in neuromyelitis optica than in multiple sclerosis and correlates with clinical disability. *J. Int. Med. Res.* 40, 1483–1491. doi: 10.1177/147323001204000427

Vorbrodt, A. W., and Dobrogowska, D. H. (2003). Molecular anatomy of intercellular junctions in brain endothelial and epithelial barriers: electron microscopist's view. *Brain Res. Rev.* 42, 221–242. doi: 10.1016/s0165-0173(03)00177-2

Wagner, F., Goertzen, A., Kiraly, O., Laube, G., Kreye, J., Witte, O. W., et al. (2020). Detailed morphological analysis of rat hippocampi treated with CSF autoantibodies from patients with anti-NMDAR encephalitis discloses two distinct types of immunostaining patterns. *Brain Res.* 1747:147033. doi: 10.1016/j.brainres.2020.147033

Wang, W., Dentler, W. L., and Borchardt, R. T. (2001). VEGF increases BMEC monolayer permeability by affecting occludin expression and tight junction assembly. *Am. J. Physiol. Heart Circ. Physiol.* 280, H434–H440. doi: 10.1152/ajpheart.2001.280.1.H434

Weksler, B. B., Subileau, E. A., Perriere, N., Charneau, P., Holloway, K., Leveque, M., et al. (2005). Blood-brain barrier-specific properties of a human adult brain endothelial cell line. *FASEB J.* 19, 1872–1874. doi: 10.1096/fj.04-3458fje

Xu, R., Feng, X., Xie, X., Zhang, J., Wu, D., and Xu, L. (2012). HIV-1 Tat protein increases the permeability of brain endothelial cells by both inhibiting occludin expression and cleaving occludin via matrix metalloproteinase-9. *Brain Res.* 1436, 13–19. doi: 10.1016/j.brainres.2011.11.052

Yoshio, T., Okamoto, H., Hirohata, S., and Minota, S. (2013). IgG anti-NR2 glutamate receptor autoantibodies from patients with systemic lupus erythematosus activate endothelial cells. *Arthritis Rheum.* 65, 457–463. doi: 10.1002/art.37745

Cell

Article

A Therapeutic Non-self-reactive SARS-CoV-2 Antibody Protects from Lung Pathology in a COVID-19 Hamster Model

Graphical Abstract

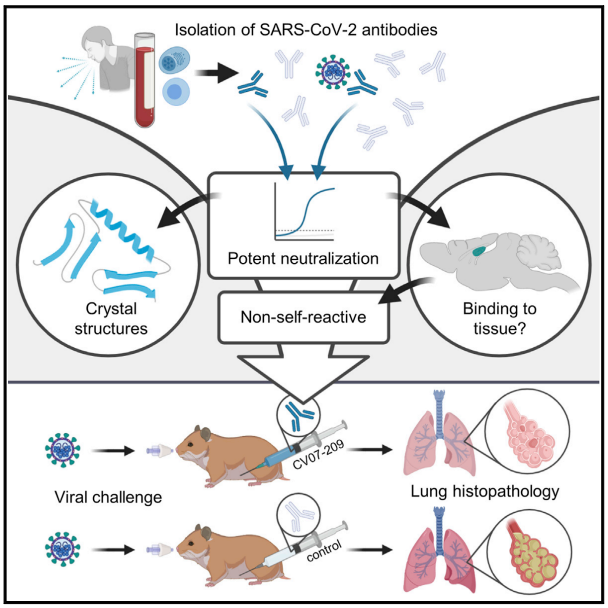

Highlights

- Characterization of potent human monoclonal SARS-CoV-2-neutralizing antibodies
- Some SARS-CoV-2 antibodies reacted with mammalian self-antigens in different organs
- Crystal structures of two antibodies in complex with SARS-CoV-2 RBD at 2.55/2.70 Å
- Post-exposure antibody treatment protected from lung damage in infected hamsters

Authors

Jakob Kreye, S. Momsen Reincke, Hans-Christian Kornau, ..., Nikolaus Osterrieder, Ian A. Wilson, Harald Prüss

Correspondence

jakob.kreye@dzne.de (J.K.), harald.pruess@dzne.de (H.P.)

In Brief

Kreye et al. report isolation and characterization of monoclonal antibodies from COVID-19 patients, some of which were found to display autoreactivity with mammalian self-antigens in different organs. Crystal structures of two antibodies in complex with the SARS-CoV-2 spike RBD reveal antibody engagement with the ACE2 binding site from different approach angles. One antibody was evaluated further for *in vivo* efficacy and found to be both protective and efficacious post-challenge in a hamster infection model.

Kreye et al., 2020, Cell *183*, 1058–1069
November 12, 2020
https://doi.org/10.1016/j.cell.2020.09.049

CellPress

CellPress
OPEN ACCESS

Cell

Article

A Therapeutic Non-self-reactive SARS-CoV-2 Antibody Protects from Lung Pathology in a COVID-19 Hamster Model

Jakob Kreye,[1,2,3,4,21,22,*] S. Momsen Reincke,[1,2,3,5,21] Hans-Christian Kornau,[1,6] Elisa Sánchez-Sendin,[1,2,3] Victor Max Corman,[7] Hejun Liu,[8] Meng Yuan,[8] Nicholas C. Wu,[8] Xueyong Zhu,[8] Chang-Chun D. Lee,[8] Jakob Trimpert,[9] Markus Höltje,[10] Kristina Dietert,[11,12] Laura Stöffler,[1,3] Niels von Wardenburg,[1,3] Scott van Hoof,[1,2,3] Marie A. Homeyer,[1,3,5] Julius Hoffmann,[1,3] Azza Abdelgawad,[9] Achim D. Gruber,[11] Luca D. Bertzbach,[9] Daria Vladimirova,[9] Lucie Y. Li,[2,10] Paula Charlotte Barthel,[10] Karl Skriner,[13] Andreas C. Hocke,[14] Stefan Hippenstiel,[14]

(Author list continued on next page)

[1]German Center for Neurodegenerative Diseases (DZNE) Berlin, 10117 Berlin, Germany
[2]Helmholtz Innovation Lab BaoBab (Brain Antibody-omics and B-cell Lab), 10117 Berlin, Germany
[3]Department of Neurology and Experimental Neurology, Charité-Universitätsmedizin Berlin, Corporate Member of Freie Universität Berlin, Humboldt-Universität Berlin, and Berlin Institute of Health, 10117 Berlin, Germany
[4]Department of Pediatric Neurology, Charité-Universitätsmedizin Berlin, Corporate Member of Freie Universität Berlin, Humboldt-Universität Berlin, and Berlin Institute of Health, 10117 Berlin, Germany
[5]Berlin Institute of Health (BIH), 10178 Berlin, Germany
[6]Neuroscience Research Center (NWFZ), Cluster NeuroCure, Charité-Universitätsmedizin Berlin, Corporate Member of Freie Universität Berlin, Humboldt-Universität Berlin, and Berlin Institute of Health, 10117 Berlin, Germany
[7]Institute of Virology, Charité-Universitätsmedizin Berlin, Corporate Member of Freie Universität Berlin, Humboldt-Universität zu Berlin, and

(Affiliations continued on next page)

SUMMARY

The emergence of SARS-CoV-2 led to pandemic spread of coronavirus disease 2019 (COVID-19), manifesting with respiratory symptoms and multi-organ dysfunction. Detailed characterization of virus-neutralizing antibodies and target epitopes is needed to understand COVID-19 pathophysiology and guide immunization strategies. Among 598 human monoclonal antibodies (mAbs) from 10 COVID-19 patients, we identified 40 strongly neutralizing mAbs. The most potent mAb, CV07-209, neutralized authentic SARS-CoV-2 with an IC_{50} value of 3.1 ng/mL. Crystal structures of two mAbs in complex with the SARS-CoV-2 receptor-binding domain at 2.55 and 2.70 Å revealed a direct block of ACE2 attachment. Interestingly, some of the near-germline SARS-CoV-2-neutralizing mAbs reacted with mammalian self-antigens. Prophylactic and therapeutic application of CV07-209 protected hamsters from SARS-CoV-2 infection, weight loss, and lung pathology. Our results show that non-self-reactive virus-neutralizing mAbs elicited during SARS-CoV-2 infection are a promising therapeutic strategy.

INTRODUCTION

Severe acute respiratory syndrome coronavirus 2 (SARS-CoV-2) started emerging in humans in late 2019 and rapidly became a pandemic with millions of cases worldwide. SARS-CoV-2 infection causes coronavirus disease 2019 (COVID-19) with severe respiratory symptoms, pathological inflammation, and multi-organ dysfunction, including acute respiratory distress syndrome, cardiovascular events, coagulopathies, and neurological symptoms (Helms et al., 2020; Zhou et al., 2020; Zhu et al., 2020). Some aspects of the diverse clinical manifestations may result from a hyperinflammatory response, as suggested by reduced mortality in hospitalized COVID-19 patients under dexamethasone therapy (Horby et al., 2020).

Understanding the immune response to SARS-CoV-2 is of utmost importance. Multiple recombinant SARS-CoV-2 monoclonal antibodies (mAbs) from convalescent patients have been reported (Brouwer et al., 2020; Cao et al., 2020; Ju et al., 2020; Kreer et al., 2020; Robbiani et al., 2020; Rogers et al., 2020; Wec et al., 2020). mAbs targeting the receptor-binding domain (RBD) of the viral spike protein S1 can compete with its binding to human angiotensin-converting enzyme 2 (ACE2) and prevent virus entry and subsequent replication (Cao et al., 2020; Ju et al., 2020; Walls et al., 2020). Potent virus-neutralizing mAbs that were isolated from diverse variable immunoglobulin (Ig) genes typically carry low levels of somatic hypermutations (SHMs). Several of these neutralizing mAbs selected for *in vitro* efficacy showed prophylactic or therapeutic potential in animal

Cell
Article

CellPress
OPEN ACCESS

Martin Witzenrath,[14] Norbert Suttorp,[14] Florian Kurth,[14,15] Christiana Franke,[3] Matthias Endres,[1,3,16,17,18] Dietmar Schmitz,[1,6] Lara Maria Jeworowski,[7] Anja Richter,[7] Marie Luisa Schmidt,[7] Tatjana Schwarz,[7] Marcel Alexander Müller,[7] Christian Drosten,[7] Daniel Wendisch,[14] Leif E. Sander,[14] Nikolaus Osterrieder,[9,19] Ian A. Wilson,[8,20] and Harald Prüss[1,2,3,*]

Berlin Institute of Health, 10117 Berlin, Germany, and German Centre for Infection Research (DZIF), 10117 Berlin, Germany
[8]Department of Integrative Structural and Computational Biology, The Scripps Research Institute, La Jolla, CA 92037, USA
[9]Institute of Virology, Freie Universität Berlin, 14163 Berlin, Germany
[10]Institute of Integrative Neuroanatomy Berlin, Charité-Universitätsmedizin Berlin, Corporate Member of Freie Universität Berlin, Humboldt-Universität zu Berlin, and Berlin Institute of Health, 10117 Berlin, Germany
[11]Institute of Veterinary Pathology, Freie Universität Berlin, 14163 Berlin, Germany
[12]Veterinary Centre for Resistance Research, Freie Universität Berlin, 14163 Berlin, Germany
[13]Department of Rheumatology and Clinical Immunology, Charité-Universitätsmedizin Berlin, Corporate Member of Freie Universität Berlin, Humboldt-Universität Berlin, and Berlin Institute of Health, 10117 Berlin, Germany
[14]Department of Infectious Diseases and Respiratory Medicine, Charité-Universitätsmedizin Berlin, Corporate Member of Freie Universität Berlin, Humboldt-Universität Berlin, and Berlin Institute of Health, 10117 Berlin, Germany
[15]Department of Tropical Medicine, Bernhard Nocht Institute for Tropical Medicine and I. Department of Medicine, University Medical Center Hamburg-Eppendorf, 20359 Hamburg, Germany
[16]Center for Stroke Research Berlin, Charité-Universitätsmedizin Berlin, Corporate Member of Freie Universität Berlin, Humboldt-Universität Berlin, and Berlin Institute of Health, 10117 Berlin, Germany
[17]Excellence Cluster NeuroCure Berlin, Charité-Universitätsmedizin Berlin, Corporate Member of Freie Universität Berlin, Humboldt-Universität Berlin, and Berlin Institute of Health, 10117 Berlin, Germany
[18]German Centre for Cardiovascular Research (DZHK), Partner Site Berlin, Charité-Universitätsmedizin Berlin, Corporate Member of Freie Universität Berlin, Humboldt-Universität Berlin, and Berlin Institute of Health, 10785 Berlin, Germany
[19]Department of Infectious Diseases and Public Health, Jockey Club College of Veterinary Medicine and Life Sciences, City University of Hong Kong, Hong Kong
[20]The Skaggs Institute for Chemical Biology, The Scripps Research Institute, La Jolla, CA 92037, USA
[21]These authors contributed equally
[22]Lead Contact
*Correspondence: jakob.kreye@dzne.de (J.K.), harald.pruess@dzne.de (H.P.)
https://doi.org/10.1016/j.cell.2020.09.049

models (Cao et al., 2020; Liu et al., 2020; Rogers et al., 2020; Zost et al., 2020). The low number of SHMs suggests limited affinity maturation in germinal centers compatible with an acute infection. Near-germline mAbs usually constitute the first line of defense against pathogens but carry the risk of self-reactivity to autoantigens (Lerner, 2016; Liao et al., 2011; Zhou et al., 2007). Although critical for therapeutic use in humans, the potential tissue reactivity of near-germline SARS-CoV-2 antibodies has so far not been examined.

Here we systematically selected 18 strongly neutralizing mAbs of 598 antibodies from 10 COVID-19 patients by characterization of their biophysical properties, authentic SARS-CoV-2 neutralization, and exclusion of off-target binding to murine tissue. Additionally, we solved two crystal structures of neutralizing mAbs in complex with the RBD, showing antibody engagement with the ACE2 binding site from different approach angles. Finally, we selected mAb CV07-209 for *in vivo* evaluation because of its *in vitro* efficacy and absence of tissue reactivity. Systemic application of CV07-209 in a hamster model of SARS-CoV-2 infection led to a profound reduction of clinical, paraclinical, and histopathological COVID-19 pathology, reflecting its potential for translational application in patients with COVID-19.

RESULTS

Antibody Repertoire Analysis of COVID-19 Patients

We first characterized the B cell response in COVID-19 using single-cell Ig gene sequencing of human mAbs (Figure 1A). From 10 COVID-19 patients with serum antibodies to the S1 subunit of the SARS-CoV-2 spike protein (Figure S1A; Table S1), we isolated two populations of single cells from peripheral blood mononuclear cells with fluorescence-activated cell sorting (FACS): $CD19^+CD27^+CD38^+$ antibody-secreting cells (ASCs) reflecting the overall humoral immune response and SARS-CoV-2-S1-labeled $CD19^+CD27^+$ memory B cells (S1-MBCs) for characterization of antigen-specific responses (Figures S1B and S1C). We obtained 598 functional paired heavy- and light-chain Ig sequences (Table S2). Of 432 recombinantly expressed mAbs, 122 were reactive to SARS-CoV-2-S1 (S1+) with a frequency of 0.0%–18.2% (median, 7.1%) within ASCs and 16.7%–84.1% (median, 67.1%) within S1-MBCs (Figures 1B and 1C). Binding to S1 did not depend on affinity maturation, as measured by the number of SHMs (Figure 1D). Compared with mAbs not reactive to SARS-CoV-2-S1, S1+ mAbs had fewer SHMs but equal lengths of their light- and heavy-chain complementarity-determining region 3 (CDR3) (Figures S1D–S1F). Within the ASC and S1-MBC population, 45.0% and 90.2% of S1+ mAbs, respectively, bound the RBD (Figure S1G).

S1+ mAbs were enriched in certain Ig genes, including variable heavy (VH)1-2, VH3-53, VH3-66, variable kappa (VK)1-33, and variable lambda (VL)2-14 (Figure S2). We identified clonally related antibody clones within patients and public and shared S1+ clonotypes from multiple patients (Figures S3A and S3B). Some public or shared clonotypes had been reported previously, such as IGHV3-53 and IGHV3-66 (Figure S3D; Cao et al., 2020; Yuan et al., 2020a), whereas others were newly identified, such as IGHV3-11 (Figure S3C).

CellPress
OPEN ACCESS

Cell
Article

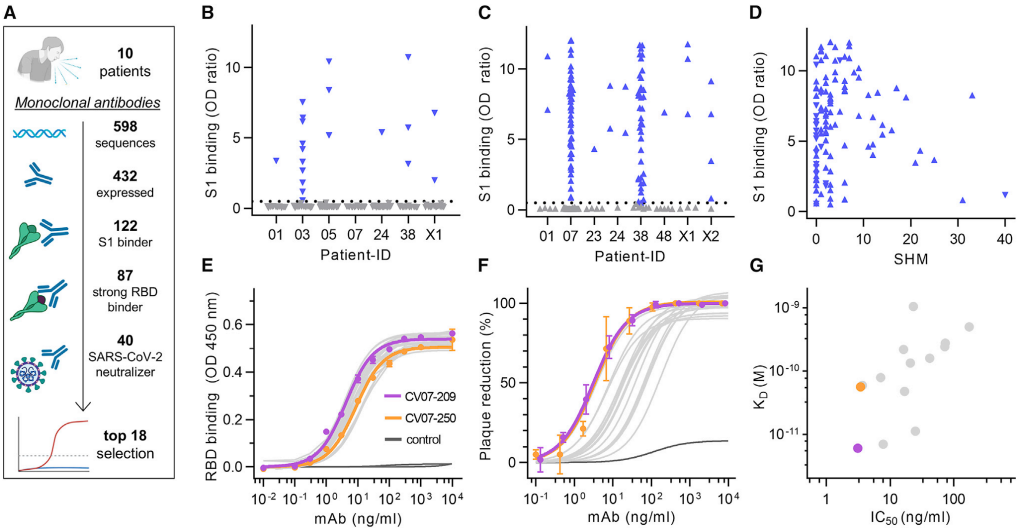

Figure 1. Identification and Characterization of Potent SARS-CoV-2-Neutralizing mAbs

(A) Diagram depicting the strategy for isolation of 18 potently neutralizing mAbs (top 18).

(B) Normalized binding to S1 of SARS-CoV-2 for mAbs isolated from ASCs (inverted triangles; blue, S1-binding; gray, not S1-binding). OD, optical density in ELISA.

(C) Normalized binding to S1 of SARS-CoV-2 for mAbs isolated from S1-stained MBCs (triangles; colors as in B).

(D) S1-binding plotted against the number of somatic hypermutations (SHMs) for all S1-reactive mAbs.

(E) Concentration-dependent binding of the top 18 SARS-CoV-2 mAbs to the RBD of S1 (mean ± SD from two wells of one experiment).

(F) Concentration-dependent neutralization of authentic SARS-CoV-2 plaque formation by the top 18 mAbs (mean ± SD from two independent measurements).

(G) Apparent affinities of mAbs to RBDs (K_D determined by surface plasmon resonance) plotted against IC_{50} of authentic SARS-CoV-2 neutralization.

See also Figures S1, S2, S3, S4, and S5 and Tables S1, S2, and S3.

Identification and Characterization of Potent SARS-CoV-2-Neutralizing mAbs

We next determined mAbs with the highest capacity to neutralize SARS-CoV-2 in plaque reduction neutralization tests (PRNTs) using an authentic virus (Munich isolate 984) (Wölfel et al., 2020). Of 87 mAbs strongly binding to the RBD, 40 showed virus neutralization with a half-maximal inhibitory concentration (IC_{50}) of 250 ng/mL or less and were considered neutralizing antibodies (Figure 1A; Table S2), of which 18 (top 18) were selected for further characterization (Table S3). The antibodies bound to the RBD with a half-maximal effective concentration (EC_{50}) of 3.8–14.2 ng/mL (Figure 1E) and an equilibrium dissociation constant (K_D) of 6.0 pM to 1.1 nM (Figure S4; Table S3), neutralizing SARS-CoV-2 with an IC_{50} value of 3.1–172 ng/mL (Figure 1F; Table S3). The antibody with the highest apparent affinity, CV07-209, was also the strongest neutralizer (Figure 1G). We hypothesized that the differences in neutralizing capacity relate to different interactions with the ACE2 binding site. Indeed, the strongest neutralizing mAbs, CV07-209 and CV07-250, reduced ACE2 binding to the RBD to 12.4% and 58.3%, respectively. Other top 18 mAbs, including CV07-270, interfered only weakly with ACE2 binding (Figure S5A).

The spike proteins of SARS-CoV-2 and SARS-CoV share more than 70% amino acid sequence identity, whereas sequence identity between SARS-CoV-2 and MERS-CoV and other endemic coronaviruses is significantly lower (Barnes et al., 2020). To analyze potential cross-reactivity of mAbs to other coronaviruses, we tested for binding of the top 18 mAbs to the RBD of SARS-CoV, MERS-CoV, and the human endemic coronaviruses 229E, NL63, HKU1, and OC43. CV38-142 detected the RBDs of SARS-CoV-2 and SARS-CoV, whereas no other mAb was cross-reactive to additional coronaviruses (Figures S5C and S5D). To further characterize the epitope of neutralizing mAbs, we performed ELISA-based epitope binning experiments using biotinylated antibodies. Co-application of paired mAbs showed competition of most neutralizing antibodies for RBD binding (Figure S5B). As an exception, the SARS-CoV cross-reactive CV38-142 bound the RBD irrespective of the presence of other mAbs, suggesting an independent and conserved target epitope (Figure S5B).

Near-Germline SARS-CoV-2 Neutralizing Antibodies Can Bind to Murine Tissue

Many SARS-CoV-2-neutralizing mAbs carry few SHMs or are in germline configuration (Figure 1D; Ju et al., 2020; Kreer et al., 2020). Antibodies close to the germline might be reactive to more than one target (Zhou et al., 2007). Prompted by the

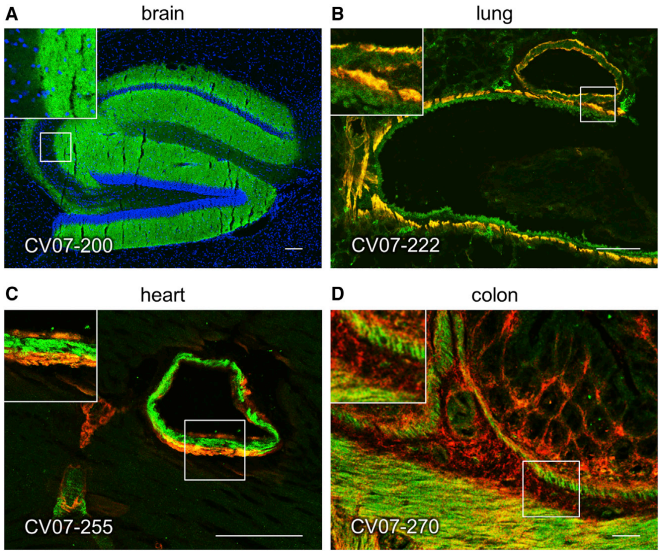

Figure 2. SARS-CoV-2-Neutralizing Antibodies Can Bind to Murine Tissue

Immunofluorescence staining of SARS-CoV-2 mAbs (green) on murine organ sections showed specific binding to distinct anatomical structures.

(A) Staining of hippocampal neuropil with CV07-200 (cell nuclei depicted in blue).

(B) Staining of bronchial walls with CV07-222.

(C) Staining of vascular walls with CV07-255.

(D) Staining of intestinal walls with CV07-270.

Smooth muscle tissue in (B)–(D) was co-stained with a commercial smooth muscle actin antibody (red). Scale bars, 100 μm. See also Table S3.

abundance of near-germline SARS-CoV-2 antibodies and to exclude potential side effects of mAb treatment, we next analyzed whether SARS-CoV-2 antibodies can bind to self-antigens.

We tested binding of S1 mAbs to unfixed murine tissues. Surprisingly, four of the top 18 potent SARS-CoV-2-neutralizing mAbs showed anatomically distinct tissue reactivities (Figure 2; Table S3). CV07-200 intensively stained brain sections in the hippocampal formation, olfactory bulb, cerebral cortex, and basal ganglia (Figure 2A). CV07-222 also bound to brain tissue as well as to smooth muscle (Figure 2B). CV07-255 and CV07-270 were reactive to smooth muscle from sections of lung, heart, kidney, and colon but not liver (Figures 2C and 2D; Table S3). None of the top 18 mAbs bound to HEp-2 cells, cardiolipin, or beta-2 microglobulin as established polyreactivity-related antigens (Jardine et al., 2016; Figure S5E).

Crystal Structures of Two mAbs Approaching the ACE2 Binding Site from Different Angles

Diffraction-quality crystals were obtained for the SARS-CoV-2 RBD complexed with two individual neutralizing mAbs, CV07-250 and CV07-270, which have notable differences in the number of SHMs, extent of ACE2 competition, and binding to murine tissue. CV07-250 (IC_{50} = 3.5 ng/mL) had 33 SHMs (17/16 on the heavy and light chain, respectively) and strongly reduced ACE2 binding and showed no binding to murine tissue. In contrast, CV07-270 (IC_{50} = 82.3 ng/mL) had only 2 SHMs (2/0), did not reduce ACE2 binding in our assay, and showed binding to smooth muscle tissue. Using X-ray crystallography, we determined the structures of CV07-250 and CV07-270 in complex with the SARS-CoV-2 RBD to resolutions of 2.55 and 2.70 Å, respectively (Figure 3; Tables S4 and S5).

The binding mode of CV07-250 to the RBD is unusual in that it is dominated by the light chain (Figures 3A and 3D), whereas in CV07-270, the heavy chain dominates, as found frequently in other antibodies (Figures 3B and 3E). Upon interaction with the RBD, CV07-250 has a buried surface area (BSA) of 399 Å^2 and 559 Å^2 on the heavy and light chains, respectively, compared with 714 Å^2 and 111 Å^2 in CV07-270. CV07-250 uses CDR H1, H3, L1, and L3 and framework region 3 (LFR3) for RBD interaction (Figures 3D and 4A–4C), whereas CV07-270 interacts with CDR H1, H3, L1, and L2 (Figures 3E and 4D–4F).

The epitope of CV07-250 completely overlaps with the ACE2 binding site with a similar angle of approach as ACE2 (Figures 3A, 3C, 4G, and 4I). In contrast, the CV07-270 epitope only partially overlaps with the ACE2 binding site, and the antibody approaches the RBD from a different angle compared with CV07-250 and ACE2 (Figures 3B, 3C, 4H, and 4I), explaining differences in ACE2 competition. Although CV07-250 and CV07-270 contact 25 epitope residues, only seven residues are shared (G446/G447/E484/G485/Q493/S494/Q498). Furthermore, CV07-270 binds to a similar epitope as the SARS-CoV-2-neutralizing antibody P2B-2F6 (Ju et al., 2020) with a similar angle of approach (Figure S5F). In fact, 18 of 20 residues in the P2B-2F6 epitope overlap with the CV07-270 epitope, although CV07-270 and P2B-2F6 are encoded by different germline genes for the heavy and light chains. Thus, these two mAbs represent antibodies encoded by different germline genes that bind to the same epitope in the RBD with near-identical binding modes and approach angles. This structural convergence is also encouraging for targeting this highly immunogenic epitope for vaccine development.

Interestingly, CV07-250 was isolated 19 days after symptom onset but had already acquired 33 SHMs, the highest number among all S1+ MBCs (Figure S1D). Some non-germline amino acids are not directly involved in RBD binding, including all five SHMs on CDR H2 (Figure S6). This observation suggests that CV07-250 could have been initially affinity matured against a different antigen.

CellPress
OPEN ACCESS

Cell
Article

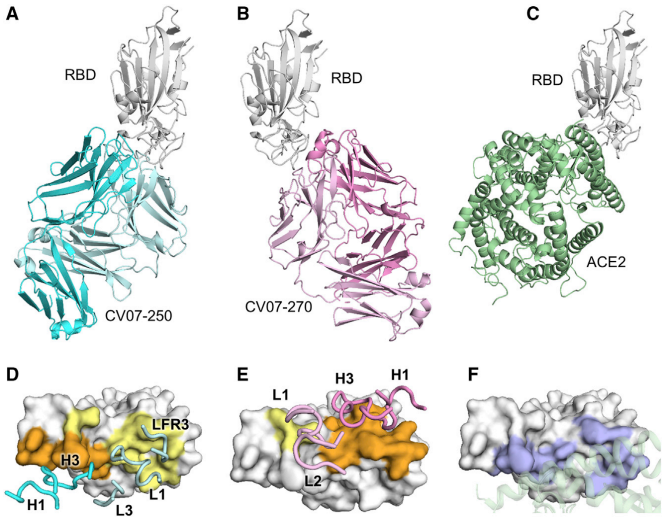

Figure 3. Crystal Structures of mAbs in Complex with the SARS-CoV-2 RBD

(A) CV07-250 (cyan) in complex with the RBD (white).

(B) CV07-270 (pink) in complex with the RBD (white).

(C) Human ACE2 with the SARS-CoV-2 RBD (PDB: 6M0J; Lan et al., 2020).

(D and E) Epitopes of (D) CV07-250 and (E) CV07-270. Epitope residues contacting the heavy chain are shown in orange and those contacting the light chain in yellow. CDR loops and the framework region that contact the RBD are labeled.

(F) ACE2-binding residues on the RBD (blue) in the same view as in (D) and (E). The ACE2-interacting region is shown in green within a semi-transparent cartoon representation.

See also Figures S5 and S6 and Tables S4 and S5.

Prophylactic and Therapeutic mAbs in a COVID-19 Animal Model

Next we selected mAb CV07-209 for evaluation of *in vivo* efficacy based on its high capacity to neutralize SARS-CoV-2 and the absence of reactivity to mammalian tissue. We used the hamster model of COVID-19 because it is characterized by rapid weight loss and severe lung pathology (Osterrieder et al., 2020). In this experimental setup, hamsters were infected intranasally with authentic SARS-CoV-2. Nine hamsters per group received a prophylactic application of CV07-209 24 h before virus challenge or a therapeutic application of CV07-209 or the control antibody mGO53 2 h after virus challenge (Figure 5A).

Hamsters under control mAb treatment lost 5.5% ± 4.4% (mean ± SD) of body weight, whereas those that received mAb CV07-209 as a therapeutic or prophylactic single dose gained 2.2% ± 3.4% or 4.8% ± 3.4% weight after 5 days post-infection (dpi), respectively. Mean body weights gradually converged in animals followed up until 13 dpi, reflecting recovery of control-treated hamsters from SARS-CoV-2 infection (Figure 5B).

To investigate the presence of SARS-CoV-2 in the lungs, we measured functional SARS-CoV-2 particles from lung tissue homogenates. Plaque-forming units were below the detection threshold for all animals in the prophylactic group and in 2 of 3 in the treatment group at 3 and 5 dpi (Figures 5C and 5D). qPCR measurements of lung viral genomic RNA copies revealed a 4–5 and 3–4 log reduction at both time points in the prophylactic and therapeutic groups, indicating a drastic decrease in SARS-CoV-2 particles in the lungs after CV07-209 application. Reduced virus replication and cell infection was confirmed by lowered detection of subgenomic viral RNA (Figures 5C and 5D). However, genomic and subgenomic RNA levels from nasal washes and laryngeal swaps were similar between all groups, indicating virus replication in the upper airways (Figures 5C and 5D).

Additionally, we performed histopathological analyses of infected hamsters. As expected, all lungs from control-treated animals sacrificed at 3 dpi revealed typical histopathological signs of necro-suppurative pneumonia with suppurative bronchitis, necrosis of bronchial epithelial cells, and endothelialitis (Figure 6A). At 5 dpi, control-treated animals showed marked bronchial hyperplasia, severe interstitial pneumonia with marked type II alveolar epithelial cell hyperplasia, and endothelialitis (Figure 6D). In contrast, animals receiving prophylactic treatment with CV07-209 showed no signs of pneumonia, bronchitis, necrosis of bronchial epithelial cells, or endothelialitis at 3 dpi. Mild interstitial pneumonia with mild type II alveolar epithelial cell hyperplasia became apparent 5 dpi. Animals receiving therapeutic CV07-209 treatment also showed a marked reduction in histopathological signs of COVID-19 pathology, although, at both time points, one of three animals showed mild bronchopulmonary pathology with signs of interstitial pneumonia and endothelialitis. These qualitative findings were mirrored in the reduction of bronchitis and edema scores (Figures 6B and 6E; Table S6).

To confirm the absence of viral particles under CV07-209 treatment, we performed *in situ* hybridization of viral RNA at 3 dpi. No viral RNA was detectable in the prophylactic group, whereas all animals in the control group and one in the therapeutic group revealed intensive staining of viral RNA in proximity of bronchial epithelial cells (Figure 6C). These findings show that systemic application of the SARS-CoV-2-neutralizing mAb CV07-209 protects hamsters from COVID-19 lung pathology and weight loss in prophylactic and therapeutic settings.

DISCUSSION

Driven by the pandemic spread of COVID-19 in early 2020, numerous groups have reported isolation, characterization, structural analysis, and animal model application of SARS-CoV-2-neutralizing mAbs (Barnes et al., 2020; Brouwer et al., 2020; Cao et al., 2020; Ju et al., 2020; Kreer et al., 2020; Robbiani

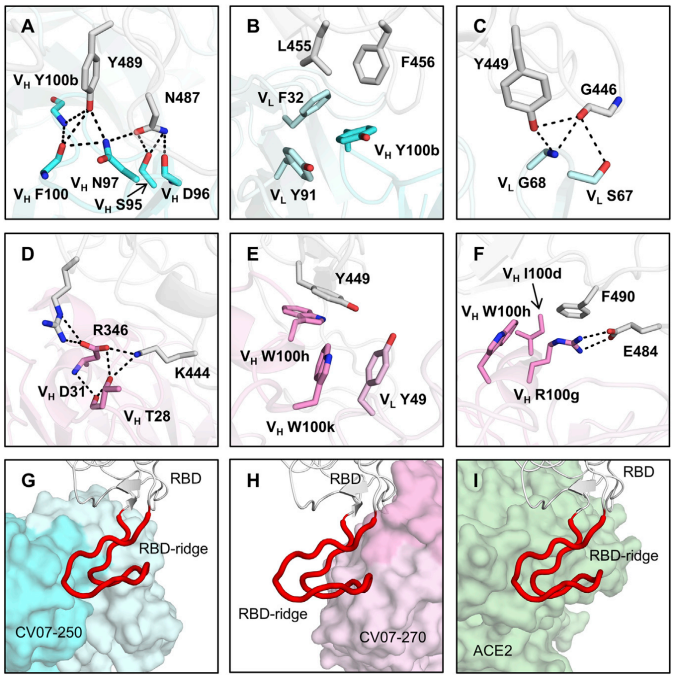

Figure 4. Interactions and Angle of Approach at the RBD-Antibody Interface

(A–C) Key interactions between CV07-250 (cyan) and the RBD (white) are highlighted.

(A) CDR H3 of CV07-250 forms a hydrogen bond network with RBD Y489 and N487.

(B) VH Y100b (CDR H3), VL F32 (CDR L1), and VL Y91 (CDR L3) of CV07-250 form a hydrophobic aromatic patch for interaction with RBD L455 and F456.

(C) The side chain of VL S67 and backbone amide of VL G68 from FR3 are engaged in a hydrogen bond network with RBD G446 and Y449.

(D–F) Interactions between CV07-270 (cyan) and the RBD (white).

(D) Residues in CDR H1 of CV07-270 participate in an electrostatic and hydrogen bond network with RBD R346 and K444.

(E) VH W100h and VH W100k on CDR H3 of CV07-270 make π-π stacking interactions with Y449. VH W100k is also stabilized by a π-π stacking interaction with VL Y49.

(F) VH R100 g on CDR H3 of CV07-270 forms an electrostatic interaction with RBD E484 as well as a π-cation interaction with RBD F490. Oxygen atoms are shown in red and nitrogen atoms in blue. Hydrogen bonds are represented by dashed lines.

(G–I) Magnified views of the different RBD ridge interactions with (G) CV07-250, (H) CV07-270, and (I) ACE2 (PDB: 6M0J; Lan et al., 2020). The ACE2-binding ridge in the RBD is represented by a backbone ribbon trace in red.

See also Figures S5 and S6 and Tables S4 and S5.

et al., 2020; Rogers et al., 2020; Wec et al., 2020). In many places, our work confirms previous results, including observation of a shared antibody response against the SARS-CoV-2 spike protein, identification of ACE2 blocking as an important mechanism of virus neutralization, isolation of high-affinity near-germline antibodies, and *in vivo* efficacy of prophylactic mAb application. Our results add several findings to the growing knowledge about the humoral immune response in SARS-CoV-2 infection.

First, we provide two structures of neutralizing mAbs identified in this study as binding to the RBD of SARS-CoV-2 at resolutions of 2.55 and 2.70 Å, allowing detailed characterization of the target epitopes and the SARS-CoV-2 neutralization mechanism of these two mAbs. SARS-CoV-2 mAbs can compete with ACE2 binding and exert neutralizing activity by inhibiting virus particle binding to host cells (Barnes et al., 2020; Brouwer et al., 2020; Cao et al., 2020; Ju et al., 2020; Kreer et al., 2020; Robbiani et al., 2020; Rogers et al., 2020; Wec et al., 2020), a key mechanism identified previously in SARS-CoV-neutralizing antibodies (Prabakaran et al., 2006; ter Meulen et al., 2006). Steric hindrance of mAbs blocking ACE2 binding to the RBD provides one mechanistic explanation of virus neutralization (Barnes et al., 2020; Cao et al., 2020; Wu et al., 2020). CV07-250 clearly belongs to this category of antibodies because its epitope lies within the ACE2 binding site, and it approaches the RBD from a similar angle as ACE2. In contrast, the epitope of CV07-270 only partially overlaps with the ACE2 binding site and approaches the RBD ridge from a different angle. In line with these findings, competition of CV07-270 with ACE2 binding, as detected by ELISA, was very weak; therefore, its mechanism of virus neutralization remains elusive. Of note, there have been reports of neutralizing antibodies targeting epitopes distant to the ACE2 binding site (Chi et al., 2020). Future research will need to clarify whether additional mechanisms, like triggering conformational changes in the spike protein upon antibody binding, contribute to virus neutralization, as reported for SARS-CoV (Walls et al., 2019).

Second, the majority of our SARS-CoV-2 mAbs are close to germline configuration, supporting previous studies (Kreer et al., 2020; Robbiani et al., 2020). Binding of some antibodies to HEp-2 cells has been reported before (Kreer et al., 2020), a finding we could confirm in our cohort. Given the increased probability of autoreactivity of near-germline antibodies, we additionally investigated reactivity of SARS-CoV-2 mAbs with unfixed murine tissue, allowing detection of reactivity to potential self-antigens in their natural conformation. Indeed, we found that a fraction of SARS-CoV-2-neutralizing antibodies also bound to brain-, lung-, heart-, kidney-, or gut-expressed epitopes. Such reactivity with host antigens should ideally be prevented by immunological tolerance mechanisms, but complete exclusion of such antibodies would generate "holes" in the antibody

CellPress
OPEN ACCESS

Cell
Article

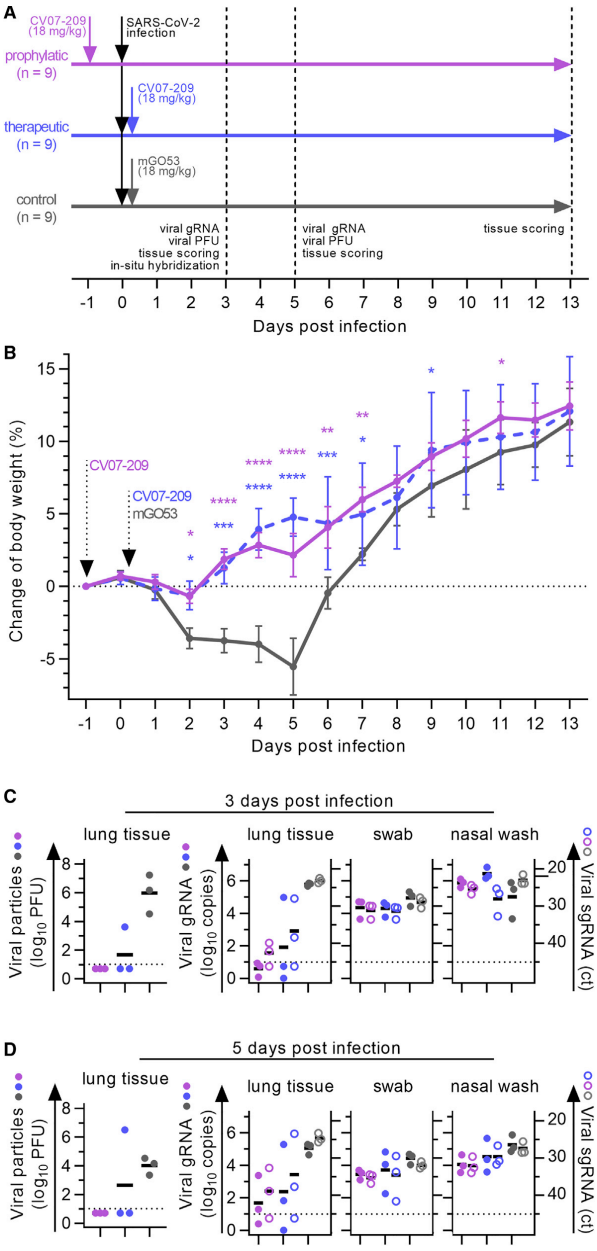

Figure 5. Prophylactic and Therapeutic Application of mAb CV07-209 in a COVID-19 Hamster Model

(A) Schematic overview of the animal experiment.

(B) Body weight of hamsters after virus challenge and prophylactic (pink) or therapeutic (blue) application of the SARS-CoV-2-neutralizing mAb CV07-209 or control antibody (mean ± SEM from 9 animals per group from days −1 to 3, n = 6 from days 4–5; n = 3 from days 6–13; mixed-effects model with post hoc Dunnett's multiple tests in comparison with the control group; significance levels are shown as *p < 0.05, **p < 0.01, ***p < 0.001, and ****p < 0.0001 or not shown when not significant.

(C and D) Left: quantification of plaque-forming units (PFU) from lung homogenates. Right: quantification of genomic SARS-CoV-2 RNA (gRNA) as copies per 10^5 cellular transcripts (left y axis, filled circles) and cycle threshold (ct) of subgenomic SARS-CoV-2 RNA (sgRNA) detection (right y axis, unfilled circles) from samples and time points as indicated. Values for PFUs were set to 5 when not detected, gRNA copies below 1 were set to 1, and the ct of sgRNA was set to 46 when not detected. Bars indicate the mean. Dotted lines represent the detection threshold.

See also Figure 6 and Table S6.

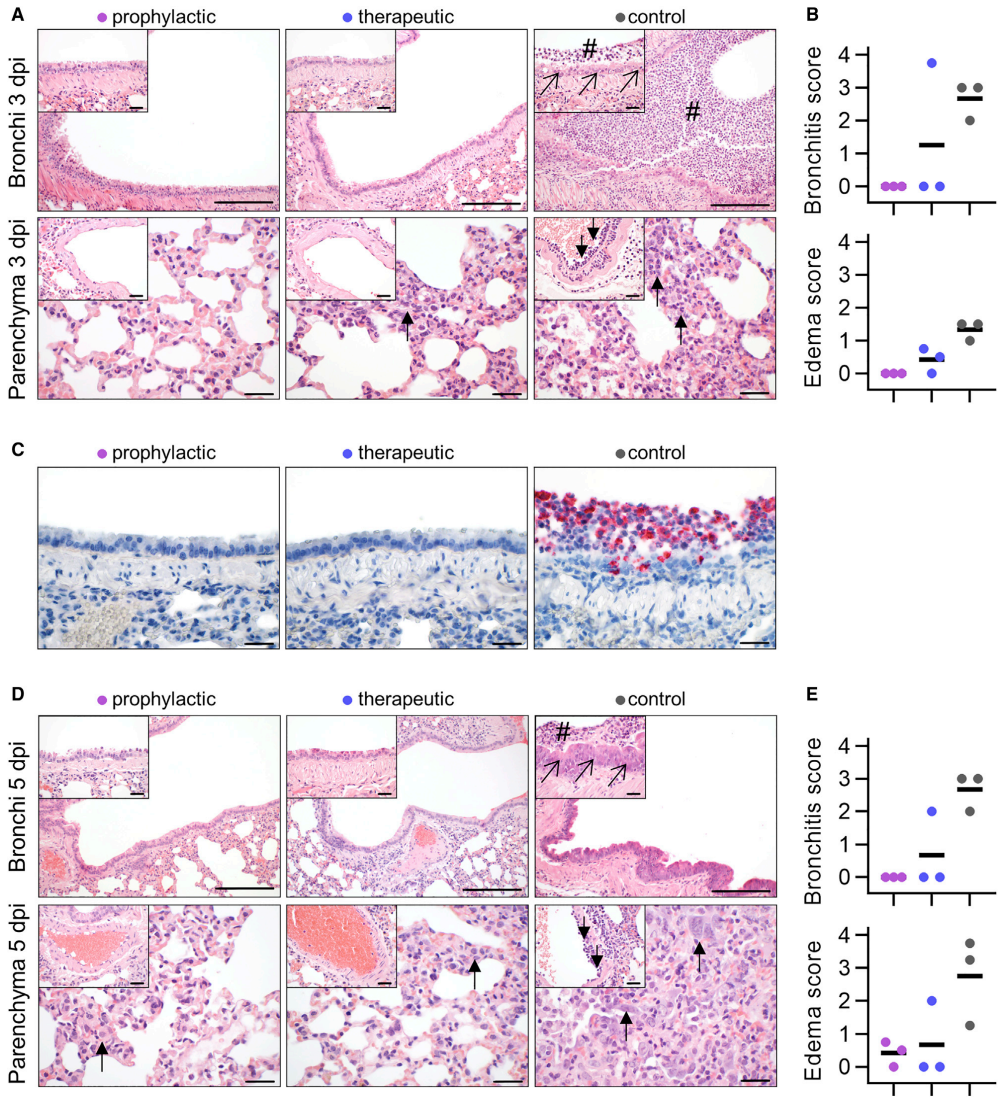

Figure 6. Histopathological Analysis of Hamsters after SARS-CoV-2 Infection

(A) Histopathology of representative hematoxylin-and-eosin-stained, paraffin-embedded bronchi with inserted epithelium (top row) and lung parenchyma with inserted blood vessels (bottom row) at 3 dpi. Severe suppurative bronchitis with immune cell infiltration (hash symbol) is apparent only in the control-treated animals with necrosis of bronchial epithelial cells (diagonal arrows). Necro-suppurative interstitial pneumonia (upward arrows) with endothelialitis (downward arrows) is prominent in control-treated animals. Scale bars, 200 μm in the bronchus overview, 50 μm in all others.

(B) Bronchitis and edema score at 3 dpi. Bars indicate the mean.

(C) Detection of viral RNA (red) using *in situ* hybridization of representative bronchial epithelium present only in the control group. Scale bars, 50 μm.

(D) Histopathology of representative lung sections from areas comparable with (A) at 5 dpi. Staining of bronchi of control-treated animals showed marked bronchial hyperplasia with hyperplasia of epithelial cells (diagonal arrow) and still existing bronchitis (hash symbol), absent in all prophylactically treated and in 2/3

(legend continued on next page)

repertoire. In fact, HIV utilizes epitopes shared by its envelope and mammalian self-antigens, harnessing immunological tolerance to impair anti-HIV antibody responses (Yang et al., 2013) and impeding successful vaccination (Jardine et al., 2016). To defy virus escape in HIV and, similarly, COVID-19, anergic, strongly self-reactive B cells likely enter germinal centers and undergo clonal redemption to mutate away from self-reactivity while retaining HIV or SARS-CoV-2 binding (Reed et al., 2016). Interestingly, longitudinal analysis of mAbs in COVID-19 showed that the number of SHMs in SARS-CoV-2-neutralizing antibodies only increased marginally over time (Kreer et al., 2020). This finding suggests that the self-reactivity observed in this study may not be limited to mAbs of the early humoral immune response in SARS-CoV-2 infection. Whether self-reactive antibodies could contribute to extra-pulmonary symptoms in COVID-19 awaits further studies and should be closely monitored in vaccination trials.

Finally, we evaluated in detail the *in vivo* efficacy of the most potent neutralizing antibody, CV07-209, in a Syrian hamster model of SARS-CoV-2 infection. This model is characterized by a severe phenotype including weight loss and distinct lung pathology. Our results demonstrated that prophylaxis and treatment with a single dose of CV07-209 not only led to clinical improvement, as shown by the absence of weight loss, but also to markedly reduced lung pathology. Although the findings confirm the efficacy of prophylactic mAb administration as described by other groups in mice, hamsters, and rhesus macaques (Cao et al., 2020; Liu et al., 2020; Rogers et al., 2020; Zost et al., 2020), our work also demonstrates the efficacy of post-exposure treatment in hamsters leading to virus clearance, clinical remission, and prevention of lung injury. We provide detailed insights into the lung pathology of SARS-CoV-2-infected hamsters at multiple times during the disease course, including the regeneration phase. It complements two very recent demonstrations of a therapeutic effect of mAbs in a hamster model of COVID-19 (Baum et al., 2020; Li et al., 2020). These data expand the growing knowledge about post-exposure treatment from transgenic hACE2 mice (Cao et al., 2020) and a mouse model using adenovector delivery of human ACE2 before virus challenge (Liu et al., 2020). Collectively, our results indicate that mAb treatment can be fine-tuned for exclusion of self-reactivity with mammalian tissues and that mAb administration can also be efficacious after infection, which will be the prevailing setting in COVID-19 patients.

Limitations of Study

Although our study confirms the potential of therapeutic mAb application for treatment of COVID-19, interpretation of the data is limited to a first exploration of a short window between infection and antibody administration. Although our paradigm mimics the relevant scenario of immediate post-exposure treatment, we cannot conclude whether the therapeutic benefit can also be translated into the more common clinical setting of treatment at heterogenous time points after symptoms have occurred. For this, follow-up studies will have to focus on delayed mAb application after symptom onset.

We also describe the reactivity of SARS-CoV-2 mAbs to self-antigens from different tissues. These findings require attention and, simultaneously, careful interpretation and thorough investigation to provide a better understanding of their functional relevance beyond the observed binding. This includes identification of non-viral target antigens, functional *in vitro* studies, and *in vivo* models. The self-reactive mAbs identified in this study derived from patients without severe extra-pulmonary symptoms. To address a possible connection between self-reactive antibodies and the diverse clinical manifestations of COVID-19, expression and characterization of mAbs from patients with such disease courses are needed.

STAR★METHODS

Detailed methods are provided in the online version of this paper and include the following:

- KEY RESOURCES TABLE
- RESOURCE AVAILABILITY
  - Lead Contact
  - Materials Availability
  - Data and Code Availability
- EXPERIMENTAL MODELS AND SUBJECT DETAILS
  - SARS-CoV-2-infected individuals and sample collection
  - Animal experiment approval and animal care
- METHOD DETAILS
  - PBMC collection and FACS staining
  - Generation of recombinant human monoclonal antibodies
  - SARS-CoV-2-S1 ELISA
  - RBD ELISA
  - Circos plot of public clonotypes
  - Identification of 18 strongly neutralizing antibodies
  - Surface plasmon resonance measurements
  - Plaque reduction neutralization test
  - Immunocytochemistry
  - Crystal structure determination of Fab-RBD complexes
  - Murine tissue reactivity screening
  - HEp2 cell assay
  - Polyreactivity screening ELISA
  - Hamster model of SARS-CoV-2 infection

therapeutically treated animals (top row). Lung parenchyma staining of control-treated animals showed severe interstitial pneumonia with marked type II alveolar epithelial cell hyperplasia and endothelialitis (insets, downward arrows). Compared with control-treated animals, prophylactically treated animals showed only mild signs of interstitial pneumonia with mild type II alveolar epithelial cell hyperplasia (upward arrow), whereas therapeutically treated animals showed a more heterogeneous picture, with 1/3 animals showing no signs of lung pathology, 1/3 animals showing only mild signs of interstitial pneumonia, and 1/3 animals showing moderate multifocal interstitial pneumonia. Scale bars, 200 μm in the bronchus overview, 50 μm in all others.
(E) Bronchitis and edema score at 5 dpi. Bars indicate the mean.
See also Figure 5 and Table S6.

- Histopathology and *in situ* hybridization
- Virus titrations, RNA extractions and RT-qPCR

● QUANTIFICATION AND STATISTICAL ANALYSIS

SUPPLEMENTAL INFORMATION

Supplemental Information can be found online at https://doi.org/10.1016/j.cell.2020.09.049.

ACKNOWLEDGMENTS

We thank Stefanie Bandura, Matthias Sillmann, and Doreen Brandl for excellent technical assistance; Christian Meisel for performing a cardiolipin ELISA; and Martin Barner for assistance with generating the circos plot in Figure S3B. We acknowledge BIAFFIN GmbH & Co. KG (Kassel, Germany) for performance of SPR measurements and Dr. Désirée Kunkel from the Flow & Mass Cytometry Core Facility at Charité-Universitätsmedizin Berlin for support with single-cell sorting. S.M.R. is a participant in the BIH-Charité Junior Clinician Scientist Program funded by Charité – Universitätsmedizin Berlin and the Berlin Institute of Health. Work at Scripps was supported by NIH K99 AI139445 (to N.C.W.) and the Bill and Melinda Gates Foundation OPP1170236 (to I.A.W.). Use of the SSRL, SLAC National Accelerator Laboratory, is supported by the U.S. Department of Energy, Office of Science, Office of Basic Energy Sciences under contract DE-AC02–76SF00515. The SSRL Structural Molecular Biology Program is supported by the DOE Office of Biological and Environmental Research and the National Institutes of Health, National Institute of General Medical Sciences (including P41GM103393). This work was supported by COVID-19 grants from Freie Universität Berlin and Berlin University Alliance (to N.O. and L.E.S.); by the German Research Foundation (DFG) (SFB-TR84 to A.D.G., A.C.H., S.H., N.S., M.W., C.D., and L.E.S.; EXC2049 to M.E. and D.S.; and PR 1274/2-1, PR 1274/3-1, and PR 1274/5-1 to H.P.); by the Helmholtz Association (ExNet0009 to H.-C.K. and HIL-A03 to H.P.); and by the Federal Ministry of Education and Research (Connect-Generate 01GM1908D to H.P. and PROVID 01KI20160A and SYMPATH 01ZX1906A to M.W., A.C.H., S.H., N.S., and L.E.S.).

AUTHOR CONTRIBUTIONS

Conceptualization, J.K., S.M.R., H.-C.K., V.M.C., J.T., K.D., H.L., M.Y., N.C.W., N.O., I.A.W., and H.P.; Software, J.K. and S.M.R.; Formal Analysis, J.K., S.M.R., H.-C.K., E.S.-S., V.M.C., H.L., M.Y., N.C.W., J.T., M.H., L.D.B., K.D., A.D.G., M.E., D.S., A.D.G., M.A.M., C.D., N.O., I.A.W., and H.P.; Investigation, J.K., S.M.R., H.-C.K., E.S.-S., V.M.C., H.L., M.Y., N.C.W., X.Z., C.-C.D.L., J.T., M.H., K.D., L.S., N.v.W., S.v.H., M.A.H., J.H., A.A., L.D.B., D.V., L.Y.L., P.C.B., A.C.H., K.S., L.M.J., A.R., M.L.S., T.S., and D.W.; Resources, S.H., M.W., N.S., F.K., C.F., M.E., D.S., D.W., L.E.S., and H.P.; Writing – Original Draft, J.K., S.M.R., and H.P.; Writing – Review & Editing, all authors; Supervision, J.K., S.M.R., I.A.W., and H.P.

DECLARATION OF INTERESTS

Related to this work, the German Center for Neurodegenerative Diseases (DZNE) and Charité-Universitätsmedizin Berlin have filed a patent application on which J.K., S.M.R., H.-C.K., E.S.-S., V.M.C., M.A.M., D.W., L.E.S., and H.P. are named as inventors.

Received: August 11, 2020
Revised: September 14, 2020
Accepted: September 18, 2020
Published: September 23, 2020

REFERENCES

Adams, P.D., Afonine, P.V., Bunkóczi, G., Chen, V.B., Davis, I.W., Echols, N., Headd, J.J., Hung, L.W., Kapral, G.J., Grosse-Kunstleve, R.W., et al. (2010). PHENIX: a comprehensive Python-based system for macromolecular structure solution. Acta Crystallogr. D Biol. Crystallogr. *66*, 213–221.

Bailey, L.J., Sheehy, K.M., Dominik, P.K., Liang, W.G., Rui, H., Clark, M., Jaskolowski, M., Kim, Y., Deneka, D., Tang, W.J., and Kossiakoff, A.A. (2018). Locking the Elbow: Improved Antibody Fab Fragments as Chaperones for Structure Determination. J. Mol. Biol. *430*, 337–347.

Barnes, C.O., West, A.P., Jr., Huey-Tubman, K.E., Hoffmann, M.A.G., Sharaf, N.G., Hoffman, P.R., Koranda, N., Gristick, H.B., Gaebler, C., Muecksch, F., et al. (2020). Structures of Human Antibodies Bound to SARS-CoV-2 Spike Reveal Common Epitopes and Recurrent Features of Antibodies. Cell *182*, 828–842.e16.

Baum, A., Copin, R., Ajithdoss, D., Zhou, A., Lanza, K., Negron, N., Ni, M., Wei, Y., Atwal, G.S., Oyejide, A., et al. (2020). REGN-COV2 antibody cocktail prevents and treats SARS-CoV-2 infection in rhesus macaques and hamsters. bioRxiv. https://doi.org/10.1101/2020.08.02.233320.

Brouwer, P.J.M., Caniels, T.G., van der Straten, K., Snitselaar, J.L., Aldon, Y., Bangaru, S., Torres, J.L., Okba, N.M.A., Claireaux, M., Kerster, G., et al. (2020). Potent neutralizing antibodies from COVID-19 patients define multiple targets of vulnerability. Science *369*, 643–650.

Buchholz, U., Müller, M.A., Nitsche, A., Sanewski, A., Wevering, N., Bauer-Balci, T., Bonin, F., Drosten, C., Schweiger, B., Wolff, T., et al. (2013). Contact investigation of a case of human novel coronavirus infection treated in a German hospital, October-November 2012. Euro Surveill. *18*, 20406.

Cao, Y., Su, B., Guo, X., Sun, W., Deng, Y., Bao, L., Zhu, Q., Zhang, X., Zheng, Y., Geng, C., et al. (2020). Potent neutralizing antibodies against SARS-CoV-2 identified by high-throughput single-cell sequencing of convalescent patients' B cells. Cell *182*, 73–84.e16.

Chi, X., Yan, R., Zhang, J., Zhang, G., Zhang, Y., Hao, M., Zhang, Z., Fan, P., Dong, Y., Yang, Y., et al. (2020). A neutralizing human antibody binds to the N-terminal domain of the Spike protein of SARS-CoV-2. Science *369*, 650–655.

Corman, V.M., Landt, O., Kaiser, M., Molenkamp, R., Meijer, A., Chu, D.K., Bleicker, T., Brünink, S., Schneider, J., Schmidt, M.L., et al. (2020). Detection of 2019 novel coronavirus (2019-nCoV) by real-time RT-PCR. Euro Surveill. *25*, 2000045.

Dietert, K., Gutbier, B., Wienhold, S.M., Reppe, K., Jiang, X., Yao, L., Chaput, C., Naujoks, J., Brack, M., Kupke, A., et al. (2017). Spectrum of pathogen- and model-specific histopathologies in mouse models of acute pneumonia. PLoS ONE *12*, e0188251.

Ekiert, D.C., Friesen, R.H., Bhabha, G., Kwaks, T., Jongeneelen, M., Yu, W., Ophorst, C., Cox, F., Korse, H.J., Brandenburg, B., et al. (2011). A highly conserved neutralizing epitope on group 2 influenza A viruses. Science *333*, 843–850.

Emsley, P., and Cowtan, K. (2004). Coot: model-building tools for molecular graphics. Acta Crystallogr. D Biol. Crystallogr. *60*, 2126–2132.

Erickson, N.A., Gruber, A.D., and Mundhenk, L. (2020). The Family of Chloride Channel Regulator, Calcium-activated Proteins in the Feline Respiratory Tract: A Comparative Perspective on Airway Diseases in Man and Animal Models. J. Comp. Pathol. *174*, 39–53.

Gruber, A.D., Osterrieder, N., Bertzbach, L.D., Vladimirova, D., Greuel, S., Ihlow, J., Horst, D., Trimpert, J., and Dietert, K. (2020). Standardization of Reporting Criteria for Lung Pathology in SARS-CoV-2 Infected Hamsters – What Matters? Am. J. Respir. Cell Mol. Biol. Published online September 8, 2020. https://doi.org/10.1165/rcmb.2020-0280LE.

Gu, Z., Gu, L., Eils, R., Schlesner, M., and Brors, B. (2014). circlize Implements and enhances circular visualization in R. Bioinformatics *30*, 2811–2812.

Helms, J., Kremer, S., Merdji, H., Clere-Jehl, R., Schenck, M., Kummerlen, C., Collange, O., Boulay, C., Fafi-Kremer, S., Ohana, M., et al. (2020). Neurologic Features in Severe SARS-CoV-2 Infection. N. Engl. J. Med. *382*, 2268–2270.

Hoffmann, M., Kleine-Weber, H., Schroeder, S., Krüger, N., Herrler, T., Erichsen, S., Schiergens, T.S., Herrler, G., Wu, N.-H., Nitsche, A., et al. (2020). SARS-CoV-2 Cell Entry Depends on ACE2 and TMPRSS2 and Is Blocked by a Clinically Proven Protease Inhibitor. Cell *181*, 271–280.e8.

Horby, P., Lim, W.S., Emberson, J.R., Mafham, M., Bell, J.L., Linsell, L., Staplin, N., Brightling, C., Ustianowski, A., Elmahi, E., et al. (2020). Dexamethasone in Hospitalized Patients with Covid-19 - Preliminary Report. N. Engl. J. Med. Published online July 17, 2020. https://doi.org/10.1056/NEJMoa2021436.

Jardine, J.G., Sok, D., Julien, J.P., Briney, B., Sarkar, A., Liang, C.H., Scherer, E.A., Henry Dunand, C.J., Adachi, Y., Diwanji, D., et al. (2016). Minimally Mutated HIV-1 Broadly Neutralizing Antibodies to Guide Reductionist Vaccine Design. PLoS Pathog. *12*, e1005815.

Ju, B., Zhang, Q., Ge, J., Wang, R., Sun, J., Ge, X., Yu, J., Shan, S., Zhou, B., Song, S., et al. (2020). Human neutralizing antibodies elicited by SARS-CoV-2 infection. Nature *584*, 115–119.

Kornau, H.C., Kreye, J., Stumpf, A., Fukata, Y., Parthier, D., Sammons, R.P., Imbrosci, B., Kurpjuweit, S., Kowski, A.B., Fukata, M., et al. (2020). Human Cerebrospinal Fluid Monoclonal LGI1 Autoantibodies Increase Neuronal Excitability. Ann. Neurol. *87*, 405–418.

Kreer, C., Zehner, M., Weber, T., Ercanoglu, M.S., Gieselmann, L., Rohde, C., Halwe, S., Korenkov, M., Schommers, P., Vanshylla, K., et al. (2020). Longitudinal Isolation of Potent Near-Germline SARS-CoV-2-Neutralizing Antibodies from COVID-19 Patients. Cell *182*, 843–854.e12.

Kreye, J., Wenke, N.K., Chayka, M., Leubner, J., Murugan, R., Maier, N., Jurek, B., Ly, L.T., Brandl, D., Rost, B.R., et al. (2016). Human cerebrospinal fluid monoclonal N-methyl-D-aspartate receptor autoantibodies are sufficient for encephalitis pathogenesis. Brain *139*, 2641–2652.

Krissinel, E., and Henrick, K. (2007). Inference of macromolecular assemblies from crystalline state. J. Mol. Biol. *372*, 774–797.

Kurth, F., Roennefarth, M., Thibeault, C., Corman, V.M., Müller-Redetzky, H., Mittermaier, M., Ruwwe-Glösenkamp, C., Heim, K.M., Krannich, A., Zvorc, S., et al. (2020). Studying the pathophysiology of coronavirus disease 2019: a protocol for the Berlin prospective COVID-19 patient cohort (Pa-COVID-19). Infection *48*, 619–626.

Lan, J., Ge, J., Yu, J., Shan, S., Zhou, H., Fan, S., Zhang, Q., Shi, X., Wang, Q., Zhang, L., and Wang, X. (2020). Structure of the SARS-CoV-2 spike receptor-binding domain bound to the ACE2 receptor. Nature *581*, 215–220.

Lerner, R.A. (2016). Combinatorial antibody libraries: new advances, new immunological insights. Nat. Rev. Immunol. *16*, 498–508.

Li, W., Schäfer, A., Kulkarni, S.S., Liu, X., Martinez, D.R., Chen, C., Sun, Z., Leist, S.R., Drelich, A., Zhang, L., et al. (2020). High potency of a bivalent human VH domain in SARS-CoV-2 animal models. Cell, S0092-8674(20)31148-X.

Liao, H.X., Chen, X., Munshaw, S., Zhang, R., Marshall, D.J., Vandergrift, N., Whitesides, J.F., Lu, X., Yu, J.S., Hwang, K.K., et al. (2011). Initial antibodies binding to HIV-1 gp41 in acutely infected subjects are polyreactive and highly mutated. J. Exp. Med. *208*, 2237–2249.

Liu, L., Wang, P., Nair, M.S., Yu, J., Rapp, M., Wang, Q., Luo, Y., Chan, J.F., Sahi, V., Figueroa, A., et al. (2020). Potent neutralizing monoclonal antibodies directed to multiple epitopes on SARS-CoV-2 spike. Nature *584*, 450–456.

McCoy, A.J., Grosse-Kunstleve, R.W., Adams, P.D., Winn, M.D., Storoni, L.C., and Read, R.J. (2007). Phaser crystallographic software. J. Appl. Cryst. *40*, 658–674.

Minor, W., Cymborowski, M., Otwinowski, Z., and Chruszcz, M. (2006). HKL-3000: the integration of data reduction and structure solution–from diffraction images to an initial model in minutes. Acta Crystallogr. D Biol. Crystallogr. *62*, 859–866.

Nakamura, T., Karakida, N., Dantsuka, A., Ichii, O., Elewa, Y.H.A., Kon, Y., Nagasaki, K.I., Hattori, H., and Yoshiyasu, T. (2017). Effects of a mixture of medetomidine, midazolam and butorphanol on anesthesia and blood biochemistry and the antagonizing action of atipamezole in hamsters. J. Vet. Med. Sci. *79*, 1230–1235.

Osterrieder, N., Bertzbach, L.D., Dietert, K., Abdelgawad, A., Vladimirova, D., Kunec, D., Hoffmann, D., Beer, M., Gruber, A.D., and Trimpert, J. (2020). Age-Dependent Progression of SARS-CoV-2 Infection in Syrian Hamsters. Viruses *12*, 779.

Otwinowski, Z., and Minor, W. (1997). Processing of X-ray diffraction data collected in oscillation mode. Methods Enzymol *276*, 307–326.

Prabakaran, P., Gan, J., Feng, Y., Zhu, Z., Choudhry, V., Xiao, X., Ji, X., and Dimitrov, D.S. (2006). Structure of severe acute respiratory syndrome coronavirus receptor-binding domain complexed with neutralizing antibody. J. Biol. Chem. *281*, 15829–15836.

Reed, J.H., Jackson, J., Christ, D., and Goodnow, C.C. (2016). Clonal redemption of autoantibodies by somatic hypermutation away from self-reactivity during human immunization. J. Exp. Med. *213*, 1255–1265.

Reincke, S.M., Prüss, H., and Kreye, J. (2020). Brain Antibody Sequence Evaluation (BASE): an easy-to-use software for complete data analysis in single cell immunoglobulin cloning. BMC Bioinformatics *21* (446). https://doi.org/10.1186/s12859-020-03741-w.

Robbiani, D.F., Gaebler, C., Muecksch, F., Lorenzi, J.C.C., Wang, Z., Cho, A., Agudelo, M., Barnes, C.O., Gazumyan, A., Finkin, S., et al. (2020). Convergent antibody responses to SARS-CoV-2 in convalescent individuals. Nature *584*, 437–442.

Rogers, T.F., Zhao, F., Huang, D., Beutler, N., Burns, A., He, W.T., Limbo, O., Smith, C., Song, G., Woehl, J., et al. (2020). Isolation of potent SARS-CoV-2 neutralizing antibodies and protection from disease in a small animal model. Science *369*, 956–963.

Schritt, D., Li, S., Rozewicki, J., Katoh, K., Yamashita, K., Volkmuth, W., Cavet, G., and Standley, D.M. (2019). Repertoire Builder: high-throughput structural modeling of B and T cell receptors. Mol. Syst. Des. Eng. *4*, 761–768.

ter Meulen, J., van den Brink, E.N., Poon, L.L., Marissen, W.E., Leung, C.S., Cox, F., Cheung, C.Y., Bakker, A.Q., Bogaards, J.A., van Deventer, E., et al. (2006). Human monoclonal antibody combination against SARS coronavirus: synergy and coverage of escape mutants. PLoS Med. *3*, e237.

Tiller, T., Meffre, E., Yurasov, S., Tsuiji, M., Nussenzweig, M.C., and Wardemann, H. (2008). Efficient generation of monoclonal antibodies from single human B cells by single cell RT-PCR and expression vector cloning. J. Immunol. Methods *329*, 112–124.

Walls, A.C., Xiong, X., Park, Y.J., Tortorici, M.A., Snijder, J., Quispe, J., Cameroni, E., Gopal, R., Dai, M., Lanzavecchia, A., et al. (2019). Unexpected Receptor Functional Mimicry Elucidates Activation of Coronavirus Fusion. Cell *176*, 1026–1039.e15.

Walls, A.C., Park, Y.J., Tortorici, M.A., Wall, A., McGuire, A.T., and Veesler, D. (2020). Structure, Function, and Antigenicity of the SARS-CoV-2 Spike Glycoprotein. Cell *181*, 281–292.e6.

Wec, A.Z., Wrapp, D., Herbert, A.S., Maurer, D.P., Haslwanter, D., Sakharkar, M., Jangra, R.K., Dieterle, M.E., Lilov, A., Huang, D., et al. (2020). Broad neutralization of SARS-related viruses by human monoclonal antibodies. Science *369*, 731–736.

Wölfel, R., Corman, V.M., Guggemos, W., Seilmaier, M., Zange, S., Müller, M.A., Niemeyer, D., Jones, T.C., Vollmar, P., Rothe, C., et al. (2020). Virological assessment of hospitalized patients with COVID-2019. Nature *581*, 465–469.

Wu, Y., Wang, F., Shen, C., Peng, W., Li, D., Zhao, C., Li, Z., Li, S., Bi, Y., Yang, Y., et al. (2020). A noncompeting pair of human neutralizing antibodies block COVID-19 virus binding to its receptor ACE2. Science *368*, 1274–1278.

Yang, G., Holl, T.M., Liu, Y., Li, Y., Lu, X., Nicely, N.I., Kepler, T.B., Alam, S.M., Liao, H.X., Cain, D.W., et al. (2013). Identification of autoantigens recognized by the 2F5 and 4E10 broadly neutralizing HIV-1 antibodies. J. Exp. Med. *210*, 241–256.

Yuan, M., Liu, H., Wu, N.C., Lee, C.D., Zhu, X., Zhao, F., Huang, D., Yu, W., Hua, Y., Tien, H., et al. (2020a). Structural basis of a shared antibody response to SARS-CoV-2. Science *369*, 1119–1123.

Yuan, M., Wu, N.C., Zhu, X., Lee, C.D., So, R.T.Y., Lv, H., Mok, C.K.P., and Wilson, I.A. (2020b). A highly conserved cryptic epitope in the receptor binding domains of SARS-CoV-2 and SARS-CoV. Science *368*, 630–633.

Zhou, Z.H., Tzioufas, A.G., and Notkins, A.L. (2007). Properties and function of polyreactive antibodies and polyreactive antigen-binding B cells. J. Autoimmun. *29*, 219–228.

Zhou, P., Yang, X.L., Wang, X.G., Hu, B., Zhang, L., Zhang, W., Si, H.R., Zhu, Y., Li, B., Huang, C.L., et al. (2020). A pneumonia outbreak associated with a new coronavirus of probable bat origin. Nature *579*, 270–273.

Zhu, N., Zhang, D., Wang, W., Li, X., Yang, B., Song, J., Zhao, X., Huang, B., Shi, W., Lu, R., et al.; China Novel Coronavirus Investigating and Research Team (2020). A Novel Coronavirus from Patients with Pneumonia in China, 2019. N. Engl. J. Med. *382*, 727–733.

Zivcec, M., Safronetz, D., Haddock, E., Feldmann, H., and Ebihara, H. (2011). Validation of assays to monitor immune responses in the Syrian golden hamster (Mesocricetus auratus). J. Immunol. Methods *368*, 24–35.

Zost, S.J., Gilchuk, P., Case, J.B., Binshtein, E., Chen, R.E., Nkolola, J.P., Schafer, A., Reidy, J.X., Trivette, A., Nargi, R.S., et al. (2020). Potently neutralizing and protective human antibodies against SARS-CoV-2. Nature *584*, 443–449.

Curiculum Vitae

Mein Lebenslauf wird aus datenschutzrechtlichen Gründen in der elektronischen Version meiner Arbeit nicht veröffentlicht.

Curiculum Vitae

Mein Lebenslauf wird aus datenschutzrechtlichen Gründen in der elektronischen Version meiner Arbeit nicht veröffentlicht.

Publication List

1. Barthel PC, Staabs F, Li LY, Buthut M, Otto C, Ruprecht K, Prüss H, Höltje M. Immunoreactivity to astrocytes in different forms of dementia: High prevalence of autoantibodies to GFAP. Brain Behav Immun Health. 2023;29:100609.

2. Li LY, Kreye J, Burek M, Cordero-Gomez C, Barthel PC, Sánchez-Sendín E, Kornau HC, Schmitz D, Scharf M, Meybohm P, Reincke SM, Prüss H, Höltje M. Brain blood vessel autoantibodies in patients with NMDA and GABA(A) receptor encephalitis: identification of unconventional Myosin-X as target antigen. Front Cell Neurosci. 2023;17:1077204.

3. Kreye J, Reincke SM, Kornau HC, Sánchez-Sendin E, Corman VM, Liu H, Yuan M, Wu NC, Zhu X, Lee CD, Trimpert J, Höltje M, Dietert K, Stöffler L, von Wardenburg N, van Hoof S, Homeyer MA, Hoffmann J, Abdelgawad A, Gruber AD, Bertzbach LD, Vladimirova D, Li LY, Barthel PC, Skriner K, Hocke AC, Hippenstiel S, Witzenrath M, Suttorp N, Kurth F, Franke C, Endres M, Schmitz D, Jeworowski LM, Richter A, Schmidt ML, Schwarz T, Müller MA, Drosten C, Wendisch D, Sander LE, Osterrieder N, Wilson IA, Prüss H. A Therapeutic Non-self-reactive SARS-CoV-2 Antibody Protects from Lung Pathology in a COVID-19 Hamster Model. Cell. 2020;183(4):1058-69.e19.

4. Scheuer T, dem Brinke EA, Grosser S, Wolf SA, Mattei D, Sharkovska Y, Barthel PC, Endesfelder S, Friedrich V, Bührer C, Vida I, Schmitz T. Reduction of cortical parvalbumin-expressing GABAergic interneurons in a rodent hyperoxia model of preterm birth brain injury with deficits in social behavior and cognition. Development. 2021;148(20).

Acknowledgments

Ich bedanke mich bei PD Dr. Markus Höltje für die durchweg exzellente Betreuung meiner Doktorarbeit. Beginnend mit der Erarbeitung des Themas über die zahl- und lehrreichen Tage im Labor, bis hin zur Veröffentlichung der Publikationen und der Erstellung dieses Manuskriptes, wurde ich stets herzlich und geduldig begleitet, ermutigt, gefordert und gefördert.

Mein Dank gilt weiterhin Prof. Dr. Harald Prüß, so wie Prof. Dr. Klemens Ruprecht von deren engagierter Betreuung ich ebenfalls profitieren durfte. Besonders die intensive, interdisziplinäre Zusammenarbeit und die lebhaften Diskussionen waren für mich und das gesamte Projekt sehr wertvoll und bereichernd.

Ebenfalls bedanken möchte ich mich bei dem gesamten Team der AG Höltje, insbesondere bei Birgit Metze, Marion Möbes und Antje Dräger für das herzliche Willkommen und die engagierte Einarbeitung in das Labor, sowie für die große Unterstützung während des gesamtes Projekts. Lucie Y. Li danke ich, neben ihrer wertvollen fachlichen Meinung, auch für das Sitzen im selben Boot, das gemeinsame Durchbeißen und allem, was dazu gehörte.

Außerdem bedanke ich mich bei allen meinen Koautor*innen für ihren wertvollen Beitrag und die erfolgreiche Zusammenarbeit in unseren spannenden Projekten.

Liebe Familie, liebe Freund*innen – ein riesiges Dankeschön an jede und jeden von euch, für euer unerschütterliches bei mir Sein und für alles, was weit darüber hinaus geht.